



UNIVERSITÀ
DEGLI STUDI
DI PADOVA

UNIVERSITÀ DEGLI STUDI DI PADOVA

Dipartimento di Ingegneria Industriale DII

Corso Di Laurea Magistrale In Ingegneria Dell'Energia Elettrica

**NUMERICAL MODELS FOR DISSYMMETRIC ELECTRIC NETWORKS
STEADY-STATE ANALYSIS**

*Relatore: Ch.mo Prof. Roberto Turri
Department of industrial engineering*

*Correlatore: Ing. Roberto Andolfato
SINT Ingegneria Srl*

*Laureando: ISACCO FARA
n° matricola 1150694*

ANNO ACCADEMICO 2018 – 2019

to Alessia

ABSTRACT

In electrical plants design, a proper earthing system design is certainly one of the most important steps.

A well-made design of the earthing system, ensures that dangerous step and touch voltage values for human life are not reached, with a particular focus on the economic issue (oversizing the earthing system, based on the total fault current instead of the current that indeed flows through the earth, can be very uneconomical).

Studying the fault current distribution into the system and, in particular, what is the value of the *split factor*, is one of the main purposes of the NETS (NETwork Solver) software.

NETS is based on the phase components method, hence it permits to study how current divides itself into each component of the network (whether a phase conductor, an overhead earth wire or a cable screen), regardless of the symmetry of the network and of the number of conductors taken into account in the network under study, and also considering mutual couplings between each conductor.

The phase components method goes beyond the first limit of programs based on symmetrical components method, that is the hypothesis of symmetric network; in fact this assumption is only true in transmission lines, but not in case of distribution lines, where the major part of the loads are single-phase and the distributed generation can be single-phase too, mainly in case of domestic photovoltaic power plants.

A validation, through a comparison with results gave by an open source software, OpenDSS (Open Distribution System Simulator), highlights that a phase components method allows a very extensive study of the current distribution in the network, phase by phase.

SOMMARIO

Nella progettazione degli impianti elettrici, il corretto dimensionamento dell'impianto di terra assume fondamentale importanza.

Dimensionare correttamente tale impianto di terra significa garantire che non vengano raggiunti valori di tensione di passo e contatto tali da risultare pericolosi per la sicurezza delle persone in caso di guasto monofase a terra, senza perdere di vista l'aspetto economico (sovradimensionare l'impianto di terra, basandosi sulla totale corrente di guasto invece che sulla reale corrente che ritorna via terra, può essere molto dispendioso).

Studiare come si distribuisce la corrente di guasto, ed in particolare calcolare lo *split factor*, è uno dei principali scopi del programma NETS (NETwork Solver).

NETS è un software basato sul metodo alle fasi, quindi permette di studiare come si ripartisce la corrente in ogni singolo componente della rete (sia esso un conduttore di fase, una fune di guardia aerea o lo schermo di un cavo interrato), indipendentemente dalla condizione di simmetria della rete e indipendentemente dal numero di conduttori presenti nella rete considerata, valutando i mutui accoppiamenti tra i diversi conduttori.

Questo metodo supera il limite principale dei programmi basati sul metodo alle sequenze, cioè quello di considerare la rete simmetrica, situazione veritiera nel caso di linea di trasmissione, ma non più vera nel caso di reti di distribuzione, dove la maggior parte dei carichi è monofase e l'aumento della diffusione della generazione distribuita, che inietta in rete principalmente potenza monofase, fa sì che si abbiano continue situazioni di squilibrio sul sistema elettrico di distribuzione.

Una validazione, mediante confronto con i risultati ottenuti da un software open source, OpenDSS (Open Distribution System Simulator), mette in risalto il fatto che metodo alle fasi permette uno studio capillare della distribuzione della corrente nella rete, fase per fase.

ACKNOWLEDGEMENTS

I would like to thank Prof. Roberto Turri, who gave me the opportunity to firstly get in touch with SINT Ingegneria.

I also would like to thank Ing. Massimiliano Coppo, for helping me to use OpenDSS.

I am grateful to Ing. Roberto Andolfato, for supporting and helping me every time I needed it, during these seven months.

Many thanks to my “unibests”, for the good time spent together at the university and outside of it. I would also like to thank all the friends who have shared experiences and adventures with me, and my colleagues of pizzeria Terrazza, with which I passed many weekends during my student life, sharing good and bad moments from the numerous exams periods.

I sincerely want to thank my parents, Antonella e Giovanni, my sister Mary and Marco, who all believed in me since the beginning and who motivated and supported me during these eight years.

CONTENTS

CONTENTS	xi
List of Figures	xiii
List of Tables.....	xvii
1. INTRODUCTION.....	1
2. NUMERICAL METHODS FOR NETWORK ANALYSIS	3
2.1 Symmetrical Components Method	3
2.2 Phase Components Method	6
2.3 Comparison Between Methods.....	7
3. COMMERCIAL SOFTWARE	9
3.1 NETS	9
3.2 OpenDSS	10
3.3 Other Codes	11
4. NETS.....	13
4.1 General.....	13
4.2 Topology.....	16
4.3 Components	18
4.3.1 Feeders.....	18
4.3.2 Ideal Voltage and Current Sources	20
4.3.3 Transverse Impedances.....	21
4.3.4 Longitudinal Impedances	21
4.3.5 Lines and Cables.....	22
4.3.6 Transformers Yy Yd Dy Dd.....	27
4.3.7 Transformers Yz Dz	34
5. NETS RESULTS VALIDATION.....	37
5.1 Overhead Lines	37
5.1.1 Overhead line, frequency domain – NETS vs OpenDSS	37
5.1.2 Overhead line, various conditions – NETS vs OpenDSS.....	40
5.1.2.1 Steady state condition.....	43
5.1.2.2 Three-phase fault condition.....	50
5.1.2.3 Phase to phase to earth fault condition.....	54
5.1.2.4 Phase to earth fault condition.....	58
5.1.3 Overhead line, electromagnetic interaction – NETS vs OpenDSS.....	63
5.2 Underground Cables	66
5.2.1 Underground cables, frequency domain – NETS vs OpenDSS	66
5.2.1.1 Solid bonding condition	68

xii *CONTENTS*

5.2.1.2	Single bonding condition	71
5.2.2	Underground cables, various condition – NETS vs OpenDSS.....	74
5.2.2.1	Steady state condition	76
5.2.2.2	Phase to earth fault condition.....	78
5.3	Transformers	80
5.3.1	Two windings transformer	81
5.3.1.1	Steady state condition - Balanced Load Without Neutral.....	82
5.3.1.2	Steady state condition - Unbalanced Load Without Neutral	83
5.3.1.3	Steady state condition - Unbalanced Load With Neutral	84
5.3.1.4	Phase to earth fault condition.....	84
5.3.2	Three windings transformers	86
5.3.2.1	ZigZag transformer Yzn1	87
5.3.2.2	ZigZag transformer Dzn0	88
5.4	Meshed Network	89
5.4.1	Steady state condition	94
5.4.1.1	Steady state condition, 1 [MVA] load	95
5.4.1.2	Steady state condition, 100 [MVA] load	96
5.4.2	Phase to earth fault condition.....	97
CONCLUSIONS	101
6. ANNEXES.....		103
6.1	Cross Bonding Transposition.....	103
BIBLIOGRAPHY.....		109

List of Figures

Figure 2-1 – Schematic representation of a sequence components approach	5
Figure 2-2 – Schematic representation of a power system with multi-conductor approach [3]	6
Figure 2-3 – Lumped parameter representation of a transmission line with double circuit and single earth wire [3]	7
Figure 4-1 – Line splitting in cells.	13
Figure 4-2 – π -representation of a cell.	14
Figure 4-3 – $2n$ -port cell.....	15
Figure 4-4 – Equations obtained from topological conditions	17
Figure 4-5 – Representation of a Feeder	19
Figure 4-6 – Representation of an Ideal Voltage Source	20
Figure 4-7 – Representation of an Ideal Current Source.....	20
Figure 4-8 – Representation of a Transverse Impedance	21
Figure 4-9 – Representation of a Longitudinal Impedance.....	22
Figure 4-10 – Equivalent circuit for line or cable cell, referred to the link between two ports	23
Figure 4-11 – Carson’s two-conductor circuit with ground return (left); physical layout of two conductors with ground return (right) [13]	24
Figure 4-12 – Simplified equivalent model of a single-phase transformer.....	31
Figure 4-13 – Simplified equivalent model of a Zig Zag three-phase transformer.....	35
Figure 5-1: Single Line Diagram of an Ideal Voltage Source + Overhead Line + Load	37
Figure 5-2: Graphical differences between overhead line phase A current at difference frequencies, NETS vs OpenDSS (NETS = azure, OpenDSS = grey).....	40
Figure 5-3: Tower lattice layout.....	41
Figure 5-4: Single Line Diagram of an Overhead Line with a Load at the End	44
Figure 5-5: Magnitude Current Distribution along Left Overhead Earth Wire – NETS	46
Figure 5-6: Magnitude Current Distribution along Right Overhead Earth Wire – NETS	46
Figure 5-7: Magnitude Current Distribution along Left and Right Overhead Earth Wire – OpenDSS.....	47
Figure 5-8: Magnitude Potential Distribution along Left and Right Overhead Earth Wire – NETS.....	47
Figure 5-9: Magnitude Potential Distribution along Left and Right Overhead Earth Wire – OpenDSS.....	48
Figure 5-10: Magnitude Current Distribution along Left Overhead Earth Wire – NETS	49
Figure 5-11: Magnitude Current Distribution along Right Overhead Earth Wire – NETS	49
Figure 5-12: Single Line Diagram of an Overhead Line with a Load and a Fault at the End	50
Figure 5-13: Magnitude Current Distribution along Left Overhead Earth Wire – NETS	51
Figure 5-14: Magnitude Current Distribution along Right Overhead Earth Wire – NETS	52
Figure 5-15: Magnitude Current Distribution along Left and Right Overhead Earth Wire – OpenDSS.....	52

xiv List of Figures

Figure 5-16: Magnitude Potential Distribution along Left and Right Overhead Earth Wire – NETS	53
Figure 5-17: Magnitude Potential Distribution along Left and Right Overhead Earth Wire – OpenDSS	53
Figure 5-18: Single Line Diagram of an Overhead Line with a Load and a Fault at the End.....	54
Figure 5-19: Magnitude Current Distribution along Left Overhead Earth Wire – NETS.....	55
Figure 5-20: Magnitude Current Distribution along Right Overhead Earth Wire – NETS.....	56
Figure 5-21: Magnitude Current Distribution along Left and Right Overhead Earth Wire – OpenDSS	56
Figure 5-22: Magnitude Potential Distribution along Left and Right Overhead Earth Wire – NETS	57
Figure 5-23: Magnitude Potential Distribution along Left and Right Overhead Earth Wire – OpenDSS	57
Figure 5-24: Magnitude Current Distribution along Left Overhead Earth Wire – NETS.....	59
Figure 5-25: Magnitude Current Distribution along Right Overhead Earth Wire – NETS.....	59
Figure 5-26: Magnitude Current Distribution along Left and Right Overhead Earth Wire – OpenDSS	60
Figure 5-27: Magnitude Potential Distribution along Left Overhead Earth Wire – NETS.....	60
Figure 5-28: Magnitude Potential Distribution along Left and Right Overhead Earth Wire – OpenDSS	61
Figure 5-29: Magnitude Current Distribution along Left Overhead Earth Wire – NETS.....	62
Figure 5-30: Magnitude Current Distribution along Right Overhead Earth Wire – NETS.....	62
Figure 5-31: Tower lattices cross section layout	64
Figure 5-32: Single Line Diagram of an Ideal Voltage Source + Underground Cable + Solid Bonding + Load..	67
Figure 5-33: Graphical differences between phase A core currents at difference frequencies in case of solid bonding, NETS vs OpenDSS (NETS = azure, OpenDSS = grey).....	70
Figure 5-34: Graphical differences between phase A screen currents at difference frequencies in case of solid bonding, NETS vs OpenDSS (NETS = azure, OpenDSS = grey).....	70
Figure 5-35: Ratio between current along screen and phase of the phase A (calculated by NETS).....	71
Figure 5-36: Graphical differences between phase A core currents at difference frequencies in case of single bonding, NETS vs OpenDSS (NETS = azure, OpenDSS = grey).....	73
Figure 5-37: Graphical differences between phase A screen currents at difference frequencies in case of single bonding, NETS vs OpenDSS (NETS = azure, OpenDSS = grey).....	73
Figure 5-38: Single Line Diagram of Feeder + Underground Cable + Intermediate Traspositions + Solid Bonding + Load.....	74
Figure 5-39: Single Line Diagram of Feeder + Underground Cable + Intermediate Traspositions with Voltage Limiter Triggered + Solid Bonding + Load.....	79
Figure 5-40: Single Line Diagram of Feeder – Transformer and Load.....	81
Figure 5-41: Single Line Diagram of Feeder – Transformer, Load and Fault	85
Figure 5-42: Single Line Diagram of Feeder – Transformer and Load.....	86
Figure 5-43: Graphical comparison between primary side currents in case of Yzn1 transformer, NETS vs OpenDSS (X log, Y linear).....	88
Figure 5-44: Graphical comparison between primary side currents in case of Dzn0 transformer, NETS vs OpenDSS (X log, Y linear).....	89
Figure 5-45: Single Line Diagram of a Meshed Network	90
Figure 5-46: Tower lattice layout	92

Figure 5-47: Single Line Diagram of an the Meshed Network (Voltage Limiter triggered in the Left Cable)..... 98

Figure 7-1: Magnitude Current Distribution along phase A – Transposition 10+10+10 [km] – NETS 103

Figure 7-2: Magnitude Current Distribution along screens on phase A – Transposition 10+10+10 [km] – NETS 104

Figure 7-3: Magnitude Current Distribution along phase A – Transposition 2·(5+5+5) [km] – NETS 104

Figure 7-4: Magnitude Current Distribution along screens on phase A – Transposition 2·(5+5+5) [km] – NETS 105

Figure 7-5: Magnitude Current Distribution along screens on phase B – Transposition 2·(5+5+5) [km] – NETS 105

Figure 7-6: Magnitude Current Distribution along screens on phase C – Transposition 2·(5+5+5) [km] – NETS 106

Figure 7-7: Magnitude Current Distribution along screens on phases A+B+C – Transposition 2·(5+5+5) [km] – NETS 106

List of Tables

Table 5-1: Differences between overhead line phase A current at difference frequencies, NETS vs OpenDSS ..	39
Table 5-2: Current and voltage variations along the overhead line in steady state condition, NETS vs OpenDSS	45
Table 5-3: Current and voltage variations along the overhead line in three phase fault condition, NETS vs OpenDSS	51
Table 5-4: current and voltage variations along the overhead line in phase to phase fault condition, NETS vs OpenDSS	55
Table 5-5: Current and voltage variations along the overhead line in phase to earth fault condition, NETS vs OpenDSS	58
Table 5-6: The result does not change, modifying the length of each line in NETS	62
Table 5-7: Current and voltage variations along the overhead line with electromagnetic interaction, NETS vs OpenDSS	66
Table 5-8: Differences between underground cable phase A core current and phase A screen current at difference frequencies, in solid bonding condition, NETS vs OpenDSS	69
Table 5-9: Differences between underground cable phase A core current and phase A screen current at difference frequencies, in single bonding condition, NETS vs OpenDSS	72
Table 5-10: Current and voltage variations along the underground cable in steady state condition, NETS vs OpenDSS	76
Table 5-11: Current and voltage variations along the underground cable, neglecting the conductance effect between screen and earth, NETS vs OpenDSS	77
Table 5-12: Current and voltage variations along the underground cable in phase to earth fault condition, NETS vs OpenDSS	78
Table 5-13: Potential rise in cable screen transposition points, NETS vs OpenDSS.....	79
Table 5-14: Current and voltage variations along the underground cable with voltage limiter triggered, NETS vs OpenDSS	80
Table 5-15: Current and voltage at the primary side and at the secondary side, balanced load without neutral, in steady state condition, NETS vs OpenDSS.....	83
Table 5-16: Current and voltage at the primary side and at the secondary side, unbalanced load without neutral, in steady state condition, NETS vs OpenDSS.....	83
Table 5-17: Current and voltage at the primary side and at the secondary side, unbalanced load with neutral, in steady state condition, NETS vs OpenDSS.....	84
Table 5-18: Current and voltage at the primary side and at the secondary side, balanced load without neutral in phase to earth fault condition, NETS vs OpenDSS.....	85
Table 5-19: Current and voltage trends along phase A of longitudinal elements of the network in steady state condition, NETS vs OpenDSS	95

xviii List of Tables

Table 5-20: Load current with a 1 [MVA] load	96
Table 5-21: Load current with a 100 [MVA] load	96
Table 5-22: Current and voltage trends along phase A of longitudinal elements of the network in phase to earth fault condition, NETS vs OpenDSS	97
Table 5-23: : Potential rise in cables screen transposition points, NETS vs OpenDSS	98
Table 5-24: Current and voltage trends along phase A of longitudinal elements of the network in phase to earth fault condition with left underground cable voltage limiter triggered , NETS vs OpenDSS	99

Chapter 1

INTRODUCTION

The study of electrical networks may require specific numerical simulation programs.

XGSLab is a versatile software for electromagnetic simulations and can be applied in power, grounding and lightning protection systems.

The XGSLab application field is so wide because the implemented model is for general use and solves the Maxwell equations in non-stationary conditions taking into account the earth lack of homogeneity by the Green functions, the earth reaction by the Sommerfeld integrals and moving from the frequency to the time domain by means the Fourier transforms.

A new module of this software, NETS, has been developed to solve multi-conductor and multi-phase full meshed networks.

NETS has the primary purpose to calculate the earth return current when a fault occurs.

During normal conditions, a power system network is reasonably balanced so that the soil current or electromagnetic induction may be easily neglected; hence; the network is practically decoupled from the earth and its characteristics are practically irrelevant.

Phase to ground short circuit calculations are very often made assuming that the impedances of the neutral to ground interconnections, such as grounding grids or transmission tower footings, are negligible (zero conductivity soil) or infinite (ungrounded skywire).

These two assumptions are not always true and NETS are able to take in account these phenomena.

The earthing system has to be designed to keep, firstly, the touch voltage value below a safety threshold established by standards (a person must be able to work in safety condition); in case of transmission line tower earthing system, the earthing system has to be designed to preserve the insulators chain from a lightning discharge, by ensuring that the lightning current, when it hits the overhead earth wire, flows down into the earthing system instead of breaking the insulators. Around the pylons, a protection against the step voltage has to be guaranteed.

In order to design a good earthing system, it is important to study the share of the current that effectively flows down through the earth. This share is named *split factor* and it is given by the ratio between the current that flows back into the earth and the total fault current. The remaining part that does not flow towards the earth, returns back passing through the overhead earth wire-in overhead line, the cable screen or all other metallic paths, as pipelines.

This means that a smaller quantity of copper is necessary to compose the earthing system, resulting in significant cost savings in terms of money: as it can be seen in chapter 5, *split factor* can reach values that permits to use a quantity of copper equal to half, or less, with respect to a case that considers the entire fault current.

Knowing the magnitude of quantities for each phase, is important also to understand the voltage rise in the circuit under study when a fault occurs, as it can be on a bus that simulates a sheath voltage limiter in a screen transposition point with a cable line.

The aim of this thesis is to validate the results obtained by NETS, with a comparison using OpenDSS (Open Distribution System Simulator); there are other programs that are able to do the same calculations here performed by NETS (for example EMTP, CDEGS, etc.) but, trivially, OpenDSS is a free tool available on the web.

The second chapter presents a short description of the two different methods to represent a network, with the most important characteristics of each and a comparison between the two methods, bringing out advantages and disadvantages of each approach.

In the third chapter there is a brief description of the capabilities and the limits of the two software used to do the comparison.

A better comprehensive discussion of the phase components method is explained in the fourth chapter. It consists on the theoretical background used to develop the NETS software.

The fifth chapter describes the comparison between NETS and OpenDSS. Overhead earth wires, screened cables and transformers are dealt with, as well as an example of a simple meshed network in which all the elements treated separately are joint together.

Finally, conclusions are drawn and possible future developments will be listed.

Chapter 2

NUMERICAL METHODS FOR NETWORK ANALYSIS

2.1 Symmetrical Components Method

Electric generation plants feed the national grid with sinusoidal power. Electric distribution systems are mainly three-phase and a group of three quantities, i.e. potentials, currents, impedances (or admittances) can be used to describe them.

Hence, it is useful to represent each single quantity as a rotating phasor in the Gauss-plan, using the Steinmetz transformer: the corresponding phasor includes the module and phase values, in a complex form.

A set of three voltages is symmetric if each component has the same module, they differ by a phase shift of 120° and, in the same way, a set of three currents is balanced if each component has the same module and they differ by a phase shift of 120° .

In the ideal case, the vector sum of each group of components is equal to zero. But in a real case, distribution systems are neither symmetrical nor balanced, because of the dissymmetry of the system and, overall, the insertion of single-phase loads. A more complex analysis caused by different component of the system, is then necessary for not ideal systems.

To face this problem, the symmetrical components theory can help. This theory was developed by Fortescue in 1918 [1] and it states that a system of n vectors can be resolved in n different symmetrical groups or systems (where n is a prime number). One of these systems consists of n equal vectors and the remaining $(n-1)$ systems consist of n equi-spaced vectors that, with the first mentioned groups of equal vectors, form an equal number of symmetrical n -phase systems.

In case of $n=3$, a three-phase voltage system could be decomposed into three sequence circuits:

- Positive sequence, composed by three phasors with equal module which differ by a phase shift of 120° , rotating in clockwise direction. The positive sequence has the same phase sequence as the system under study and it is always present in each network situation, in particular with balanced load

- Negative sequence, composed by three phasors with equal module which differ by a phase shift of 120°, rotating in counterclockwise direction. This sequence is present when there is an unbalanced load
- Zero sequence, composed by three phasors with equal module and phase. This sequence takes into account unbalanced conditions and earth is involved

The sum of these three sequences gives back the original circuit under study.

Essentially, this method converts three unbalanced phases into three independent sources, which makes asymmetric fault analysis more tractable.

The core of the Fortescue transform is the shifting operator α :

$$\alpha = e^{j\frac{2\pi}{3}} \quad (2.1)$$

Note that:

$$\begin{aligned} \alpha^3 &= 1 \\ \alpha^{-1} &= \alpha^2 \end{aligned} \quad (2.2)$$

The transformation can be expressed using the following formulas:

$$\mathbf{e}_{abc} = \begin{Bmatrix} E_0 \\ E_0 \\ E_0 \end{Bmatrix} + \begin{Bmatrix} E_1 \\ \alpha^2 E_1 \\ \alpha E_1 \end{Bmatrix} + \begin{Bmatrix} E_2 \\ \alpha E_2 \\ \alpha^2 E_2 \end{Bmatrix} = \begin{bmatrix} 1 & 1 & 1 \\ 1 & \alpha^2 & \alpha \\ 1 & \alpha & \alpha^2 \end{bmatrix} \begin{Bmatrix} E_0 \\ E_1 \\ E_2 \end{Bmatrix} = [A] \mathbf{E}_{012} \quad (2.3)$$

The inverse relation gives:

$$\mathbf{E}_{012} = [A]^{-1} \mathbf{e}_{abc} \quad (2.4)$$

$$[A]^{-1} = \frac{1}{3} \begin{bmatrix} 1 & 1 & 1 \\ 1 & \alpha & \alpha^2 \\ 1 & \alpha^2 & \alpha \end{bmatrix}$$

This representation can be applied to every entity and it is useful because a complex problem can be reduced to a sum of easier problems.

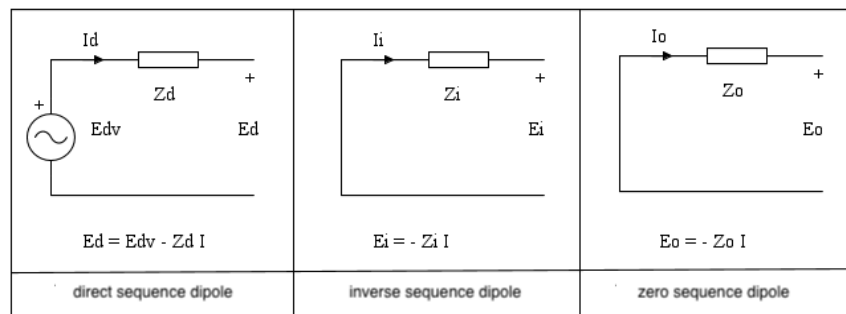


Figure 2-1 – Schematic representation of a sequence components approach

As it can be seen in the previous figure, the positive sequence circuit is represented by a generator with an applied voltage equal to E_d (i.e. the star voltage of the circuit under study) and with the series impedance Z_d ; the negative sequence circuit is represented only by the series impedance Z_i (because there is no negative sequence voltage applied) and the zero sequence circuit is represented by the Z_o impedance (for the same reason of the inverse impedance).

The Symmetrical components method, in addition of being a powerful analytical tool, is also conceptually useful.

The great utility of symmetrical components is that, for most types of network elements, the symmetrical components are independent from each other.

In particular, balanced impedances and rotating machines will draw only positive sequence currents in response to positive sequence voltages.

A completely balanced network will have three separated sequence networks.

If a network is unbalanced at a particular point, the sequence networks will be interconnected at that point.

The key to use symmetrical components in handling unbalanced situations is in learning how to formulate those interconnections.

This method can be applied in studying the faults in the medium or high voltage networks, (the, usually, without the neutral conductor). In this type of networks, can be affected by the following types of faults may occur:

- Phase to earth fault condition
- Phase to phase fault condition
- Phase to phase to earth fault condition
- Three-phase fault condition
- Three-phase to earth fault condition

Short circuits determine, in the fault sections, specific constraints that correspond to equal number of constraints between relative sequence components. Linking together in a specific

way the three sequence dipoles, the different types of faults can be modeled and the real short circuit current can be computed.

As reported in [2], each of the three sequence networks are decoupled from each other (there are no mutual couplings between sequence circuits) and can be studied using three single-phase circuits.

2.2 Phase Components Method

The symmetrical components method introduces a sort of facilitation, hence it does not consider in a proper way the ground return current during faults. On the other hand, the phase components method, does not introduce any kind of simplification in the circuit, but it analyses the network in its entirety; in fact, each single component is taken into account in the model.

The phase components method applies the basic electrical science laws, as the Kirchhoff current law (which declares that the sum of the currents that enters in a node shall be equal to the sum of the currents that leaves the same node at any time), and the Kirchhoff voltage law (which declares that the sum of the algebraic voltages along a closed line, taking into account their sign, is equal to zero).

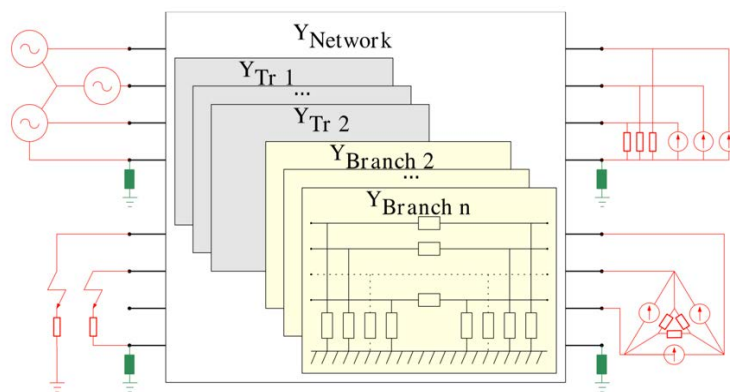


Figure 2-2 – Schematic representation of a power system with multi-conductor approach [3]

In the figure above, a generic power system is represented taking into consideration lines, generators, loads and grounding conditions.

The network can be represented by an admittance matrix, built by using an incidence matrix that takes into account the couplings between the buses.

Shunt elements and grounding impedances represent the link between the phase potential and the ground.

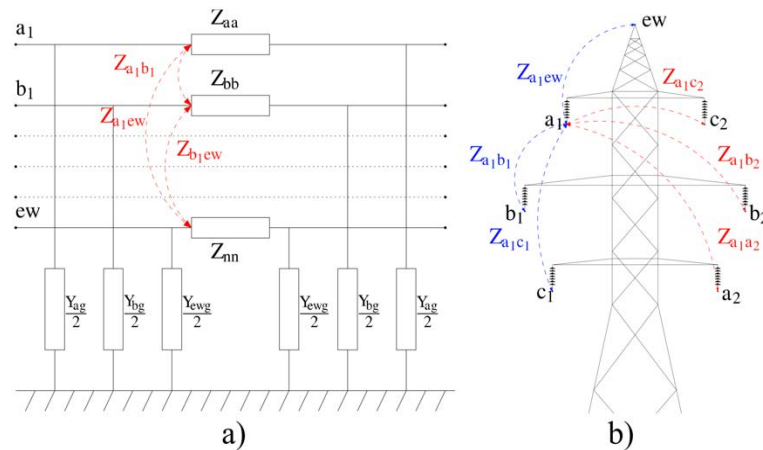


Figure 2-3 – Lumped parameter representation of a transmission line with double circuit and single earth wire [3]

As better described in chapter 4, branch elements are represented through an n -phase lumped parameters circuits, in which we got longitudinal impedances Z and transverse admittances Y_t representing respectively the self and mutual couplings within the circuits and between each circuit and ground.

These terms can be used to build the admittance matrix:

$$Y_{branch} = \begin{bmatrix} Z^{-1} + \frac{Y_t}{2} & -Z^{-1} \\ -Z^{-1} & Z^{-1} + \frac{Y_t}{2} \end{bmatrix} \tag{2.5}$$

This matrix explains the correlation between currents and voltages, for the $2n$ ports of the branch elements. It is assumed that currents are positive if enter the node and potentials are calculated based on a common zero-voltage reference.

2.3 Comparison Between Methods

In all cases, symmetrical and balanced multiphase networks can be reduced to the equivalent single-phase network.

In general, systems are unbalanced and sometime also unsymmetrical and, in these cases, the network solution requires one of the previously described methods.

The two methods are not alternative each other and cannot be directly compared.

It is however important to know advantages and disadvantages and limits of both methods as below described.

The Symmetrical components method is a powerful analytical tool and also conceptually useful; in case of symmetrical network, the calculation of unbalanced conditions is quite simple because the unbalanced system is converted in balanced systems easy to solve.

This method also has the advantage of reducing the size of the linear system involved with the problem, requiring limited computing power. For transmission lines, a condition with balanced load can be supposed, hence the approximation could be valid.

This method has been used for many years in industry and engineering for short circuit and load flow analysis, thus it is widely validated.

The drawbacks of this approach are that it can be used only for symmetrical systems or for systems that have been reduced to symmetrical. It could be anyway used with quasi symmetrical systems like common power lines and cables.

Finally, symmetrical components method does not take into consideration mutual couplings among the conductors, and this could be a problem in order to evaluate how current distributes, for example, in a double circuit line.

All these assumptions and limitations have been exceeded with the phase components method, because it treats each single conductor as a phase, and it does not introduce any kind of facilitation. Furthermore, it can be used to study any circuit, regardless of the level of unbalance and asymmetry of the network. Hence, it can be a useful approach when studying low voltage networks (networks with a fourth conductor, the neutral one) or high voltage networks, because there is one, or more, overhead earth wires. In case of phase to earth fault, current flows through these passive conductors, and it can be useful to observe how much current flows back through the overhead earth wires and how much flows back to the earth.

The multi-conductor approach is advantageous especially when two or more circuits are studied, because it allows to correctly consider the mutual couplings among conductors both in the same direction and from one circuit to the other.

The great advantage of this method is that any kind of circuit can be studied, because the number of circuits can be expanded with no limitations.

The most important drawback is that the size of the linear system involved with the problem is increased and considerable memory resources and computing power are required. Nonetheless, taking into account the memory resources and computing power of modern PC, the phase components method is today an often feasible approach and in any case sometimes the only applicable method.

Chapter 3

COMMERCIAL SOFTWARE

In this chapter, a short presentation of the two software used in this thesis, NETS and OpenDSS.

3.1 NETS

The code has been implemented using actual values and not per-unit quantities.

The computer codes based on per-unit quantities were diffused in the past because this approach offered some advantages with digital computers with fixed-point arithmetic. Modern computers work with floating-point arithmetic and so, today there is no reasons to use per-unit quantities.

Moreover actual-values offered some important advantages are summarized in [4].

NETS is a very flexible tool to solve full meshed multi-conductor and multi-phase networks taking into account all the neutral conductors paths as well as the earth path.

This approach is general and overcomes the classic method of symmetrical components and can be used to represent power systems as multi-conductor networks enabling the consideration of asymmetrical and/or unbalanced systems also in presence of grounding circuits or circuits with a different phases number.

The grounding systems (substation grids, tower footings ...) can be specified in an arbitrary way.

NETS calculates lines, cables and transformers parameters starting on data normally available on commercial data sheets.

Like the other XGS modules, also NETS has been thought for a use as general as possible.

NETS can be used to solve transmission and distribution networks in steady state or fault conditions and to calculate potentials, currents or short circuit currents (three-phase, phase to phase, phase to phase to earth, single-phase to earth) with or without fault impedances.

In particular, NETS can be used for the calculation of the fault current distribution in power networks and between power circuits and earth. An accurate knowledge of the fault current distribution is crucial in grounding, mitigation to reduce interference on communication circuits and pipelines, power systems protections calibration and coordination, neutral grounding resistor sizing and many other applications.

NETS is thus a very useful tool to calculate data input for other XGS modules (for instance the split factor or the current to earth) without unrealistic assumptions as for instance,

magnitude of fault current known and unaffected by grounding impedances, impedances of overhead earth wires or tower footing resistances uniform along the line, or again, infinite length of lines ...

Moreover, NETS represents the link between XGS and the most diffused commercial software for power systems analysis.

3.2 OpenDSS

OpenDSS is a power distribution system simulator released by EPRI (Electrical Power Research Institute). It is a frequency-domain simulation engine with many characteristics found in other commercial simulation tools. OpenDSS can be used for planning and analysis of multi-phase distribution systems, analysis of distributed generation interconnection, annual simulations, storage modeling and analysis, and other studies.

It is a powerful tool based on a command line interface, which represents its strength, if a user is used to this type of interface (for example Matlab) but, it might be uncomfortable, because it the construction of the circuit string by string is very time consuming.

OpenDSS also supports many other types of frequency-domain circuit simulations commonly performed on utility electric power distribution systems.

Another advantage is that users commonly drive the OpenDSS with the familiar Mathworks MATLAB program, Python, C#, R, and other languages. This provides powerful external analytical capabilities as well as better graphics for displaying results, but it also means that there are other commands to learn.

This software, although it is powerful, has some negative aspects which should not be neglected. The mains are:

- It does not have a library where user can set materials properties, cable or line types or the transformers characteristics. It means that, for each script, user has to set the characteristics of the elements he wants to use
- If user wants to represent a line with n spans, he has to write n strings, one for each span. With more complex network, work becomes increasingly difficult
- Default values may distort the results and it is not so easy to find them
- It is not possible to define the conductor conductivity; hence, only copper and aluminum conductors can be simulated; in fact, at first a steel overhead earth wire was taken into account in the comparison with NETS, but it has been changed with an aluminum one, to allow a comparison between the two software
- It is not possible to define a permittivity value, and this is a limitation because, by rising the frequency, this parameter gets less and less negligible
- If user wants to study an underground screened cable, and it wants to consider the screen current, it has to calculate by hand the primitive matrices R,X,C of the cable and insert the result into the OpenDSS script.

- It is possible to set each type of transformer, but it is necessary to impose the phase connections port by port. In addition, user has to calculate by hand the input data for each winding, because OpenDSS requires data that are not commonly available in datasheets.

A better understanding of the program can be found in [5].

3.3 Other Codes

There are other programs that may perform calculation applying the phase components method; the most important are:

- CDEGS modules SPLIT and SPLITS [6]
- EMTP, that is able to perform time-domain calculation [4], [7]

Chapter 4

NETS

4.1 General

The electric networks analysis can be conveniently formulated with conventional techniques that can be implemented in calculation programs. This is certainly right in case of multi-conductor, linked and complex networks.

The aim is to get a “full mesh multi-conductor network solver”, flexible and suitable to solve practical cases generalizing the context as much as possible.

It must be possible to calculate potentials and currents on the buses and along the linked network branches in steady state conditions or three-phase, phase to phase to earth and phase to earth fault conditions.

The calculation is performed in steady state fault condition, hence when the transient is completed.

The frequency application range goes from DC up to a limit dependent on the components included in the system (10 kHz for lines and a few kHz for cables and transformers).

This method is based on lumped parameters equivalent circuits (as it can be seen in the following figure). For each cell the admittance matrix is built, taking into account the equivalent π -model, as it can be seen in Figure 4-2.

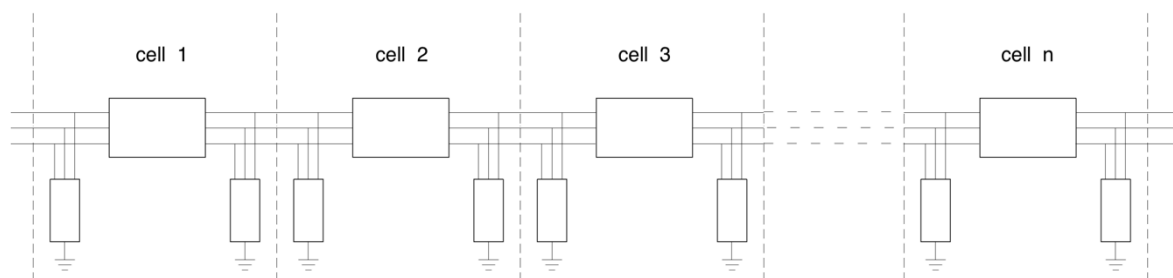


Figure 4-1 – Line splitting in cells.

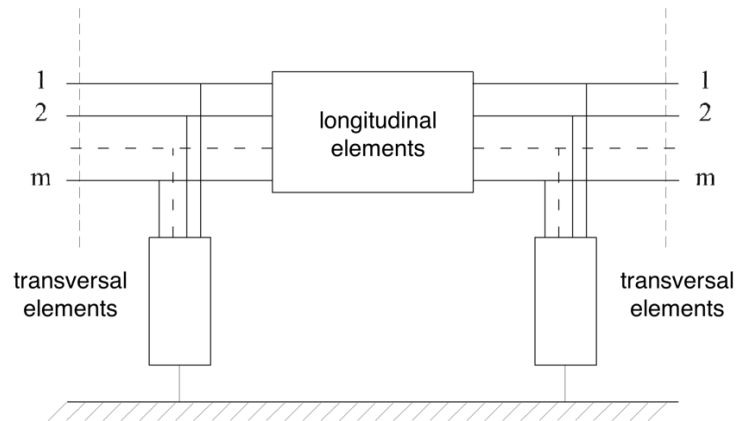


Figure 4-2 – π -representation of a cell.

The precision of the computation improves as the numbers of cells increases, as the discretization of the lines increases as well. In addition, the discretization must grow along with the frequency [8].

The model is based on the network theory suited for the specific case.

It will be used the following terminology:

- Bus or Node: a point in which one or more cells can be connected
- Cell or Branch: an element (line, generator, transformer, etc...)
- Mesh: a set of cells linked together to form a loop
- Port: a terminal of a cell

Each component of the network can be represented starting from a cell. In order to represent components like generators or transverse impedances a cell with p input ports is used.

For representing components that connect two parts of the network as lines, transformers or longitudinal impedances an oriented cell with p input ports and p output ports is used.

The number p can be 3 for three-phase network without neutral connection, 4 for three-phase network with neutral connection or another number if screens, Overhead Earth wires or systems composed by more than one circuit are considered.

The positive direction of currents was chosen according to the literature rule for double dipoles with the entering exiting current hence, with opposite convention to the one treated in [9].

The p ports cells will be named “Type-1 cells” and the $2p$ ports cells will be named “Type-2 cells”.

The maximum number of the ports, as well as maximum number of phases, is limited to 26, as the English alphabet letters; in some cases, cells linked together could have a different number of ports.

Usually, transformers and generators have three or four ports, whereas lines can have a greater number of ports, to consider more circuits including, cable screens or armors, overhead earth wires, etc.

For example, a system with two three-phase overhead line and two overhead earth wires includes eight conductors and require eight ports, whereas a three-phase cable with single core screened cables requires six ports.

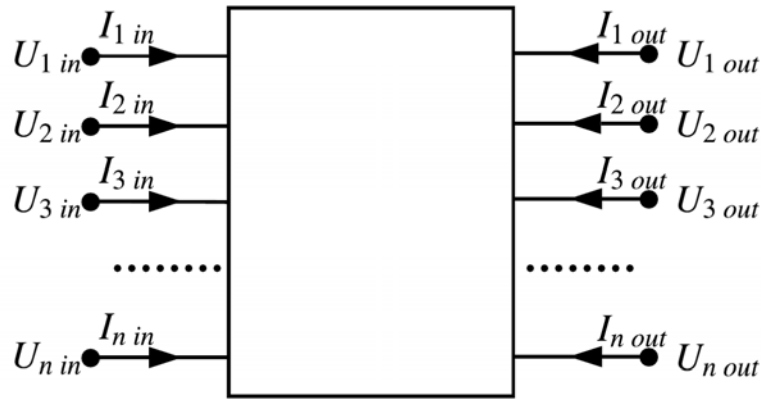


Figure 4-3 – $2n$ -port cell

Each port can be related to a potential and a current.

Each *Type-1* cell introduces $2p$ unknowns (p potentials + p currents) and each *Type-2* cell introduces $4p$ unknowns ($2p$ potentials + $2p$ currents); hence, the total ports number is equal to:

$$P = \sum_{i=1}^{C_1} p_i + 2 \sum_{i=1}^{C_2} p_i = P_1 + 2P_2 \quad (4.1)$$

and the total number of unknowns is:

$$N = 2P \quad (4.2)$$

The same amount of independent equations is needed.

The complete linear system can be written as follow:

$$\begin{bmatrix} [A_{11}] & [A_{12}] & [A_{13}] & [A_{14}] \\ [A_{21}] & [A_{22}] & [A_{23}] & [A_{24}] \\ [B_{11}] & [B_{12}] & [B_{13}] & [B_{14}] \\ [B_{21}] & [B_{22}] & [B_{23}] & [B_{24}] \end{bmatrix} \begin{Bmatrix} \{I_{in P_1+P_2}\} \\ \{I_{out P_2}\} \\ \{U_{in P_1+P_2}\} \\ \{U_{out P_2}\} \end{Bmatrix} = \begin{Bmatrix} \{N_{1P_1+P_2}\} \\ \{N_{2P_2}\} \\ \{0_{P_1+P_2}\} \\ \{0_{P_2}\} \end{Bmatrix} \quad (4.3)$$

and in a compact way:

$$\begin{bmatrix} [A_{P \times 2P}] \\ [B_{P \times 2P}] \end{bmatrix} \begin{Bmatrix} \{I_P\} \\ \{U_P\} \end{Bmatrix} = \begin{Bmatrix} \{N_P\} \\ \{0_P\} \end{Bmatrix} \quad (4.4)$$

The first p equations (submatrix A), can be obtained from the Y_{bus} or Z_{bus} matrix of cells, and the second p equations (submatrix B), can be obtained from the topology conditions on potentials and currents.

The solution of the linear system, get potential and current in each port.

The computational cost requires the solution of a $2p$ order sparse complex system.

For sparse matrices, computing the solution of the linear system can be made much more efficient with respect to both storage and computation time, if the sparsity of the matrix can be exploited.

Solver for sparse matrices are usually classified into two groups, direct and iterative [10].

NETS uses a direct solver. The calculation time required to solve a system of linear equations relatively predictable, based on the size of the matrix. For sparse matrices, the solution time decrease with the sparsity.

About storage, is important to consider with sparse matrices, it is more efficient to store only the non-zeros.

The following paragraph will first describe how to obtain the B topology submatrix, then the paragraph will show how to obtain the components equations, that is how to calculate the submatrices A and the N vectors for the following network components:

- Feeders
- Ideal Voltage Sources
- Ideal Current Sources
- Transverse Impedances
- Longitudinal Impedances
- Lines and Cables
- Transformers

4.2 Topology

For a general electrical system, the node voltages and the current injected to the system at each node can be related using the following equation:

$$I = Y_{bus} \cdot V \quad (4.5)$$

Where I is the vector of current injected to the system through each node, Y_{bus} is the nodal admittance matrix and V is the vector of nodes voltages of the system.

If a system has n nodes, the elements of the equation shall be structured as follows:

$$\begin{bmatrix} I_1 \\ I_2 \\ \vdots \\ I_n \end{bmatrix} = \begin{bmatrix} Y_{11} & Y_{12} & \cdots & Y_{1n} \\ Y_{21} & Y_{22} & \cdots & Y_{2n} \\ \vdots & \vdots & \ddots & \vdots \\ Y_{n1} & Y_{n2} & \cdots & Y_{nn} \end{bmatrix} \cdot \begin{bmatrix} V_1 \\ V_2 \\ \vdots \\ V_n \end{bmatrix} \quad (4.6)$$

Where for any row k :

- Y_{kk} ($1 \leq k \leq n$) is the sum of all the admittances connected to node k
- Y_{km} ($1 \leq k, m \leq n$) is the negative of the total admittances connected between nodes k and m .

In the figure below a network with eight branches is represented, each one with its respective cell. Hence there are eight cells, two *Type-1* cells (cells n°1 and n°3) and six *Type-2* cells (the other cells).

Nodes can be graphically represented with buses. In the following, bus and node will represent the same meaning.

Buses are arbitrarily numbered in a progressive way.

Supposing the n -conductors system, with two *Type-1* cells and six *Type-2* cells, there are $2 \cdot 2 \cdot n + 4 \cdot 6 \cdot n = 28n$ unknowns.

From Y_{bus} or Z_{bus} matrix are obtained $2 \cdot n + 2 \cdot 6 \cdot n = 14n$ equations. Applying the Kirchhoff's first law on the 5 buses, other $((c-1) \cdot n = 9n$ equations per bus can be obtained, where c is the number of cells incident the node.

In total $5 \cdot n + 9 \cdot n = 14n$ equations are obtained, which are added to the previous $14n$ equations obtained from Y_{bus} or Z_{bus} matrix, providing the $28n$ equations needed. The system is fixed.

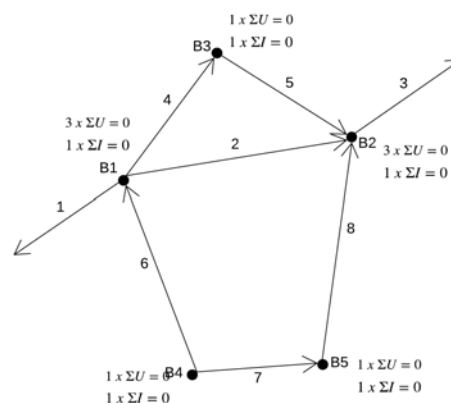


Figure 4-4 –Equations obtained from topological conditions

The system containing the topological information (that can be obtained from buses relations) can be written in a compact way:

$$\left[B_{P \times 2P} \right] \left\{ \begin{array}{l} \{ \dot{I}_P \} \\ \{ \dot{U}_P \} \end{array} \right\} = \{ 0_P \} \quad (4.7)$$

The matrix B can be found as it follows.

The cells are numbered from 1 to C and the buses are numbered from 1 to B. As agreement *Type-1* cells have only the side in and the *Type-2* cells are oriented from the entrance (side in) to the exit (side out).

It is possible to build directly the complete incident matrix:

$$\left[b_{B \times C} \right] \quad (4.8)$$

The content of the matrix B is:

- The row i is referred at the bus i
- The column j is +1 if the cell j enters the bus i going out (*Type-1* cells always, *Type-2* cells side in)
- The column j is -1 if the cell j enters the bus i going in (*Type-2* cells side out)
- The column j is 0 if the cell j does not enter the bus.

4.3 Components

As previously mentioned, it is possible to define the cells in different ways, according to the use of the cell. In the following paragraphs, the different characteristics of the various cells are described.

4.3.1 Feeders

A feeder represents an entire portion of the network or a single generator and it can be represented with a simplified model (Thevenin equivalent circuit), as it follows.

In power distribution networks, the short circuit power depends on the rated voltage. The following values can be used as reference for well meshed networks:

- Rated voltage of 400 [kV]: $I_{sc} = 50 \div 63$ [kA], $S_{sc} = 34600 \div 43600$ [MVA]
- Rated voltage of 230 [kV]: $I_{sc} = 40 \div 50$ [kA], $S_{sc} = 15900 \div 19900$ [MVA]
- Rated voltage of 132 [kV]: $I_{sc} = 31.5 \div 40$ [kA], $S_{sc} = 7200 \div 9150$ [MVA]

In power distribution and transmission networks, reactance “X” is normally much greater than resistance “R”:

- In distribution networks the “X/R” ratio is usually between 3 and 10.
- In transmission networks the “X/R” ratio is usually between 10 and 30.

If the feeder represents a synchronous generator, the reactance “X” can be chosen as in the following:

- If the clearance time is lower than 500 [ms], the the reactance can be set as the transient reactance
- If the clearance time is greater than 500 [ms], the reactance can be set as the steady state or synchronous reactance

If the fault is electrically far from the generator, the difference in result assuming transient or steady state reactance is anyway limited.

In the feeder scheme, each phase has a voltage source with an impedance Z_{p1} , Z_{p2} , ... in series, that represents the equivalent internal impedance of the feeder.

The impedance Z_e represents the impedance with which the neutral is grounded.

It is a *Type-1* cell, so it only has n input ports.

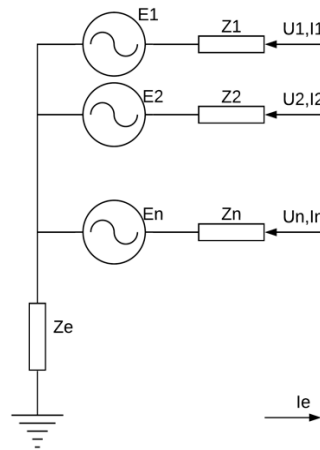


Figure 4-5 – Representation of a Feeder

The equations that represent this type of cell are:

$$\dot{U}_1 - \dot{U}_n = \dot{E}_1 + \dot{Z}_{p1} \dot{I}_1 \quad (4.9)$$

$$\dot{U}_2 - \dot{U}_n = \dot{E}_2 + \dot{Z}_{p2} \dot{I}_2 \quad (4.10)$$

$$\dot{U}_3 - \dot{U}_n = \dot{E}_3 + \dot{Z}_{p3} \dot{I}_3 \quad (4.11)$$

$$\dot{U}_4 - \dot{U}_n = \dot{E}_4 + \dot{Z}_{p4} \dot{I}_4 \quad (4.12)$$

$$\dot{U}_n = \dot{Z}_e (\dot{I}_1 + \dot{I}_2 + \dot{I}_3 + \dot{I}_4) \quad (4.13)$$

4.3.2 Ideal Voltage and Current Sources

Often, it can be useful to fix some potentials or to inject a current in one bus. These actions can be obtained with ideal voltage source cells and ideal current source cells respectively, and they can be represented with a simplified model, as it follows.

In both cases they are *Type-1* cells, so they have only n input ports.

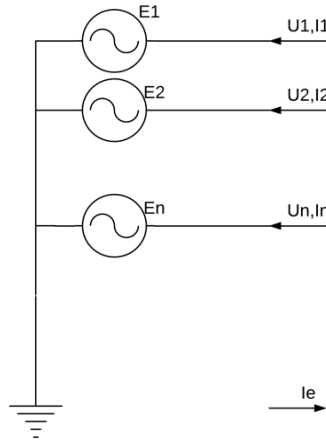


Figure 4-6 – Representation of an Ideal Voltage Source

The ideal voltage source corresponds to a feeder with Z_{p1}, Z_{p2}, \dots equal to zero and Z_e equal to zero too.

In a compact way, it can be written:

$$\{\dot{U}_{in}\} = \{\dot{E}\}, \tag{4.14}$$

where subscript U_{in} indicates the ports potential respect to the ground and E indicates the potential that is set by the user.

For the ideal current source, the following scheme shall apply.

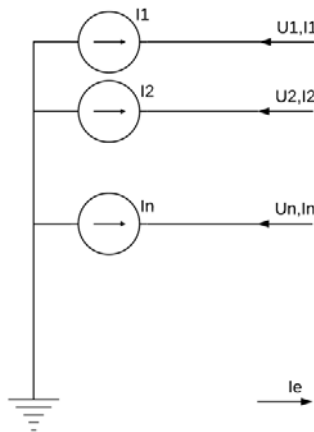


Figure 4-7 – Representation of an Ideal Current Source

In a compact way, it can be written:

$$-\{\dot{I}_{in}\} = \{\dot{J}\}, \quad (4.15)$$

where I_{in} indicates the current that flows through the cell.

4.3.3 Transverse Impedances

A transverse impedance can represent a load, an earthing system or a fault and it can be represented with a simplified model.

In this case, we consider a *Type-1* cell, so only n input ports.

A transverse impedance can be seen as a feeder, in which the voltage is set to zero in each phase. When it is used to represent a load, Z_e assumes the role of the grounding impedance of the neutral.

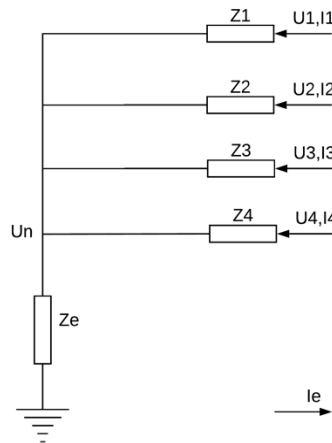


Figure 4-8 – Representation of a Transverse Impedance

In a compact way, it can be written:

$$\{\dot{U}_{in}\} - \{\dot{U}_n\} = [\dot{Z}_p] \{\dot{I}_{in}\} \quad (4.16)$$

4.3.4 Longitudinal Impedances

A longitudinal impedance can represent a lumped impedance, a switch and it can be represented using a simplified model, similar to the short line model.

It is a *Type-2* cell, so it has n input ports and n output ports.

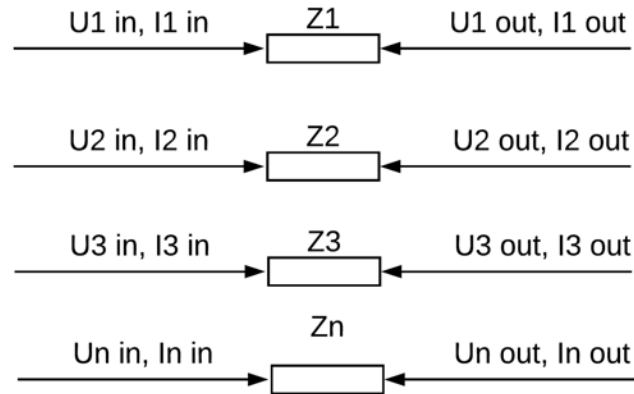


Figure 4-9 – Representation of a Longitudinal Impedance

In a compact way, it can be written as:

$$\{\dot{U}_{in}\} - [\dot{Z}]\{\dot{I}_{in}\} = \{\dot{U}_{out}\} \quad (4.17)$$

$$\{\dot{I}_{in}\} + \{\dot{I}_{out}\} = \{0\} \quad (4.18)$$

4.3.5 Lines and Cables

Lines and cables are intended as bundles (at least two) of horizontal (i.e. parallel to the ground) conductors; in order to represent this system of conductors by means of the so called “uniform transmission line model”, the following hypothesis are needed [8]:

- There are no variations along the axial direction of conductors and surrounding media characteristics
- The materials of conductors and surrounding media are linear
- The conductors spacing are much less than the wavelength relevant to the frequency under consideration
- The conductors spacing between conductors of aerial lines is at least one order of magnitude larger than the radius of the conductors so that proximity effects can be ignored
- The thin wire approximation is valid
- For ordinary calculations (meshed grids) it is possible to use lines with lumped parameters.

The π -network model is more suitable than the T-network model for long lines and cables modelling. The maximum distances to which the two models may be applied using a single π

or T cell, are the following (as it is known, the cable capacitances are 30-50 times greater than the capacitances of overhead insulated line):

- π -networks: overhead lines up to 250 km, underground or cable lines up to 100 km
- T-network: overhead lines up to 200 km, underground or cable lines up to 80 km

For longer distances, it is still possible to use the π -model, but modified impedances and admittances that modify propagation effects must be considered [11]. Alternatively, long lines and cables, can be represented with a chain of cells, each taking account of a segment of line.

The adopted model is the π -model, that corresponds with the one indicated in [8].

The line (or cable) matrix between two buses is obtained from the multi-conductor π -model, (the model applied to all conductors), and so are phases, screens, overhead earth wires to the neutral conductor.

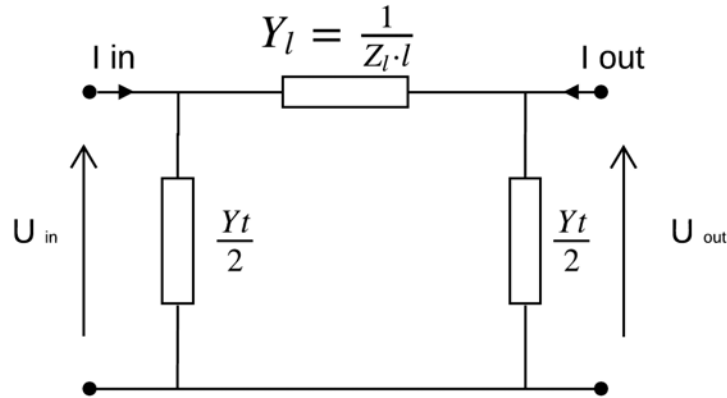


Figure 4-10 – Equivalent circuit for line or cable cell, referred to the link between two ports

With the used conventions for the current and potential signs, it is possible to write:

$$\begin{Bmatrix} \dot{I}_{in} \\ \dot{I}_{out} \end{Bmatrix} = \begin{bmatrix} \dot{Y}_l + \dot{Y}_t/2 & -\dot{Y}_l \\ -\dot{Y}_l & \dot{Y}_l + \dot{Y}_t/2 \end{bmatrix} \begin{Bmatrix} \dot{U}_{in} \\ \dot{U}_{out} \end{Bmatrix} \quad (4.19)$$

If the line (or cable) is composed by n conductors, the same relations is valid:

$$[\dot{Y}_l] = [\dot{Z}]^{-1} \quad (n \times n) \quad (4.20)$$

$$[\dot{Y}_t] = [G] + j\omega[P]^{-1} = [G] + [W]^{-1} \quad (n \times n) \quad (4.21)$$

The impedance matrix takes into account self and mutual inductances.

The matrix W take into account self and mutual coefficients of potential.

The matrix G take into account ground conductance of each conductor. In general, it is diagonal matrix and relevant only for overhead earth wires.

The entire system becomes:

$$\{I\} = [Y]\{U\} \quad (2n \times 2n) \tag{4.22}$$

Longitudinal and transverse impedances are computing with formulas which can be found in literature; in the follow commonly used formulas are described.

It was pointed out that this method takes into account the electromagnetic interaction between the conductors, which can be taken into consideration using the Carson theory for the earth returned currents [12], which is useful to determine the self and mutual admittance between each conductor, regardless of their nature (Overhead earth conductor, cable screens and armors, pipeline, etc.). In order to apply this method, it is assumed that the power line is horizontal, and that it follows a straight line in the same direction of the current. In addition, the lines, where mutual impedance are compute, are assumed to be parallel with each other.

Furthermore, soil is assumed to be homogeneous, the return current is assumed to flow in the same direction of the line and conductors are assumed to be homogeneous.

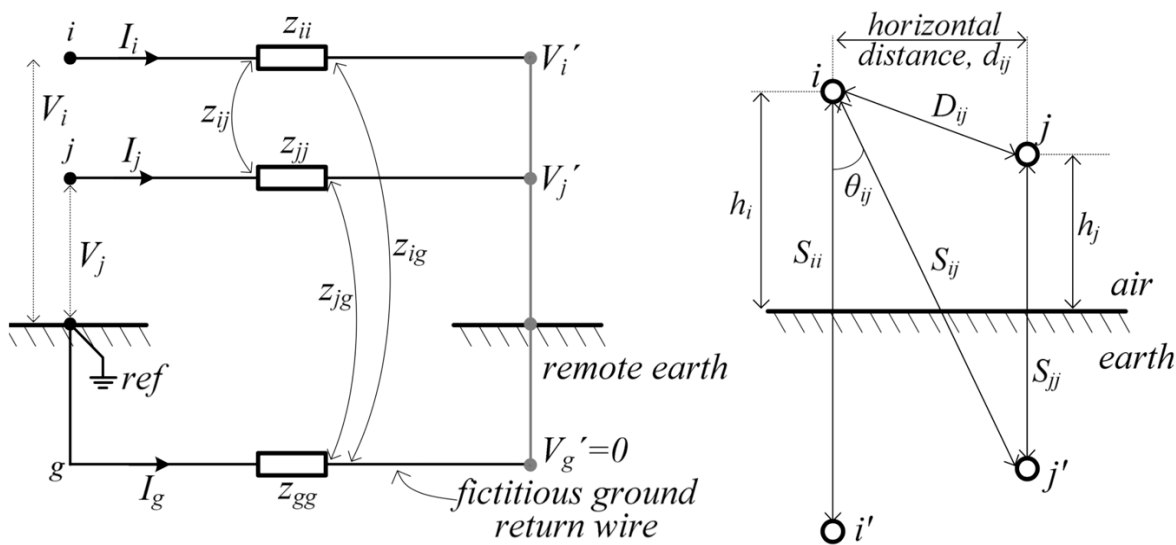


Figure 4-11 – Carson's two-conductor circuit with ground return (left); physical layout of two conductors with ground return (right) [13]

The self impedance per unit of length is given by:

$$Z_{ii} = \frac{U_{S_{ii}}}{I_i \cdot l} \quad \left[\frac{\Omega}{km} \right] \tag{4.23}$$

And it can be given by the following sum:

$$Z_{ii} = Z_{Oi} + Z_{Ei} \quad \left[\frac{\Omega}{km} \right] \quad (4.24)$$

Where:

- Z_{Oi} is the external surface impedance of a conductor with earth return. It is an inherent value of the conductor and can be compute with a measure, if it is a ferromagnetic material
- Z_{Ei} is the external part of the self impedance

These two contributions can be evaluated as:

$$Z_{Oi} = \frac{E_{Oi}}{I_i \cdot l} \quad \left[\frac{\Omega}{km} \right] \quad (4.25)$$

$$Z_{Ei} = \frac{E_{Ei}}{I_i \cdot l} \quad \left[\frac{\Omega}{km} \right] \quad (4.26)$$

The mutual impedance per unit of length between two conductors, both with earth return, is given by:

$$Z_{ij} = Z_{ji} = \frac{E_{ij}}{I_i} \quad \left[\frac{\Omega}{km} \right] \quad (4.27)$$

According to the Carson theory [14], the internal impedance Z_{Oi} can be calculated as:

$$Z_{Oi} = \left(R_i + j2 \cdot 10^{-4} \omega \frac{\mu_r}{4} \right) \quad \left[\frac{\Omega}{km} \right] \quad (4.28)$$

The external part of the self impedance Z_{Ei} is:

$$Z_{Ei} = j\omega \frac{\mu_0}{2\pi} \ln 2 \frac{h_i}{r} + 2(\Delta R_{ii} + j\Delta X_{ii}) \quad \left[\frac{\Omega}{km} \right] \quad (4.29)$$

The mutual impedance between the two conductors Z_{ij} , i and j is:

$$Z_{ij} = j\omega \frac{\mu_0}{2\pi} \ln 2 \frac{D_{ij}}{d_{ij}} + 2(\Delta R_{ij} + j\Delta X_{ij}) \quad \left[\frac{\Omega}{km} \right] \quad (4.30)$$

Where:

- D_{ij} is the distance between conductor i and conductor j image [m]
- d_{ij} is the distance between the two conductors [m]
- h_i is the height of the conductor from the soil [m]
- R_i is the DC conductor resistance [Ω/km]
- μ_0 is the vacuum permeability ($4\pi 10^{-4}$ [H/km])
- $\Delta R_{ii}, \Delta X_{ii}, \Delta R_{ij}, \Delta X_{ij}$, are correction terms that take in consideration the soil resistivity

These correction terms are obtained from indefinite integrals. An easier method, taking into account numerical series instead of indefinite integrals, can be used to have approximated expressions.

The following step is the study of simplified equations that can be easily implemented on a calculator: these formulas, called ‘‘Carson-Clem’’ equations, contain only the first term of the series for the ΔR and the first two terms for ΔX as it can be seen from [3]. Logarithmic terms are neglected.

The resulting formulas are as follows:

$$Z_{ii} = R_{ii} + R_{earth} + j4\pi f \cdot 10^{-4} \cdot \ln\left(\frac{2D_e}{d}\right) \quad \left[\frac{\Omega}{\text{km}} \right] \quad (4.31)$$

$$Z_{ij} = Z_{ji} = R_{earth} + j4\pi f \cdot 10^{-4} \cdot \ln\left(\frac{D_e}{d_{ij}}\right) \quad \left[\frac{\Omega}{\text{km}} \right] \quad (4.32)$$

Where:

- R_{ii} : is the conductor resistance per unit of length, [Ω/km]
- R_{earth} : is the equivalent earth conductor resistance, which depends on the frequency [Ω]
- d : is the phase conductor diameter [m]
- d_{ij} : is the mutual distance between conductors i and j [m]
- D_e : is the distance between the conductors and the centre of mass of the current flowing back to the earth [m]

The capacitive self and mutual susceptances matrix of the n -conductor system may be evaluated using the Maxwell potential coefficients:

$$P_{ii} = \frac{1}{2\pi\epsilon_0} \ln\left(\frac{2h_i}{r_i}\right) \quad \left[\frac{\text{km}}{F} \right] \quad (4.33)$$

$$P_{ij} = \frac{1}{2\pi\epsilon_0} \ln\left(\frac{D_{ij}}{d_{ij}}\right) \quad \left[\frac{\text{km}}{F} \right] \quad (4.34)$$

The capacitive matrix is then obtained by matrix inversion:

$$[C] = [P]^{-1} \quad (4.35)$$

The multi-conductor approach is advantageous when a double circuit line is considered, because it is possible to take in account mutual couplings between one conductor and each other.

4.3.6 Transformers Yy Yd Dy Dd

The following transformer models are referred to three-phase transformers with two windings. Usually the data available for a three-phase transformer are:

- Rated power S_n [VA]
- Rated frequency [Hz]
- Line to line input voltage V_{in} [V]
- Line to line output voltage V_{out} [V]
- Short circuit voltage v_{sc} [%]
- Short circuit losses p_{sc} [%], or P_{sc} [W]
- No load current i_0 [%]
- No load losses p_0 [%], or P_0 [W]
- In / out connections [star, delta]
- Vector Group [0 – 11]

The rated frequency has to be set to keep in mind the value of frequency of v_{sc} , p_{sc} , i_0 and p_0 . These parameters depend on the frequency, but not in a linear way. At least, it is possible to get these values in a limited range (from 50 Hz to 60 Hz, and vice versa).

Star windings are connected to the phase to neutral voltage and they are used in the transmission lines, where the voltage level is high, and it is useful to limit for insulation distances between the different conductors.

The power transformers are usually Yy type.

Delta windings are connected to the line to line voltage. The neutral conductor isn't accessible, but in case of dissymmetric load, delta connection is necessary to balance the current at the primary side. The most common distribution transformers are Dyn1 (used mainly in the American area) and Dyn11 (used primary in the European area).

Autotransformers are cheaper than the common transformers (Design power is smaller), but the insulation between the two windings is lost.

Autotransformers are always Yy type.

The short circuit and the no load data are obtained from laboratory tests. The results are different, depending on the frequency. For example, oil transformer tests are referred to 75°C, while air cooler transformer tests are referred to 100°C.

Usually, the tests consist on:

- No load test, that permits to obtain i_0 and p_0 . The transformer is without loads and it is fed by the rated value of the voltage and in the transformer flows the current involved in the iron magnetization.
- Short circuit test, that permits to obtain v_{sc} and p_{sc} . The secondary winding is in short circuit condition and the transformer is fed by a percentage of the voltage that circulates the rated current.

If required, other data related to the zero-sequence impedance can be obtained, but they are not involved in the phase transformer model. With the data available in a commercial transformer datasheet, any type of load condition (balance or unbalance load) or fault, can be treated [15]. The no load voltage ratio is defined as follows:

$$k = \frac{V_{in}}{V_{out}} \quad (4.36)$$

The voltage ratio is always referred to the module of the line to line voltage, hence it can be equal to the turns ratio, only if the two windings are connected in the same way (both star connection or both delta connection).

The transformer group indicates the voltages and currents phase shifting between side in and side out.

$$\varphi = gr \cdot 30 \frac{\pi}{180} = gr \frac{\pi}{6} \text{ [rad]} \quad (4.37)$$

For example, for transformers which belong to the group 0, it is true that $\varphi = 0 \text{ [deg]} = 0 \text{ [rad]}$ and for transformers which belong to the group 11, it is true that $\varphi = 11 \cdot 30 = 330 \text{ [deg]} = 11 \pi/6 \text{ [rad]}$.

Rated currents for both sides are equal to:

$$I_{in} = \frac{S_n}{\sqrt{3}V_{in}} \text{ [A]} \quad (4.38)$$

$$I_{out} = \frac{S_n}{\sqrt{3}V_{out}} \text{ [A]} \quad (4.39)$$

The short circuit impedance has a complex value, in which the real part represents the copper losses and the imaginary part takes into account the magnetic field that is not linked between the two windings. Hence, the imaginary part is referred to the leakage flux.

The short circuit voltage allows to get the absolute value of the short circuit impedance.

Taking into account this impedance, it follows:

$$|\dot{Z}_{scin}| = \frac{v_{sc}}{100} \frac{\frac{V_{in}}{\sqrt{3}}}{I_{in}} = \frac{v_{sc}}{100} \frac{\frac{V_{in}}{\sqrt{3}}}{\frac{S_n}{\sqrt{3}V_{in}}} = \frac{v_{sc}}{100} \frac{V_{in}^2}{S_n} \quad [\Omega] \quad (4.40)$$

The copper losses allow to get the resistive part of the short circuit impedance. If they aren't known, it is possible to put them equal to zero, with a negligible error. Instead, if they are known, this formula is valid:

$$R_{scin} = \frac{p_{sc}}{100} \frac{S_n}{3(I_{in})^2} = \frac{p_{sc}}{100} \frac{S_n}{3\left(\frac{S_n}{\sqrt{3}V_{in}}\right)^2} = \frac{p_{sc}}{100} \frac{V_{in}^2}{S_n} \quad [\Omega] \quad (4.41)$$

Then, it can obtain:

$$X_{scin} = \sqrt{|\dot{Z}_{scin}|^2 - R_{scin}^2} \quad [\Omega] \quad (4.42)$$

With a positive sign, taking into account the inductive character of the transformer reactance. So, the complex short circuit impedance is obtained below:

$$\dot{Z}_{scin} = R_{scin} + jX_{scin} \quad [\Omega] \quad (4.43)$$

Or, in a cleaner form, it can be written as:

$$\dot{Z}_{in} = R_{in} + jX_{in} \quad [\Omega] \quad (4.44)$$

The no load current permits to pull out the module of the short circuit impedance. Taking it into account, at the side in, it follows:

$$|\dot{Z}_{0in}| = \frac{\frac{V_{in}}{\sqrt{3}}}{I_0} = \frac{\frac{V_{in}}{\sqrt{3}}}{\frac{i_0 S_n}{100\sqrt{3}V_{in}}} = \frac{100}{i_0} \frac{V_{in}^2}{S_n} \quad [\Omega] \quad (4.45)$$

The no load impedance can be represented like a parallel between a resistance and an inductance.

The no load losses allow to get the no load resistance and they are, in general, negligible. Hence, the resistive part is big and often, the no load impedance is purely reactive. If the value of the no load losses is unknown, a null value can be taken, and a purely reactive impedance is considered.

Bearing in mind this, at the side in there is:

$$R_{0in} = \frac{\left(\frac{V_{in}}{\sqrt{3}}\right)^2}{\frac{P_0}{3}} = \frac{V_{in}^2}{P_0} = \frac{100 V_{in}^2}{p_0 S_n} \quad [\Omega] \quad (4.46)$$

Hence:

$$X_{0in} = \frac{1}{\sqrt{\frac{1}{|\dot{Z}_{0in}|^2} - \frac{1}{R_{0in}^2}}} = \frac{1}{\sqrt{\frac{1}{\left(\frac{100V_{in}^2}{i_0 S_n}\right)^2} - \frac{1}{\left(\frac{100V_{in}^2}{p_0 S_n}\right)^2}}} = \frac{100 V_{in}^2}{\sqrt{i_0^2 - p_0^2} S_n} \quad [\Omega] \quad (4.47)$$

$$\dot{Z}_{0in} = \frac{1}{\frac{1}{R_{0in}} + \frac{1}{jX_{0in}}} \quad [\Omega] \quad (4.48)$$

Strictly speaking, the no load impedance should be connected after the Z_{in} ; although, by considering that $Z_o \gg Z_{sc}$ [16], Z_o is put before of Z_{in} , with a small error and a big simplification. In this way, the “simplified equivalent circuit” is obtained.

This simplified model has some advantages:

- The short circuit impedance can be reported all together at one side of the transformer
- Both no load impedance and short circuit impedance can be obtained doing a no load test and a short circuit test respectively.

The single-phase equivalent circuit of the transformer is represented in the follow and, in literature, it is known as “transformer T-model as a two-port network”.

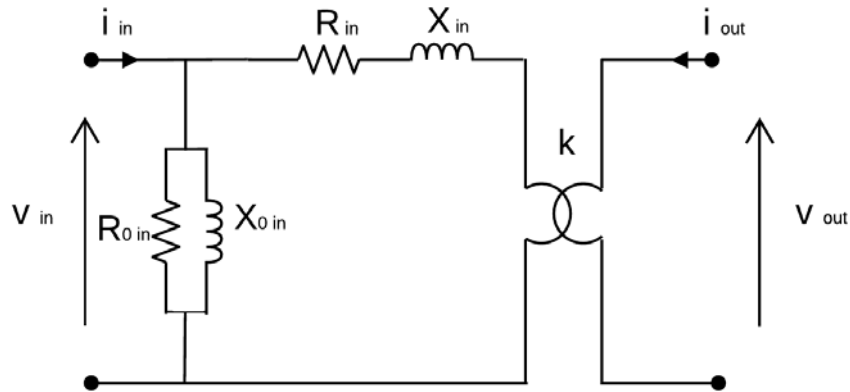


Figure 4-12 – Simplified equivalent model of a single-phase transformer

With the well-known voltages and current conventions, the equation and the related primitive admittance matrix for the simplified model of two windings single-phase transformer is as follow:

$$\begin{Bmatrix} \dot{i}_{in} \\ \dot{i}_{out} \end{Bmatrix} = \frac{1}{\dot{Z}_{in}} \begin{bmatrix} 1 + \frac{\dot{Z}_{in}}{\dot{Z}_{0in}} & -k \\ -k & k^2 \end{bmatrix} \begin{Bmatrix} \dot{v}_{in} \\ \dot{v}_{out} \end{Bmatrix} \quad (4.49)$$

Where:

- Z_{in} is the short circuit impedance referred to the side in.
- Z_{0in} is the no load impedance referred to the side in.
- k is the turns ratio, for a single-phase transformer.

$$k = \frac{V_{in}}{V_{out}} = \frac{n_{in}}{n_{out}} \quad (4.50)$$

A three-phase transformer with the neutral conductor can be represented with a four ports dipole with 16 unknowns. In case of windings without neutral conductor, the port related to the neutral will be disconnected. As usual, half equations come from the topology, half from the connections.

The first step to build the three-phase model consist of the construction of the primitive matrix.

In general, with the exception of the three single-phase transformers case, all the windings of the transformer are mutually coupled and the primitive matrix is filled [17].

Nevertheless, with acceptable approximation, mutual couples between windings that belong to different phases can be neglected [13]. Hence, a three-phase transformer can be considered

as a composition of three single-phase transformers, magnetically decoupled but electrically linked together. This approach has the advantage that it need data always available, like short circuit voltage and no load current.

The primitive admittance matrix with both sides neutral conductor could be written as:

$$[\dot{Y}_p] = \begin{bmatrix} \dot{a} & \dot{b} & 0 & 0 & 0 & 0 & 0 & 0 \\ \dot{c} & \dot{d} & 0 & 0 & 0 & 0 & 0 & 0 \\ 0 & 0 & \dot{a} & \dot{b} & 0 & 0 & 0 & 0 \\ 0 & 0 & \dot{c} & \dot{d} & 0 & 0 & 0 & 0 \\ 0 & 0 & 0 & 0 & \dot{a} & \dot{b} & 0 & 0 \\ 0 & 0 & 0 & 0 & \dot{c} & \dot{d} & 0 & 0 \\ 0 & 0 & 0 & 0 & 0 & 0 & \dot{e} & 0 \\ 0 & 0 & 0 & 0 & 0 & 0 & 0 & \dot{f} \end{bmatrix} \quad (4.51)$$

with:

$$\dot{a} = \frac{1}{\dot{Z}_{in}} + \frac{1}{\dot{Z}_{0in}} \quad \dot{b} = \dot{c} = -\frac{k}{\dot{Z}_{in}} \quad \dot{d} = \frac{k^2}{\dot{Z}_{in}} \quad \dot{e} = \frac{1}{\dot{Z}_{nin}} \quad \dot{f} = \frac{1}{\dot{Z}_{nout}} \quad (4.52)$$

In the previous matrix the submatrix related to the three single-phase transformers, the lack of mutual coupling between windings that belong to different phases and the presence of two additional impedances on the neutral conductors can be noted.

It should be noted that the matrix is symmetrical, and in the matrix construction, there are some impedances at the denominator that must be different from zero, to avoid divisions by zero. In particular, Z_{in} , $Z_{n,in}$ e $Z_{n,out}$ must be different from zero.

The short circuit impedances and the no load impedances can be calculated starting from the rated transformer initial data, usually available.

The voltage ratio, as reported in (4.50) is given by the ratio between the line-to-line voltages, with the side in voltage at the numerator and the side out voltage at the denominator.

Starting from [18] and sorting through the side in windings in the first part of the matrix, and then the side out windings, the link between currents and potentials of windings can be written as:

$$\begin{Bmatrix} \dot{i}_{1in} \\ \dot{i}_{2in} \\ \dot{i}_{3in} \\ \dot{i}_{4in} \\ \dot{i}_{1out} \\ \dot{i}_{2out} \\ \dot{i}_{3out} \\ \dot{i}_{4out} \end{Bmatrix} = \begin{bmatrix} \dot{a} & 0 & 0 & 0 & \dot{b} & 0 & 0 & 0 \\ 0 & \dot{a} & 0 & 0 & 0 & \dot{b} & 0 & 0 \\ 0 & 0 & \dot{a} & 0 & 0 & 0 & \dot{b} & 0 \\ 0 & 0 & 0 & \dot{e} & 0 & 0 & 0 & 0 \\ \dot{c} & 0 & 0 & 0 & \dot{d} & 0 & 0 & 0 \\ 0 & \dot{c} & 0 & 0 & 0 & \dot{d} & 0 & 0 \\ 0 & 0 & \dot{c} & 0 & 0 & 0 & \dot{d} & 0 \\ 0 & 0 & 0 & 0 & 0 & 0 & 0 & \dot{f} \end{bmatrix} \begin{Bmatrix} \dot{v}_{1in} \\ \dot{v}_{2in} \\ \dot{v}_{3in} \\ \dot{v}_{4in} \\ \dot{v}_{1out} \\ \dot{v}_{2out} \\ \dot{v}_{3out} \\ \dot{v}_{4out} \end{Bmatrix} \quad (4.53)$$

Taking into account windings links, and considering [19], the primitive admittance matrix can be generalized as follow:

$$\left[\dot{\mathbf{Y}}_p \right] = \begin{bmatrix} \dot{a}k_{in}^2 & 0 & 0 & 0 & \dot{b}k_{in}/k_{out} & 0 & 0 & 0 \\ 0 & \dot{a}k_{in}^2 & 0 & 0 & 0 & \dot{b}k_{in}/k_{out} & 0 & 0 \\ 0 & 0 & \dot{a}k_{in}^2 & 0 & 0 & 0 & \dot{b}k_{in}/k_{out} & 0 \\ 0 & 0 & 0 & \dot{e} & 0 & 0 & 0 & 0 \\ \dot{c}k_{in}/k_{out} & 0 & 0 & 0 & \dot{d}/k_{out}^2 & 0 & 0 & 0 \\ 0 & \dot{c}k_{in}/k_{out} & 0 & 0 & 0 & \dot{d}/k_{out}^2 & 0 & 0 \\ 0 & 0 & \dot{c}k_{in}/k_{out} & 0 & 0 & 0 & \dot{d}/k_{out}^2 & 0 \\ 0 & 0 & 0 & 0 & 0 & 0 & 0 & \dot{f} \end{bmatrix} \quad (4.54)$$

The values of the additional coefficients for star connections are:

$$k_{in} = 1, \text{ for star "side in"}$$

$$k_{out} = 1, \text{ for star "side out"}$$

The values of the additional coefficients for delta connections are:

$$k_{in} = \frac{1}{\sqrt{3}}, \text{ for delta "side in"}$$

$$k_{out} = \sqrt{3}, \text{ for delta "side out"}$$

The primitive matrix relates current and potentials on the windings, regardless from their connections.

A compact writing can be used:

$$\{\dot{i}\} = [\dot{\mathbf{Y}}_p] \{\dot{v}\} \quad (4.55)$$

The primitive matrix is invertible, provided that the short circuit impedance is different from zero, the no load impedance is not an infinite number and the neutral impedances must be different from zero.

As previously mentioned, primitive matrix is not related to the windings connections, and it relates the side in and side out currents and voltages on each winding. Currents and potentials at ports, can be obtained with the connection matrix:

$$\{\dot{v}\} = [C]\{\dot{U}\} \quad (4.56)$$

Matrix connections are different from each transformer connection and they define the transformer group. It is possible to verify that:

$$\{I\} = [C]^t \{i\} \quad (4.57)$$

hence, the final relation for the transformer will be:

$$\{I\} = [C]^t \{i\} = [C]^t [\dot{Y}_p] \{\dot{v}\} = [C]^t [\dot{Y}_p] [C] \{\dot{U}\} = [\dot{Y}_t] \{\dot{U}\} \quad (4.58)$$

The nodal admittance matrix of the transformer, is equal to:

$$[\dot{Y}_t] = [C]^t [\dot{Y}_p] [C] \quad (4.59)$$

4.3.7 Transformers Yz Dz

Zig Zag transformers are used to provide a common reference for the neutral point in lines without the neutral conductor (in the Medium Voltage level system it is useful to connect the Petersen coil) or to reduce the amount of voltage unbalance on the primary side with an unbalanced load at the secondary side [18].

Zig Zag transformer need to be treated in a different way, because it has to be modelled as a three windings transformer.

Single phase equivalent model of a transformer with Zig Zag side out, must be modelled starting from a three windings transformer, as in the following figure:

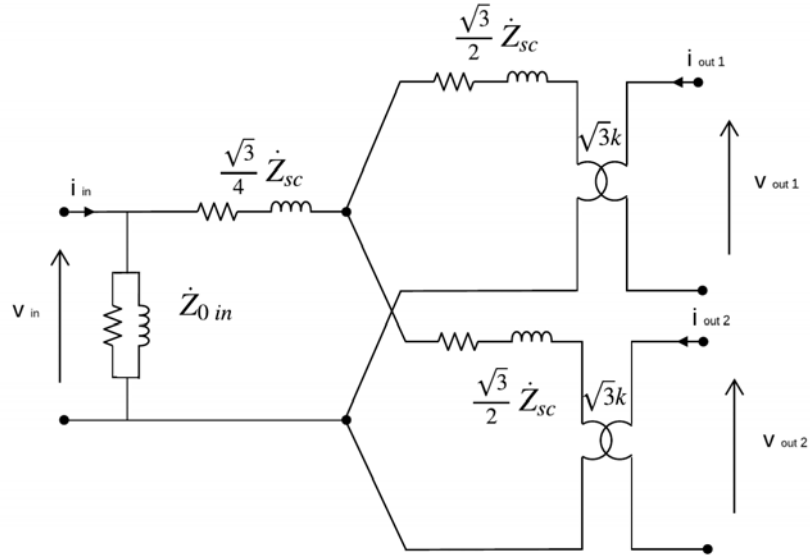


Figure 4-13 – Simplified equivalent model of a Zig Zag three-phase transformer

From the previous figure, it can be obtain the primitive admittance matrix for the simplified three windings single phase transformer model:

$$\begin{Bmatrix} \dot{i}_{in} \\ \dot{i}_{out1} \\ \dot{i}_{out2} \end{Bmatrix} = \frac{2}{\sqrt{3}\dot{Z}_{in}} \begin{bmatrix} \left(1 + \frac{\sqrt{3}\dot{Z}_{in}}{2\dot{Z}_{0in}}\right)kk_{in}^2 & -\frac{\sqrt{3}}{2}kk_{in} & -\frac{\sqrt{3}}{2}kk_{in} \\ -\frac{\sqrt{3}}{2}kk_{in} & \frac{9}{4}k^2 & -\frac{3}{4}k^2 \\ -\frac{\sqrt{3}}{2}kk_{in} & -\frac{3}{4}k^2 & \frac{9}{4}k^2 \end{bmatrix} \begin{Bmatrix} \dot{v}_{in} \\ \dot{v}_{out1} \\ \dot{v}_{out2} \end{Bmatrix} \quad (4.60)$$

The equivalent admittance primitive matrix of the three phase transformer with neutral, can be obtain composing three single phase transformers; a 12·12 matrix is built.

Hence, introducing the connection matrices, the transformer matrix can be obtained:

$$[\dot{Y}_t] = [C]' [\dot{Y}_p] [C] \quad (4.61)$$

Then, this matrix can be reduced to an 8·8 matrix, using the double inversion technique, explained in [18].

Chapter 5

NETS RESULTS VALIDATION

In this chapter, shall be presented the validation report between NETS and OpenDSS, testing all the transversal impedance elements, first individually and, in the last part of the chapter they are combined all together to form a simple network.

5.1 Overhead Lines

5.1.1 Overhead line, frequency domain – NETS vs OpenDSS

In the following, a calculation taking into account a short overhead line is shown in order to verify the agreement of the results obtained using NETS and OpenDSS (EPRI) in the frequency domain.

The case study is very simple and includes an ideal generator (symmetrical and balanced), a short overhead line without overhead earth wire and a resistive load.

The general layout is represented in the following figure.

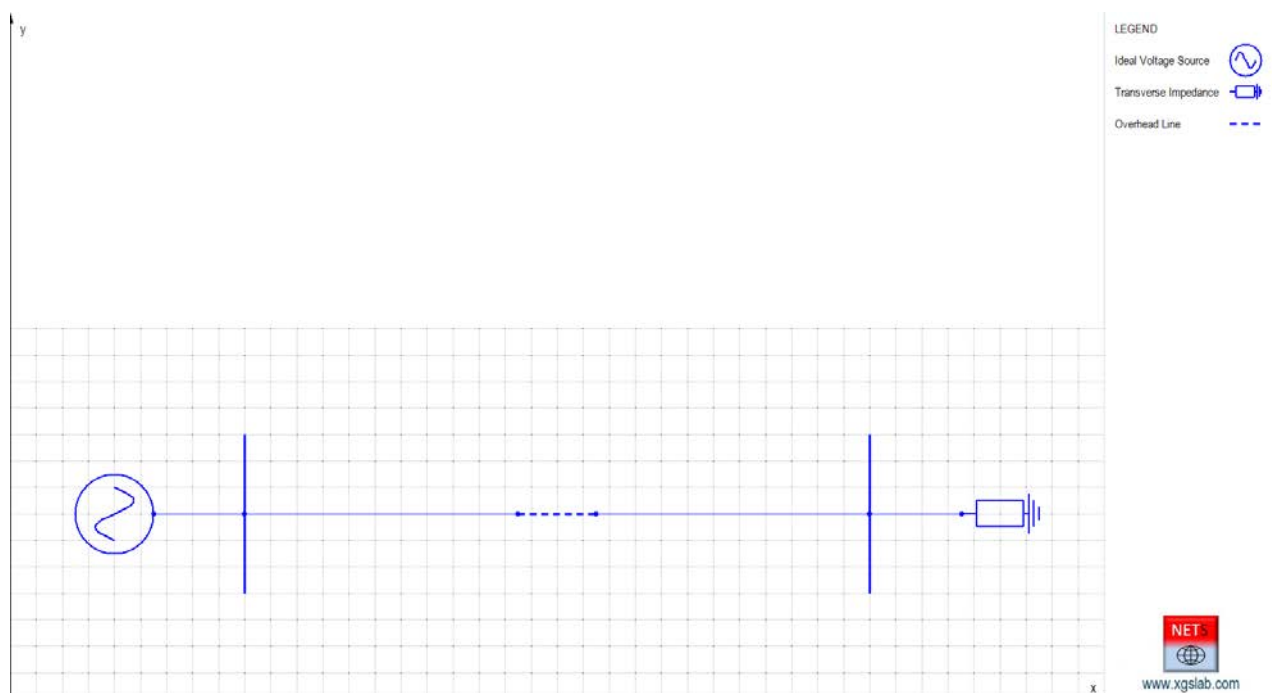


Figure 5-1: Single Line Diagram of an Ideal Voltage Source + Overhead Line + Load

In the following the main input data.

Ideal Voltage generator

Main input data:

- Phases number: 3 (symmetrical and balanced)
- Rated phase voltage: 100 [V]
- Frequency = DC, 20. 50. 100. 200. 500 [Hz], 1. 2. 5. 10. 20. 50. 100 [kHz]

In both cases, calculations cannot be provided exactly at DC condition.

If DC conditions are set, NETS automatically assumes a frequency 1 [mHz].

OpenDSS accepts a minimum frequency 1 [mHz].

Overhead Line

Main input data:

- Phases numbers: 3
- Low frequency soil resistivity = 100 [Ωm]
- High frequency soil relative permittivity = 6
- Line length = 1000 [m] (single span)
- Phases conductors layout: A (left), B (center), C (right)
- Phases conductors height = 10 [m]
- Phase conductor horizontal distance = 5 [m]
- Phase conductors: ACSR with external diameter = 31.5 [mm], cross section of steel and aluminium 65.81 and 519.5 [mm^2] respectively.

The resistance of phase conductors has to be referred to the operative temperature 75 [$^{\circ}\text{C}$] using the following formula:

$$R = R_{20} [1 + \alpha (t - 20)] [\Omega/\text{km}] \quad (5.1)$$

where:

- R_{20} [Ω/km] = resistance at 20 [$^{\circ}\text{C}$]
- α [$1/^{\circ}\text{C}$] = temperature coefficient of resistivity
- t [$^{\circ}\text{C}$] = reference temperature

Using the temperature coefficient of aluminum (0.0043 [$1/^{\circ}\text{C}$]), the phase conductor resistance is 0.6879 [Ω/km] at 75 [$^{\circ}\text{C}$].

The reference temperature for overhead earth wire can be 20 [$^{\circ}\text{C}$].

Load

Main input data:

- Phases numbers: 3
- $Z = 1 + j0 \text{ } [\Omega]$ (for all phases)
- $Z_e = 1 \text{ } [M\Omega]$

The currents on phase A calculated with NETS and OpenDSS are displayed, in the following table.

Table 5-1: Differences between overhead line phase A current at difference frequencies, NETS vs OpenDSS

f (Hz)	NETS Phase A		OpenDSS Phase A		Difference %
	I [A]	\angle [deg]	I [A]	\angle [deg]	
0.001	93.64	0.000	93.64	0.000	0.00
20	91.50	-8.220	91.46	-8.400	-0.04
50	85.64	-19.58	85.47	-19.90	-0.20
100	72.56	-34.80	72.13	-35.30	-0.59
200	50.58	-52.72	49.99	-53.20	-1.17
500	24.05	-70.42	23.60	-70.80	-1.87
1000	12.52	-77.56	12.22	-77.80	-2.40
2000	6.370	-81.27	6.180	-81.50	-2.98
5000	2.577	-83.49	2.473	-83.70	-4.04
10000	1.295	-84.18	1.217	-84.40	-6.02
20000	0.6509	-84.47	0.5655	-84.60	-13.12
50000	12.52	-84.58	0.1046	-84.00	-60.17
100000	0.1326	-84.58	0.1653	+94.20	24.66

Results for phases B and C are similar, the only differences are related to the asymmetrical conditions of phase conductors position. The comparison can be limited to phase A.

The differences in the table are related to the currents magnitude.

The differences in results up to 100 [Hz] are less than 1 % and then negligible.

The differences in results in the range 100 – 1000 [Hz] are less than 2.5 % and then acceptable. These differences are related mainly to the formulas used for the internal component of the self impedance and in particular in the reactance. It seems OpenDSS neglects the skin effects. Neglecting the skin effects (using a simplified formula) in NETS allows the same results of OpenDSS.

Difference in results at higher frequencies increase gradually.

The agreement between results provided by NETS and OpenDSS is good with differences less than 5% up to 5 [kHz].

It is evident that OpenDSS cannot be used with frequency 10 [kHz] and over.

Anyway, conservatively, 10 [kHz] can be assumed also as application limits for NETS (for overhead lines models).

The following figures represents the comparison between results in graphical way.

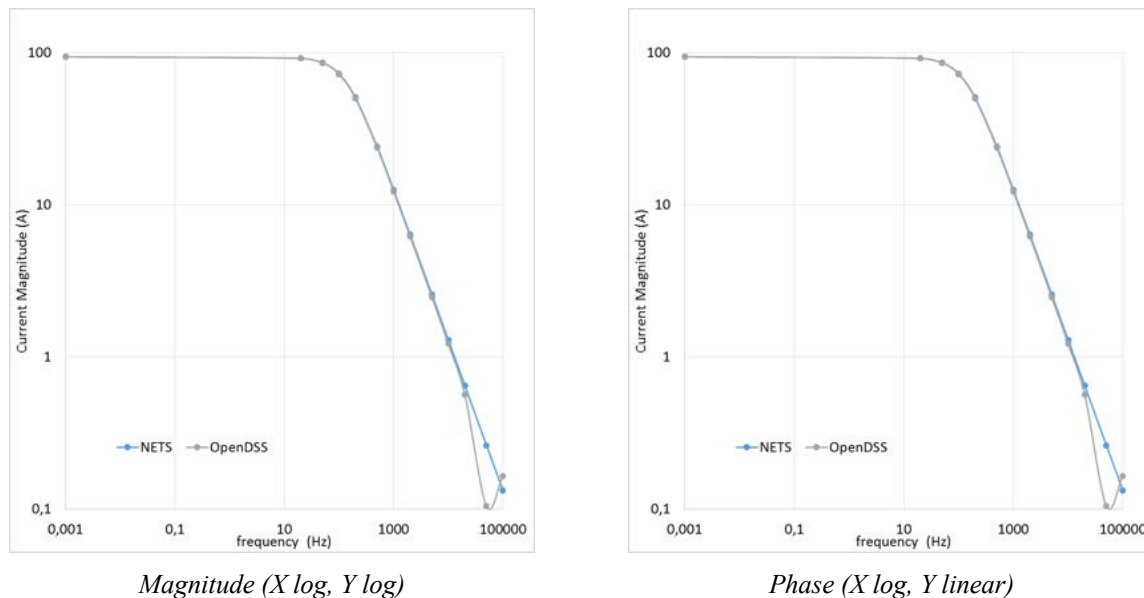


Figure 5-2: Graphical differences between overhead line phase A current at difference frequencies, NETS vs OpenDSS (NETS = azure, OpenDSS = grey)

5.1.2 Overhead line, various conditions – NETS vs OpenDSS

In the following, a calculation taking into account a medium length overhead line is shown in order to verify the agreement of the results obtained using NETS and OpenDSS (EPRI) in various conditions.

The case study is quite simple and includes a real three-phase feeder and an overhead line 80 km long, with two overhead earth wires.

The general layout is represented in the Figure 5-1.

In the following the main input data.

Feeder

Main input data:

- Phases number: 3 (symmetrical and balanced)
- Rated line voltage: 400 [kV]
- Short circuit power: 40000 [MVA]
- $X/R = 25$
- $Z_e = 0.1 [\Omega]$

The equivalent internal impedance of the feeder can be calculated with the following formulas:

$$Z = \frac{V^2}{S_{sc}} (\cos \varphi + j \sin \varphi) = \frac{V}{\sqrt{3} \cdot I_{sc}} (\cos \varphi + j \sin \varphi) = \frac{3 \cdot E}{3 \cdot I_{sc}} (\cos \varphi + j \sin \varphi) \quad (5.2)$$

$$\cos \varphi = \frac{1}{\sqrt{1 + (X/R)^2}} \quad (5.3)$$

where:

- V [V] = rated line voltage
- E [V] = rated phase voltage
- S_{sc} [VA] = short circuit power
- I_{sc} [A] = three phase short circuit current
- $\cos \varphi$ = short circuit power factor
- X/R = ratio between reactance and resistance.

It follows:

- $Z = 4.000 (0.03997 + j 0.9992) = 0.1599 + j 3.997 = \text{about } j4.000 \text{ } [\Omega]$ (for all phases)

Overhead Line

The Figure 5-3 represents the tower lattice layout and the distances between phase conductors and overhead earth wires.

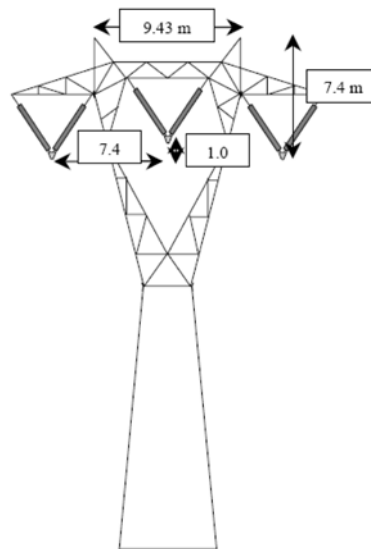


Figure 5-3: Tower lattice layout

Main input data:

- Phases numbers: 3
- Rated line voltage = 400 [kV]
- Frequency = 50 [Hz]
- Low frequency soil resistivity = 100 [Ωm]
- High frequency soil relative permittivity = 6
- Line length = 80 [km]
- Span length = 400 [m] (200 spans)
- Phases conductors layout: A (left), B (center), C (right)
- Maximum and minimum distance to the soil surface phase A and C: 24 and 11 [m]
- Maximum and minimum distance to the soil surface phase B: 25 and 12 [m]
- Maximum and minimum distance to the soil surface overhead earth wires: 31.4 and 23.4 [m]
- Phase conductors: bundle diameter = 462 [mm] - n. 3 ACSR sub conductors with external diameter = 31.5 [mm] (the steel is inside and the aluminium is outside, the cross section of steel and aluminium are respectively 65.80 and 519.5 and [mm^2]), resistance = 0.05564 [Ω/km] at 20 [$^{\circ}\text{C}$]
- Overhead wires: steel and aluminium conductors with external diameter = 11.5 [mm], cross section 80.66 [mm^2]. resistance = 1.062 [Ω/km] at 20 [$^{\circ}\text{C}$]
- Resistance to earth of each single tower: 10 [Ω]
- Resistance to earth of each terminal substation: 1 [Ω]

The resistance of phase sub conductors has to be referred to the operative temperature 75 [$^{\circ}\text{C}$] using the formula (5.1).

As anticipated, the line includes two overhead earth wires.

The limit length for lines with overhead earth wires is:

$$L \cong 10S \sqrt{\frac{R_t}{R_s}} \quad (5.4)$$

where:

- S [m] = average span length
- R_t [Ω] = average resistance to earth of each single tower
- R_s [Ω] = average resistance of a span of overhead earth wire

Using S = 400 [m], R_t = 20 [Ω] and R_s = $0.4 \cdot 1.062/2$ = 0.2124 [Ω] it follows L = about 27.5 [km].

The whole line has been divided in 4 sections of 20 [km].

Each section can be represented using a cell type “Line” with 5 ports, A, B and C for phase conductors and D, D for the overhead earth wires and will be divided in 50 equal spans.

The overhead earth wires will be connected to earth at each span. Taking into account the two overhead earth wires, the resistance to earth of each single tower for each overhead earth wires must be set doubled and then 20 [Ω].

The option “OHEW Link” has been set and then the two overhead earth wires are assumed connected at each tower (and for this reason practically equipotential at ends but also along the line).

The other line data are as above.

The average height above ground of phase conductors and overhead earth wires can be calculated using the formula:

$$h = h_{midspan} + \frac{sag}{3} \quad (5.5)$$

where:

- $h_{midspan}$ = distance to the soil surface of the conductor at the span center [m]
- sag = sag of the conductor at the span center [m]

If follows:

- Phases A and C: $h = 11 + (24 - 11) / 3 = 15.33$ [m]
- Phase B: $h = 16.33$ [m]
- Overhead earth wires: $h = 26.07$ [m].

In the following the main results in various conditions.

5.1.2.1 Steady state condition

The steady state condition is represented by the following three-phase balanced load (with insulated neutral):

- $S = 400$ [MVA] referred to the rated voltage
- $\cos \varphi = 0.8$

The steady state condition can be represented using a transverse impedance with:

- $Z = 400.0 (0.8 + j 0.6) = 320 + j 240$ [Ω] (for all phases)
- $Z_e = 1$ [M Ω]

The overhead earth wires are connected together at the line ends and then to earth using a transverse impedance with:

- $Z = 0.01 [\Omega]$
- $Z_e = 1 [\Omega]$ (resistance to earth of terminal substations)

In the following, a resistance $0.01 [\Omega]$ represents a short circuit condition.

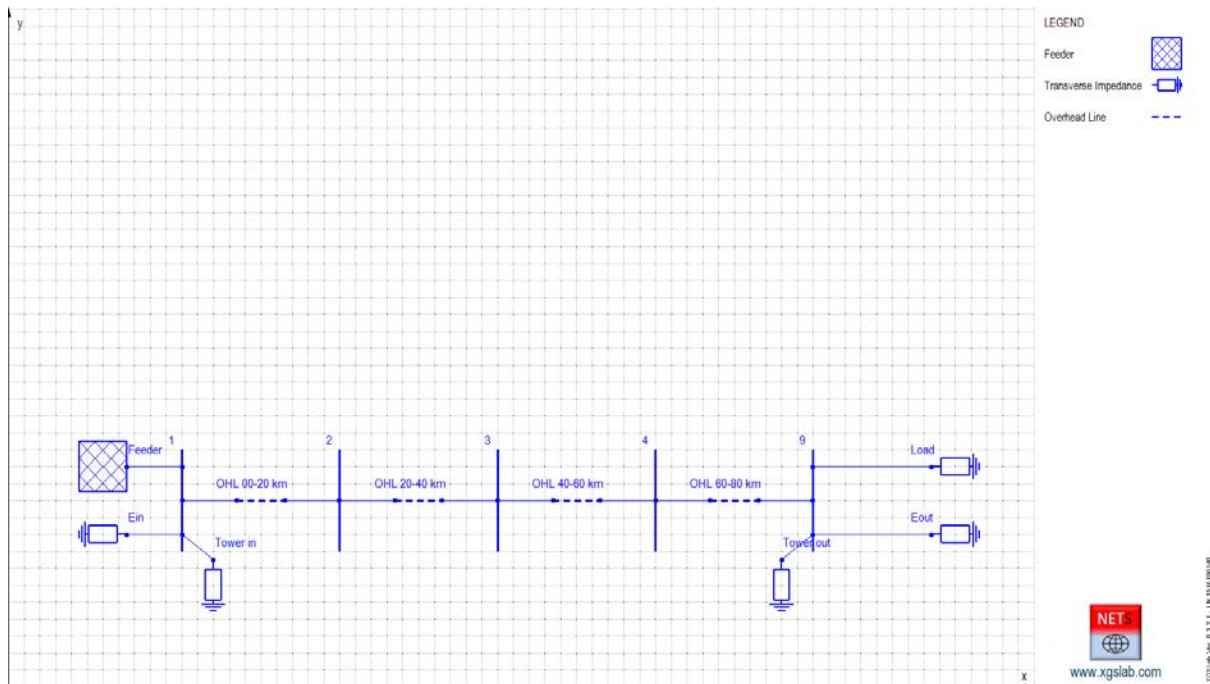


Figure 5-4: Single Line Diagram of an Overhead Line with a Load at the End

The phase voltage and currents calculated with NETS and OpenDSS are displayed, in the following table.

Table 5-2: Current and voltage variations along the overhead line in steady state condition, NETS vs OpenDSS

Cell and Phase	NETS				OpenDSS			
	I [A]	∠ [deg]	U [V]	∠ [deg]	I [A]	∠ [deg]	U [V]	∠ [deg]
Line_in A	505.4	-33.87	229753	-0.407	502.9	-33.50	229770	-0.400
Line_in B	513.1	-152.6	229772	-120.4	511.0	-152.1	229790	-120.4
Line_in C	521.8	86.63	229729	119.6	521.0	87.10	229740	119.6
OHEW_in D	8.609	161.2	6.200	-108.7	8.493	160.80	6.149	-109.4
OHEW_in D	10.75	18.08	=	=	10.81	18.80	=	=
Line_out A	552.0	140.4	220757	-2.589	552.2	140.40	220860	-2.6
Line_out B	557.0	20.58	222361	-122.6	557.3	20.60	222460	-122.6
Line_out C	556.0	-99.95	222873	116.9	556.2	-99.90	222970	116.9
OHEW_out D	9.722	-22.61	6.018	75.27	9.752	-23.50	5.944	75.2
OHEW_out D	10.82	-167.6	=	=	10.90	-167.1	=	=

It is interesting to note currents grow along line and load currents are higher than corresponding feeder currents.

This is due to the line capacitance.

It is also interesting to note the large difference in phases of currents along the two overhead earth wires. This difference can be explained taking into account currents in the overhead earth wires flow across the earth but also circulate on the overhead earth wires loop.

The agreement between results provided by NETS and OpenDSS is anyway excellent.

In the following, the magnitude of currents and potentials distribution along the overhead earth wires calculated with NETS and OpenDSS.

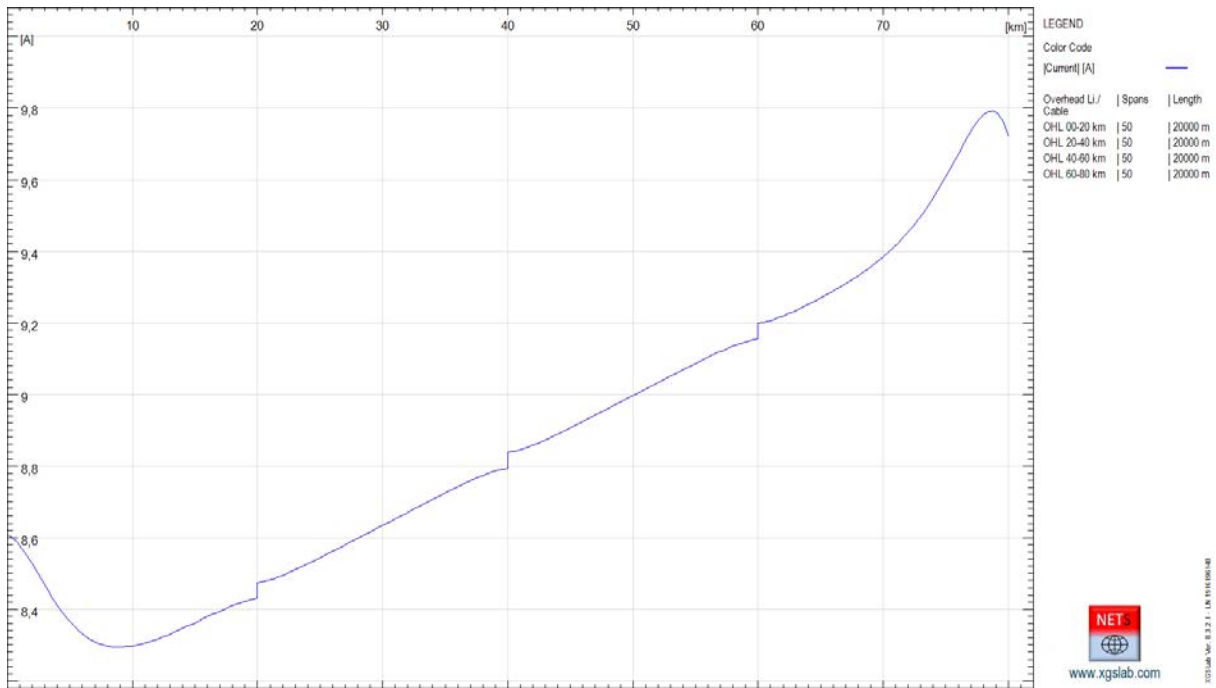


Figure 5-5: Magnitude Current Distribution along Left Overhead Earth Wire – NETS

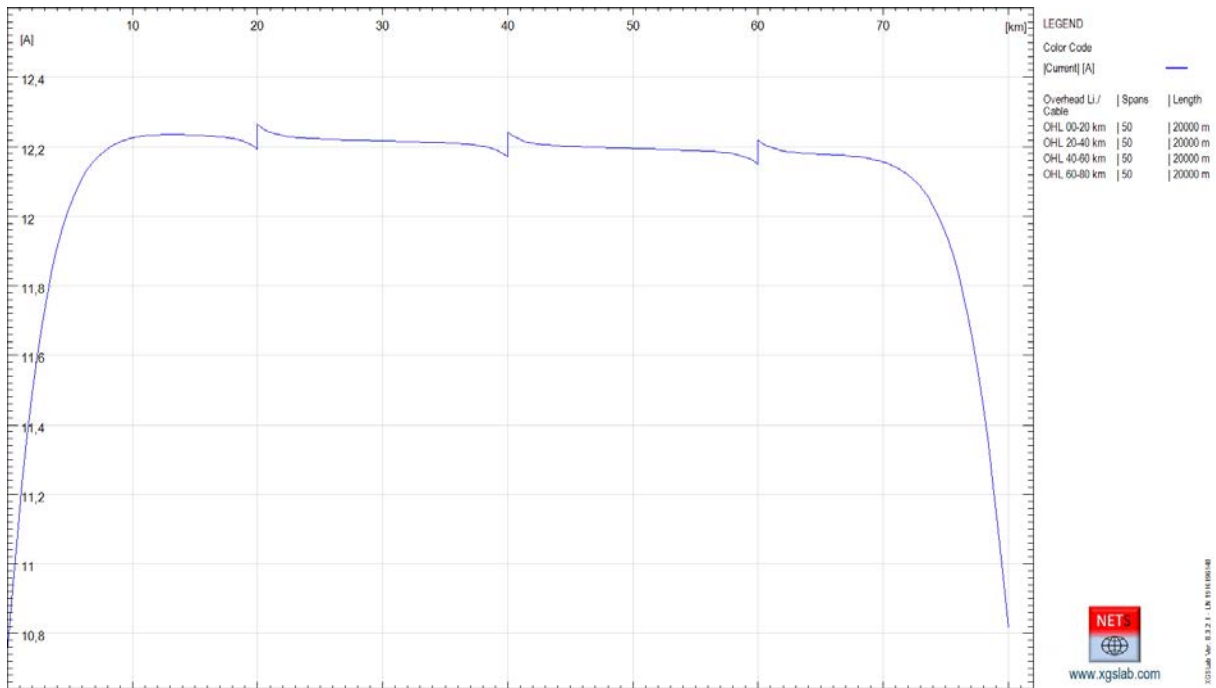


Figure 5-6: Magnitude Current Distribution along Right Overhead Earth Wire – NETS

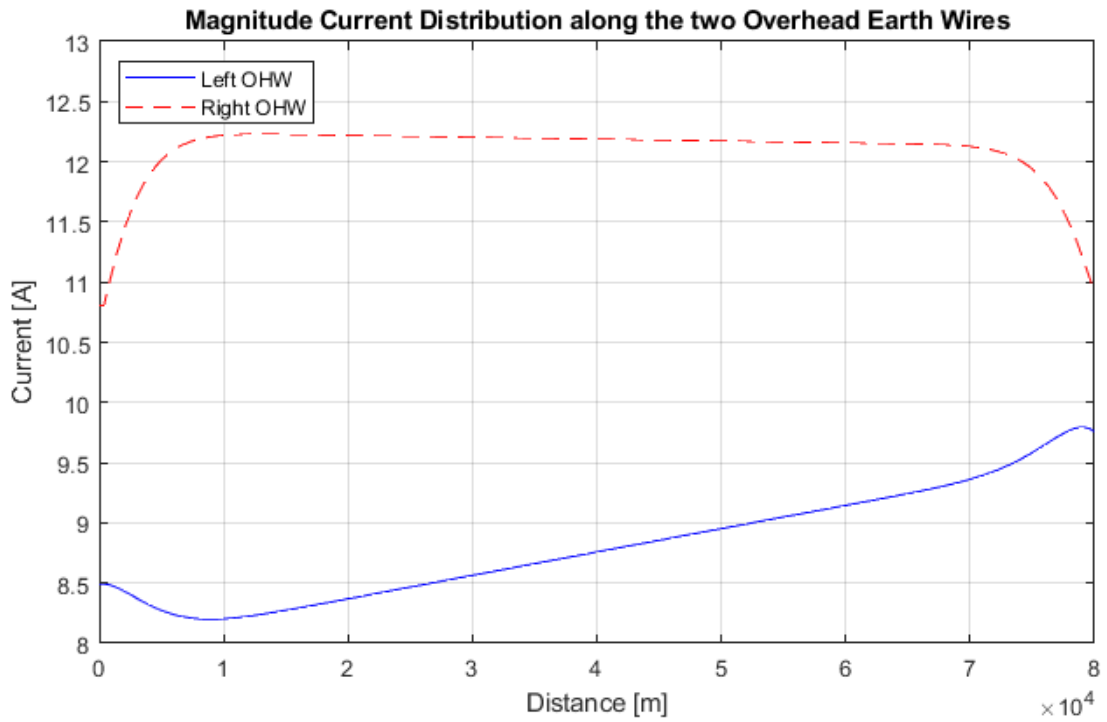


Figure 5-7: Magnitude Current Distribution along Left and Right Overhead Earth Wire – OpenDSS

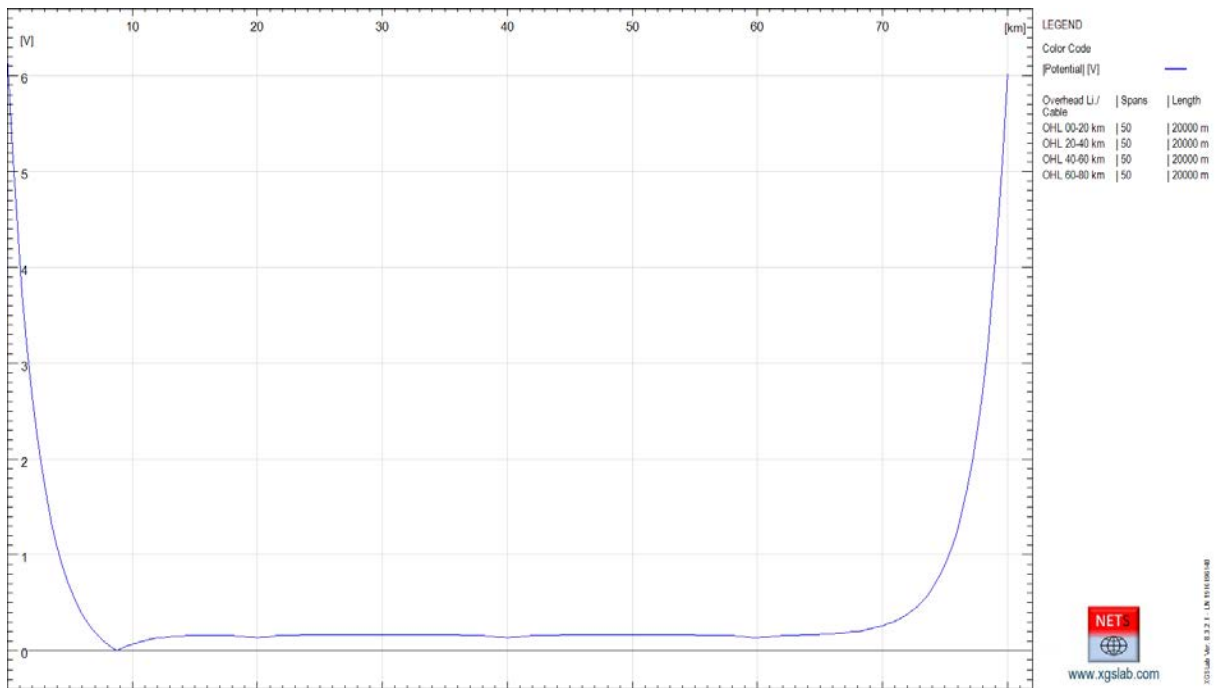


Figure 5-8: Magnitude Potential Distribution along Left and Right Overhead Earth Wire – NETS

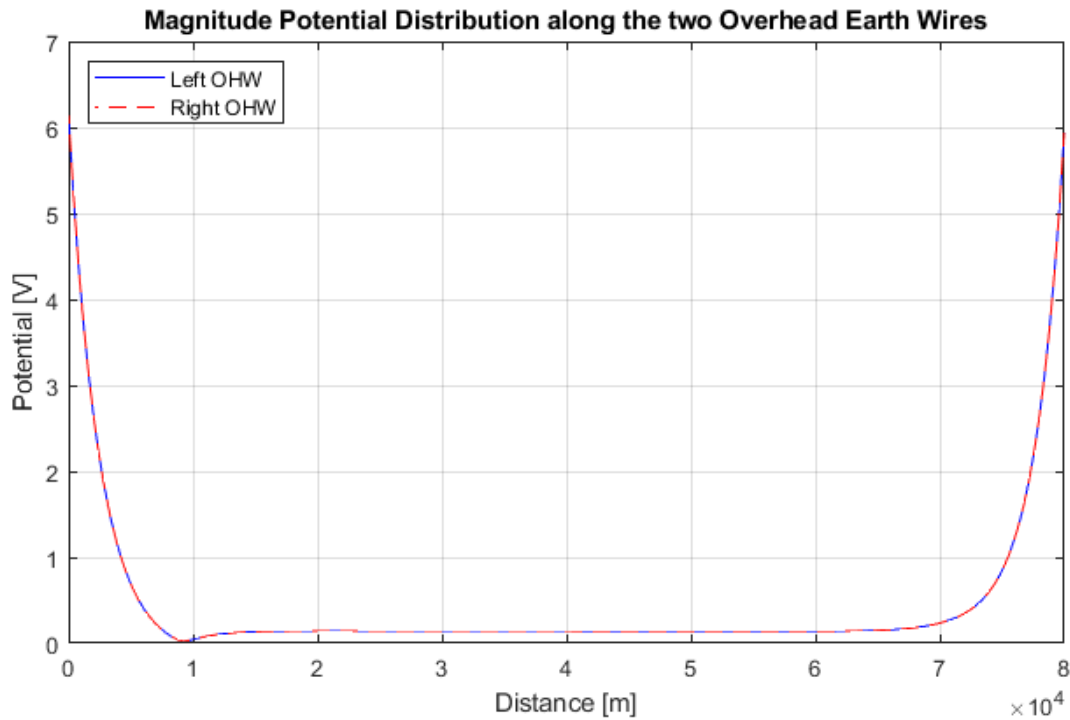


Figure 5-9: Magnitude Potential Distribution along Left and Right Overhead Earth Wire – OpenDSS

The very slight differences in current distributions calculated by NETS and OpenDSS are related to the used formulas for line parameters but also to the model modeling.

As known, OpenDSS considers each span as a short line while NETS works with blocks of spans, in this case 4 blocks of 50 spans. This offer great advantages in the data input process and makes the calculation faster.

In NETS model, the intermediate links between overhead lines at each span are taken into account using a little but not negligible resistance. Moreover, at the buses, NETS represents two distinct currents, the current of the entering and leaving conductors. These currents are in general different because the current induced in each loop formed by two overhead wires and the intermediate link at each tower.

The steps in the current distributions are in the specific case lower than 0.1 A. The differences between results provided by NETS and OpenDSS are negligible for engineering applications and they are even smaller if the comparison is between the sum of the overhead earth wire currents.

Anyway, the steps in the current distributions can be completely eliminated by assigning different phases to the two overhead wires, for instance D and E. Clearly, at the line ends, the phases must be the same, for instance D and D.

With this alternative approach, the distributions of magnitude of currents along the overhead earth wires are represented in the following figures. The steps on current distributions disappeared and values at the ends are the same.

Difference in current distributions calculated by NETS and OpenDSS are lower than 0.1 [A] with values in the range 8 – 12 [A], so the maximum difference in results is about 1%.

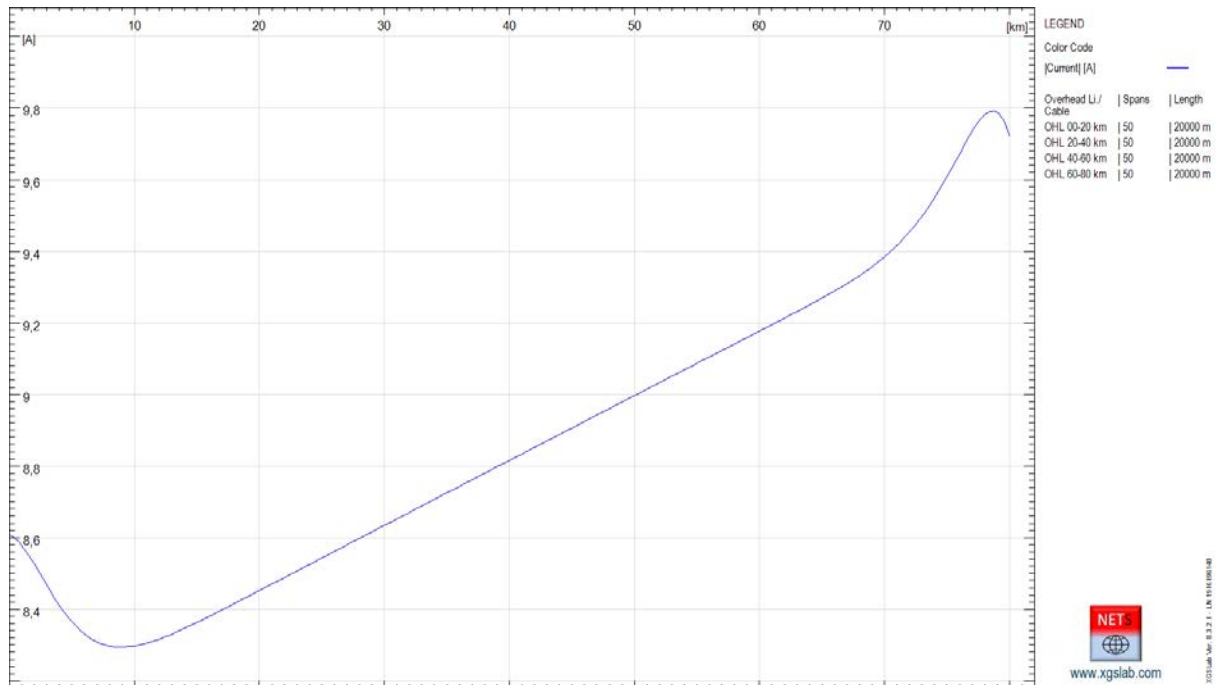


Figure 5-10: Magnitude Current Distribution along Left Overhead Earth Wire – NETS

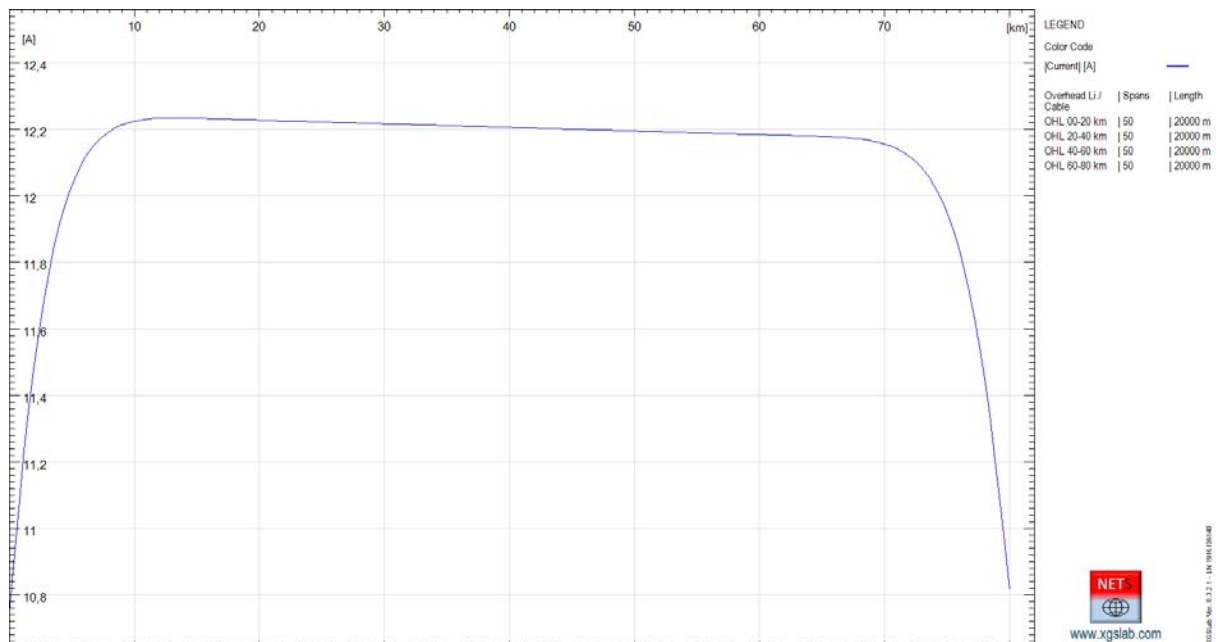


Figure 5-11: Magnitude Current Distribution along Right Overhead Earth Wire – NETS

Of course, in case of single overhead earth wire many of the problems described in the specific case do not exist and the model is simpler.

5.1.2.2 Three-phase fault condition

There are many ways to represent a three-phase fault condition:

- It is possible to modify the load impedances using $Z = 0.01 \text{ } [\Omega]$ for all phases and $Z_e = 1 \text{ } [\text{M}\Omega]$ (neutral insulated)
- It is possible to modify the bus connection the side out of the overhead line (phase B and C connected to A)
- It is possible to add a transverse impedance with $Z = 0.01 \text{ } [\Omega]$ for all phases and $Z_e = 1 \text{ } [\text{M}\Omega]$ (neutral insulated)

Probably there are more ways to represent this condition and all ways are equivalent.

Anyway, the last option in previous list is rigorous (the load is unchanged) and will be adopted.

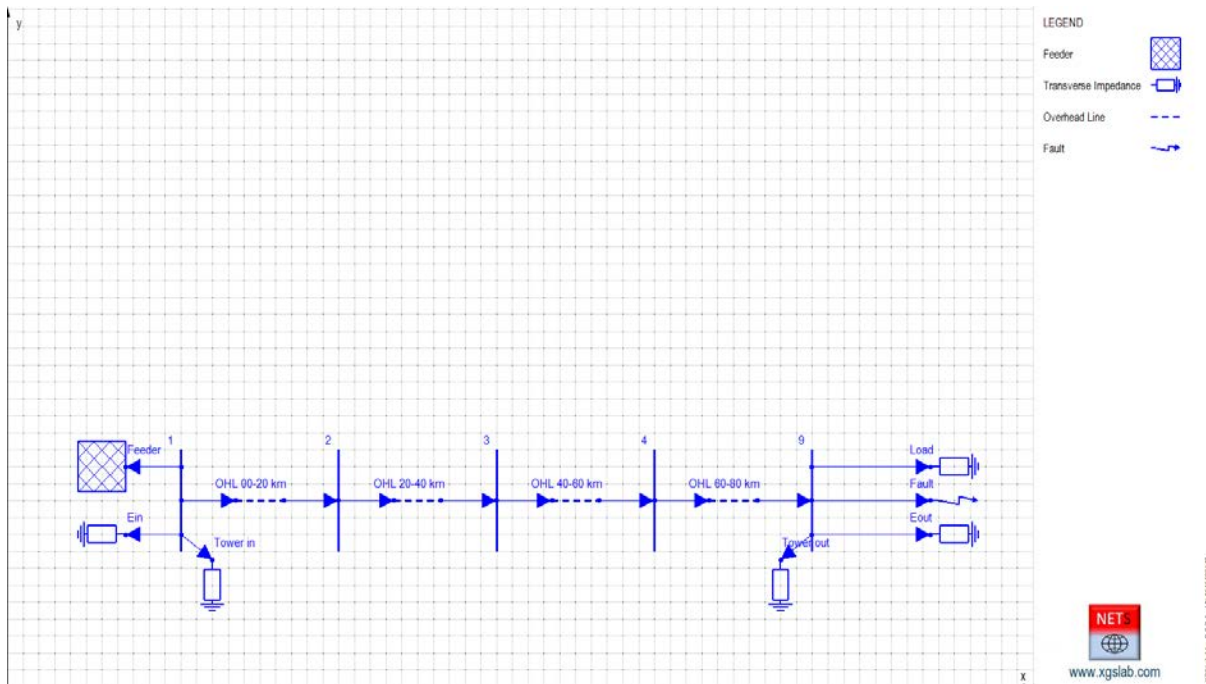


Figure 5-12: Single Line Diagram of an Overhead Line with a Load and a Fault at the End

The phase voltage and currents calculated with NETS and OpenDSS are displayed, in the following table.

Table 5-3: Current and voltage variations along the overhead line in three phase fault condition, NETS vs OpenDSS

Cell and Phase	NETS				OpenDSS			
	I [A]	L [deg]	U [V]	L [deg]	I [A]	L [deg]	U [V]	L [deg]
Line_in A	8290	-81.33	198017	-1.066	8330	-81.30	197870	-1.100
Line_in B	9428	154.7	193265	-120.5	9479	154.8	193060	-120.5
Line_in C	8385	29.85	197435	120.4	8426	29.90	197270	120.4
OHEW_in D	141.8	108.0	103.2	-150.4	142.8	106.8	102.5	-150.5
OHEW_in D	159.7	-30.83	=	=	161.3	-30.20	=	=
Line_out A	8322	98.66	8408	49.22	8363	98.70	8427	49.30
Line_out B	9461	-25.29	8438	50.27	9514	-25.30	8457	50.40
Line_out C	8415	-150.2	8542	49.46	8458	-150.2	8561	49.50
OHEW_out D	142.4	-71.80	102.6	29.79	143.5	-72.90	101.9	29.70
OHEW_out D	159.9	149.0	=	=	161.5	149.7	=	=

The agreement between results provided by NETS and OpenDSS is excellent with differences lower than 1%.

In the following, the magnitude of currents and potentials distribution along the overhead earth wires calculated with NETS and OpenDSS.

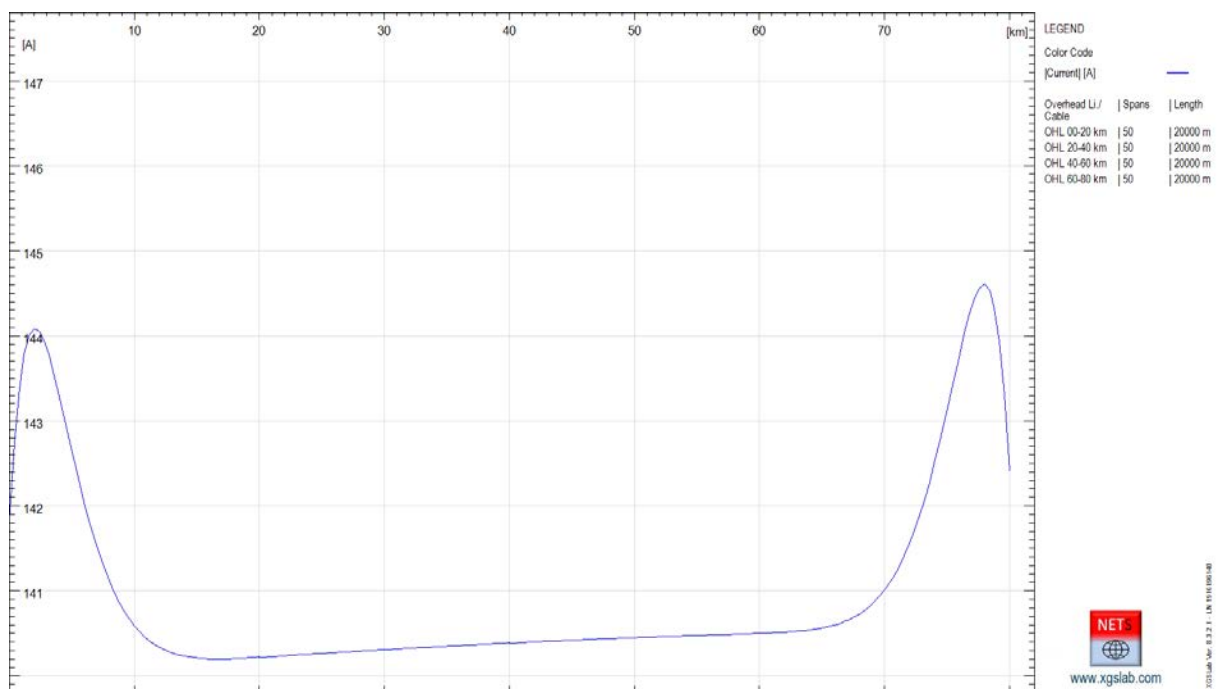


Figure 5-13: Magnitude Current Distribution along Left Overhead Earth Wire – NETS

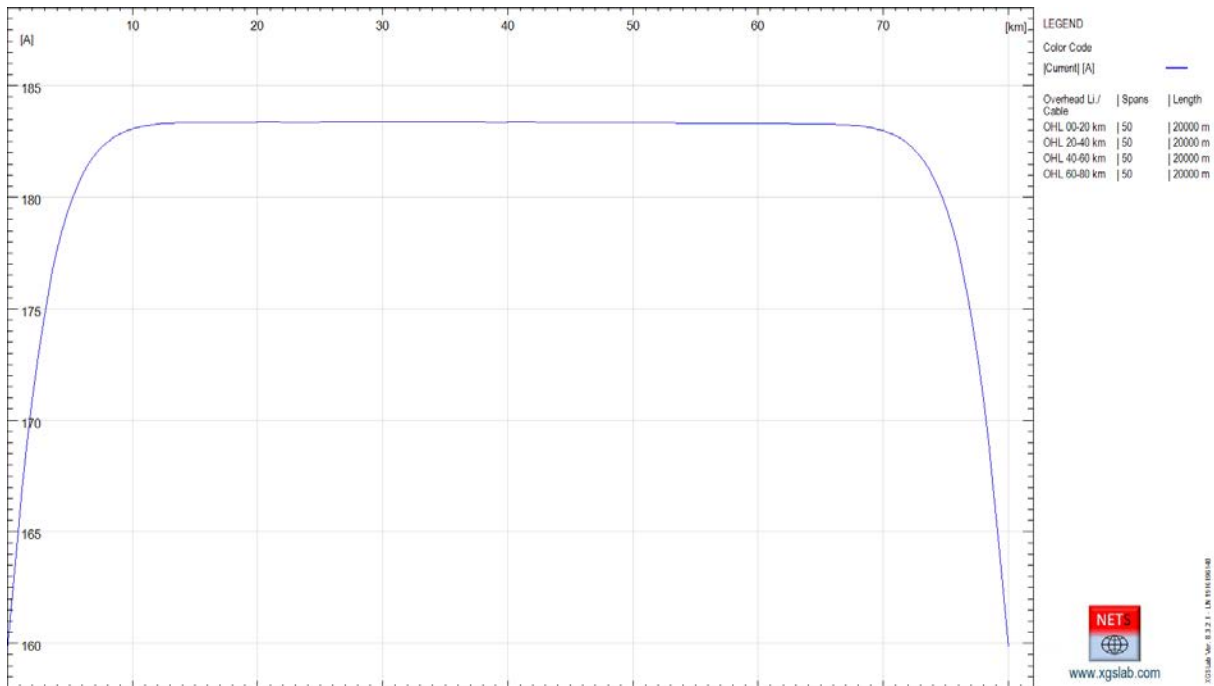


Figure 5-14: Magnitude Current Distribution along Right Overhead Earth Wire – NETS

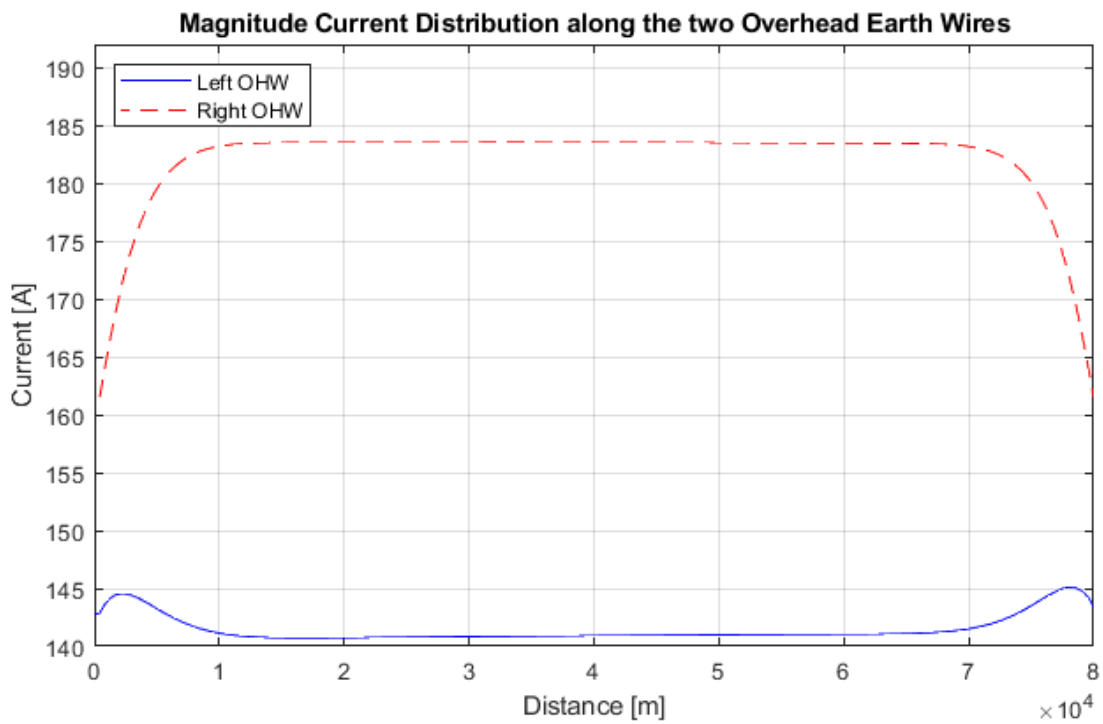


Figure 5-15: Magnitude Current Distribution along Left and Right Overhead Earth Wire – OpenDSS

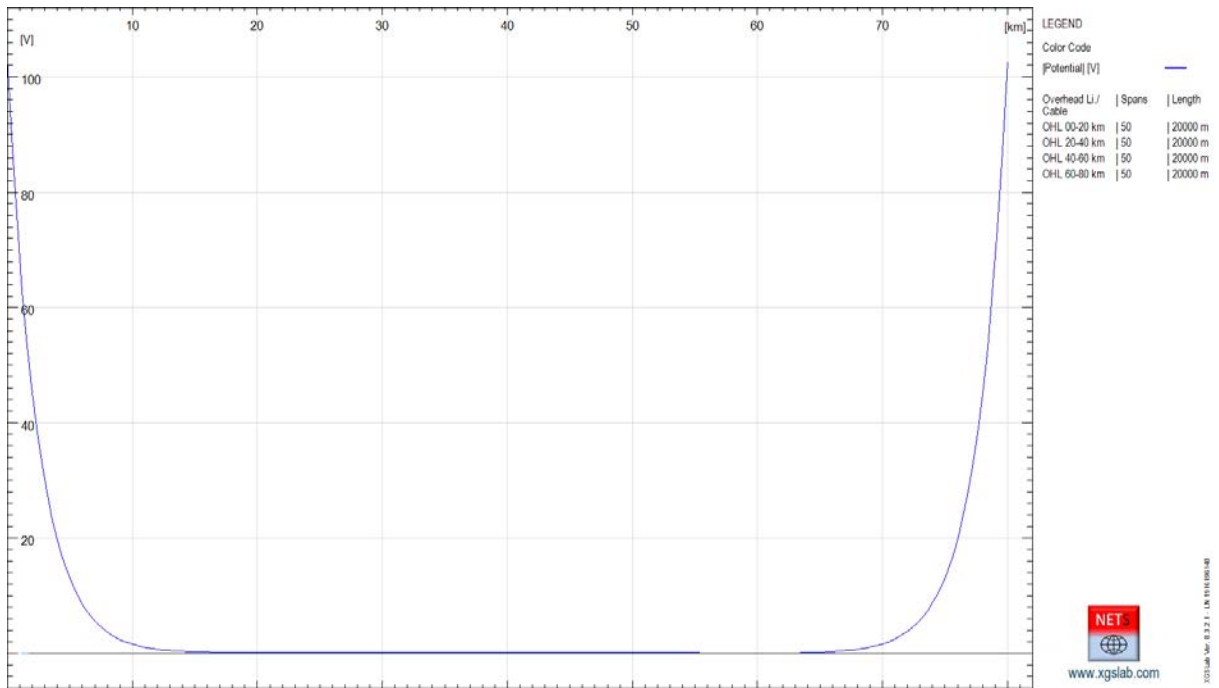


Figure 5-16: Magnitude Potential Distribution along Left and Right Overhead Earth Wire – NETS

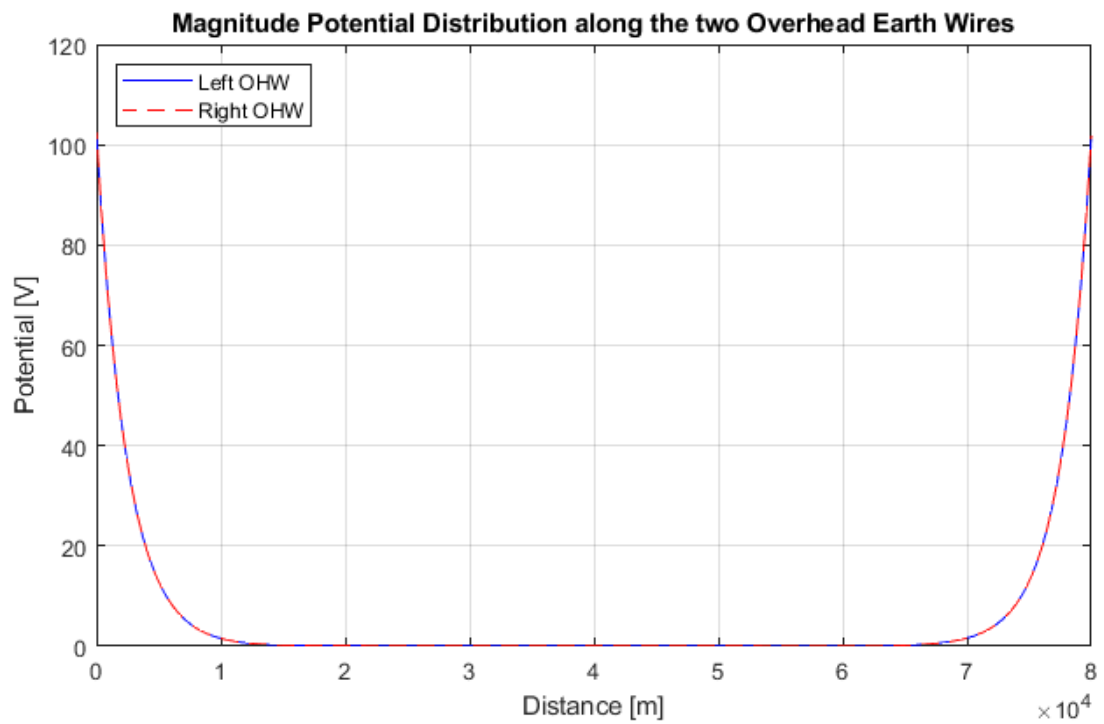


Figure 5-17: Magnitude Potential Distribution along Left and Right Overhead Earth Wire – OpenDSS

5.1.2.3 Phase to phase to earth fault condition

The phase to phase to earth fault condition can be represented modifying the transverse impedance related to the overhead lines and using a new transverse impedance with:

- $Z = 0.01 \text{ } [\Omega]$ (for all overhead earth wires)
- $Z = 0.01 \text{ } [\Omega]$ (for the fault phases, for instance A and B)
- $Z_c = 1 \text{ } [\Omega]$ (resistance to earth of the terminal substation)

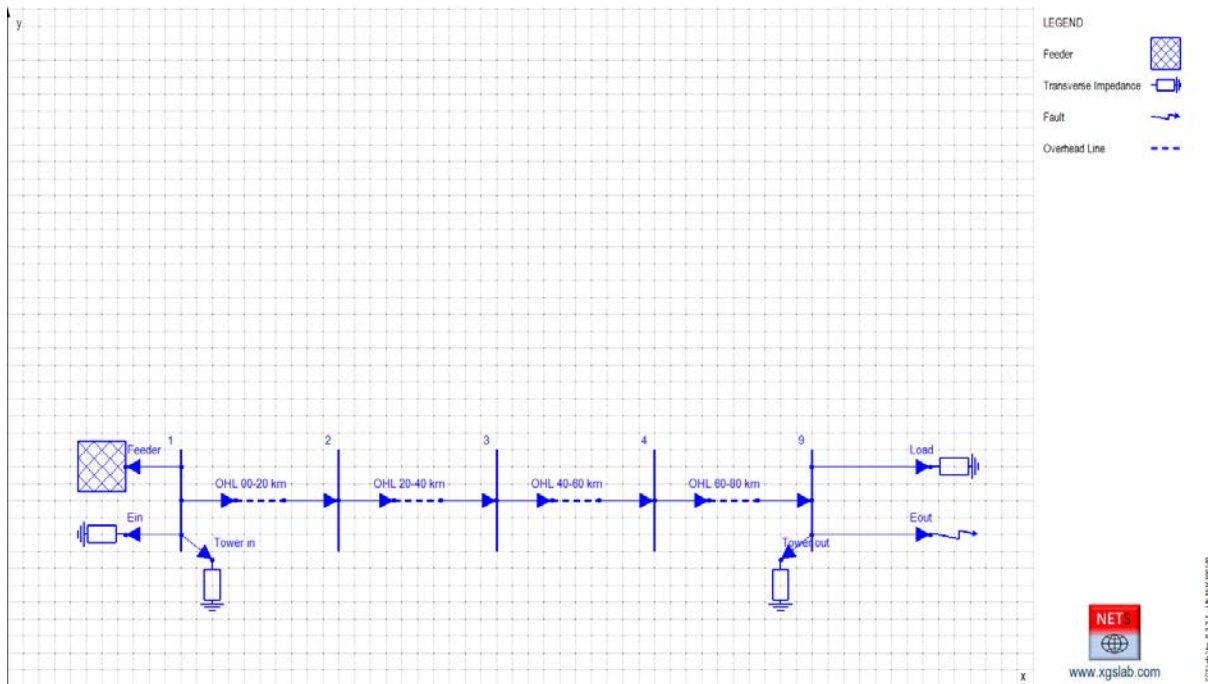


Figure 5-18: Single Line Diagram of an Overhead Line with a Load and a Fault at the End

The phase voltage and currents calculated with NETS and OpenDSS are displayed, in the following table.

Table 5-4: current and voltage variations along the overhead line in phase to phase fault condition, NETS vs OpenDSS

Cell and Phase	NETS				OpenDSS			
	I [A]	∠ [deg]	U [V]	∠ [deg]	I [A]	∠ [deg]	U [V]	∠ [deg]
Line_in A	8406	-68.51	199743	-3.103	8456	-68.20	199750	-2.40
Line_in B	7585	139.6	201114	-118.1	7599	139.3	198740	-118.3
Line_in C	436.5	81.29	229883	119.6	436.6	81.70	231980	119.2
OHEW_in D	431.7	94.74	821.5	-97.30	441.4	94.40	800.8	-97.1
OHEW_in D	441.5	70.93	=	=	452.5	71.50	=	=
Line_out A	8435	111.4	1646	-141.8	8487	111.7	1620	-140.6
Line_out B	7623	-40.33	1644	-147.2	7639	-40.50	1616	-146.2
Line_out C	479.5	-106.4	287267	110.8	481.5	-106.5	288460	110.7
OHEW_out D	902.8	-124.6	1606	-144.7	852.7	-123.4	1591	-143.6
OHEW_out D	1005	-133.6	=	=	952.7	-132.8	=	=

The agreement between results provided by NETS and OpenDSS is good with differences lower than 5%.

In the following, the magnitude of currents and potentials distribution along the overhead earth wires calculated with NETS and OpenDSS.

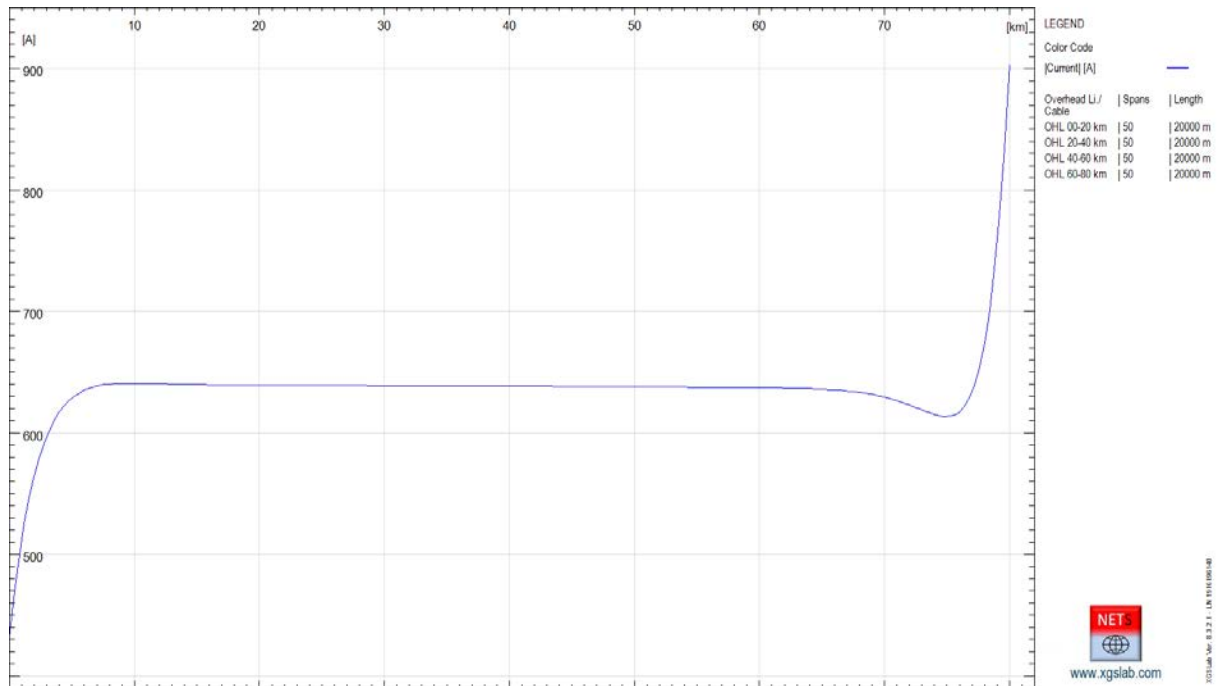


Figure 5-19: Magnitude Current Distribution along Left Overhead Earth Wire – NETS

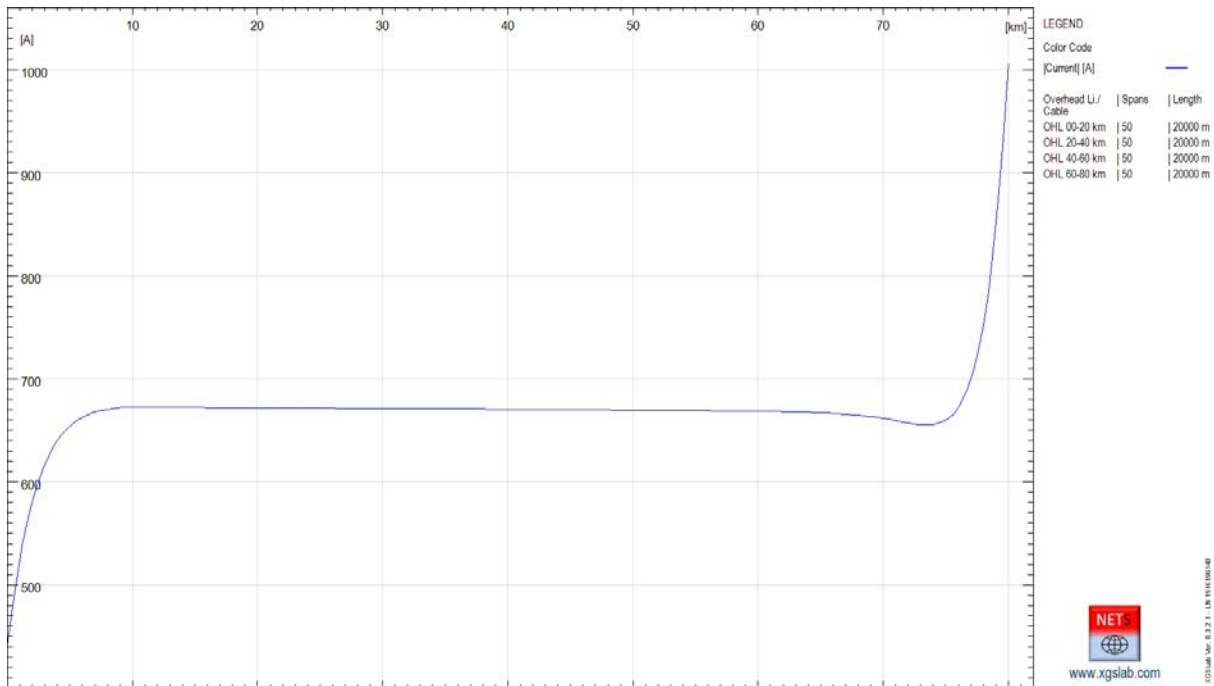


Figure 5-20: Magnitude Current Distribution along Right Overhead Earth Wire – NETS

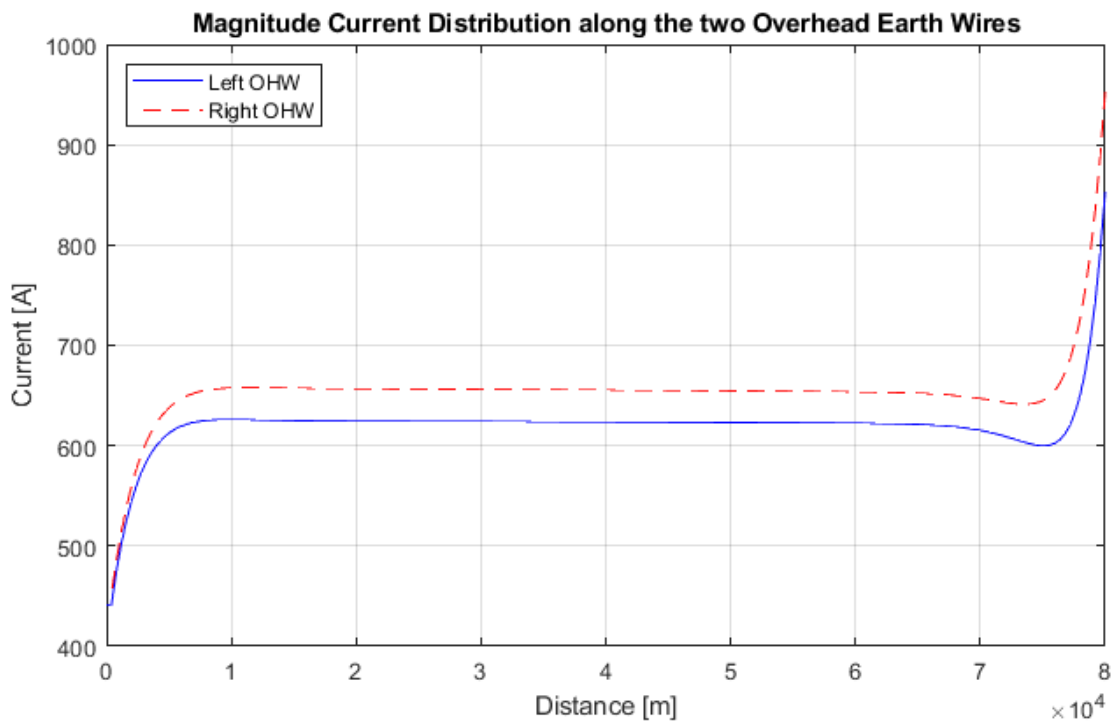


Figure 5-21: Magnitude Current Distribution along Left and Right Overhead Earth Wire – OpenDSS

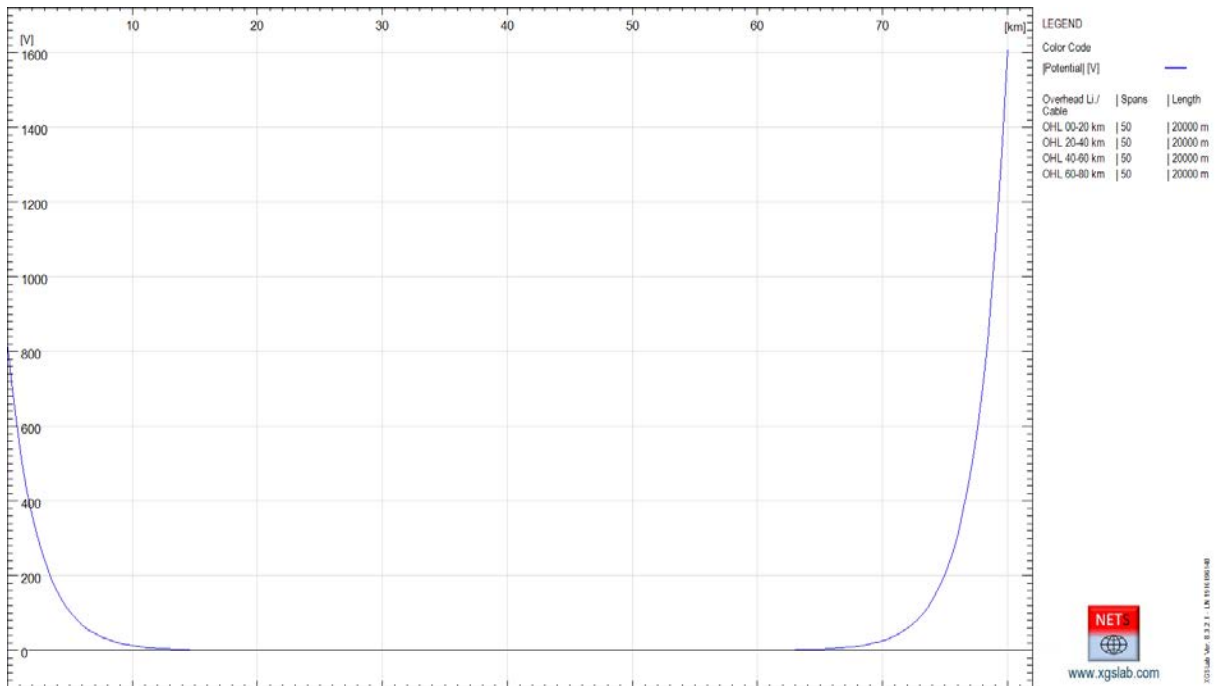


Figure 5-22: Magnitude Potential Distribution along Left and Right Overhead Earth Wire – NETS

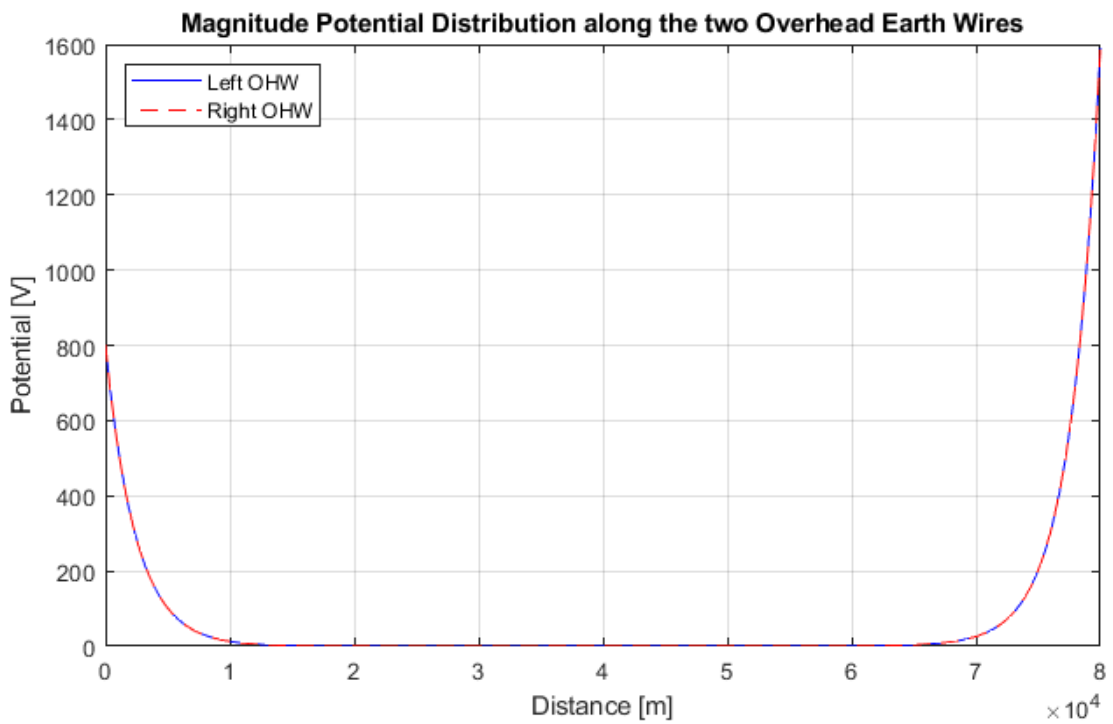


Figure 5-23: Magnitude Potential Distribution along Left and Right Overhead Earth Wire – OpenDSS

5.1.2.4 Phase to earth fault condition

The phase to earth fault condition can be represented modifying the transverse impedance related to the overhead lines and using a new transverse impedance with:

- $Z = 0.01 \text{ } [\Omega]$ (for all overhead earth wires)
- $Z = 0.01 \text{ } [\Omega]$ (for the fault phase, for instance A)
- $Z_e = 1 \text{ } [\Omega]$ (resistance to earth of the terminal substation)

The Single Line Diagram is the same of the previous case.

The phase voltage and currents calculated with NETS and OpenDSS are displayed, in the following table.

Table 5-5: Current and voltage variations along the overhead line in phase to earth fault condition, NETS vs OpenDSS

Cell and Phase	NETS				OpenDSS			
	I [A]	L [deg]	U [V]	L [deg]	I [A]	L [deg]	U [V]	L [deg]
Line_in A	5290	-76.36	210122	-0.999	5253	-75.80	207420	-0.500
Line_in B	477.0	-142.6	229763	-120.5	475.7	-142.3	229360	-121.4
Line_in C	465.9	72.85	230010	119.7	464.9	73.40	233360	120.0
OHEW_in D	639.4	148.0	1124	-33.84	656.1	148.1	1103	-33.70
OHEW_in D	530.2	143.9	=	=	550.4	144.1	=	=
Line_out A	5331	103.6	2448	-87.18	5296	104.2	2423	-86.30
Line_out B	506.0	28.87	273907	-141.8	506.1	28.7	274710	-142.2
Line_out C	520.3	-113.2	283226	129.8	522.1	-113.0	285500	130.0
OHEW_out D	1331	-67.60	2373	-87.56	1264	-66.40	2362	-86.60
OHEW_out D	1265	-71.93	=	=	1199	-70.90	=	=

The agreement between results provided by NETS and OpenDSS is good with differences lower than 5%.

In the following, the magnitude of currents and potentials distribution along the overhead earth wires calculated with NETS and OpenDSS.

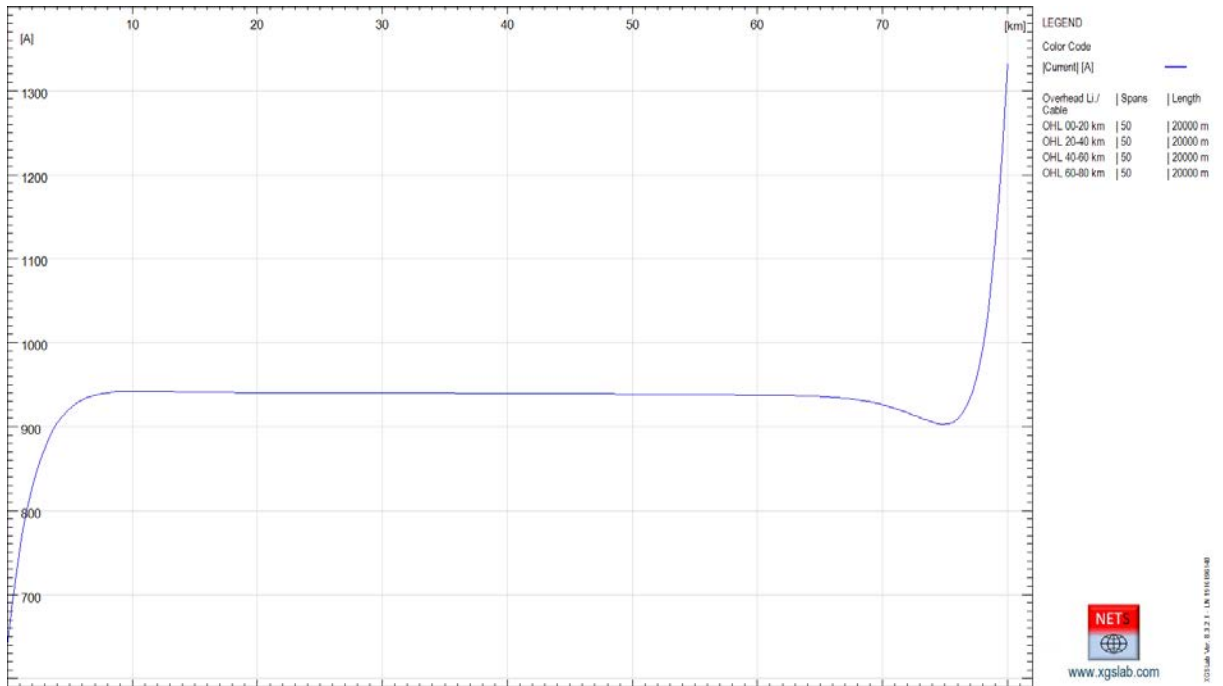


Figure 5-24: Magnitude Current Distribution along Left Overhead Earth Wire – NETS

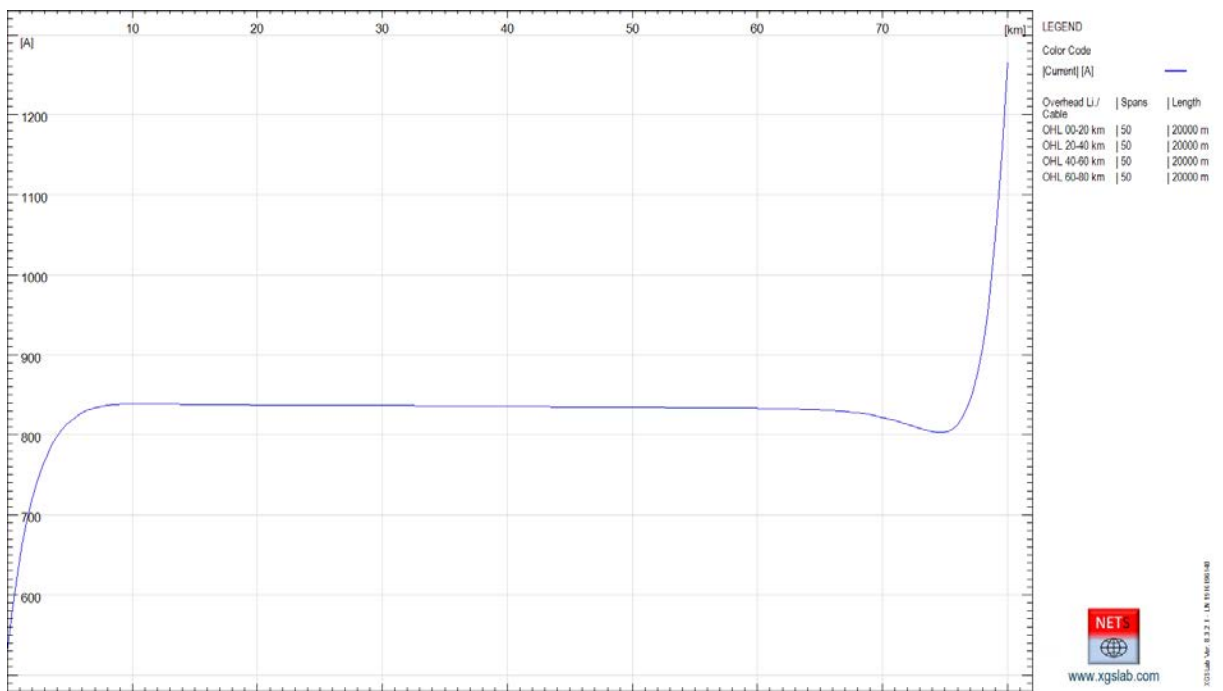


Figure 5-25: Magnitude Current Distribution along Right Overhead Earth Wire – NETS

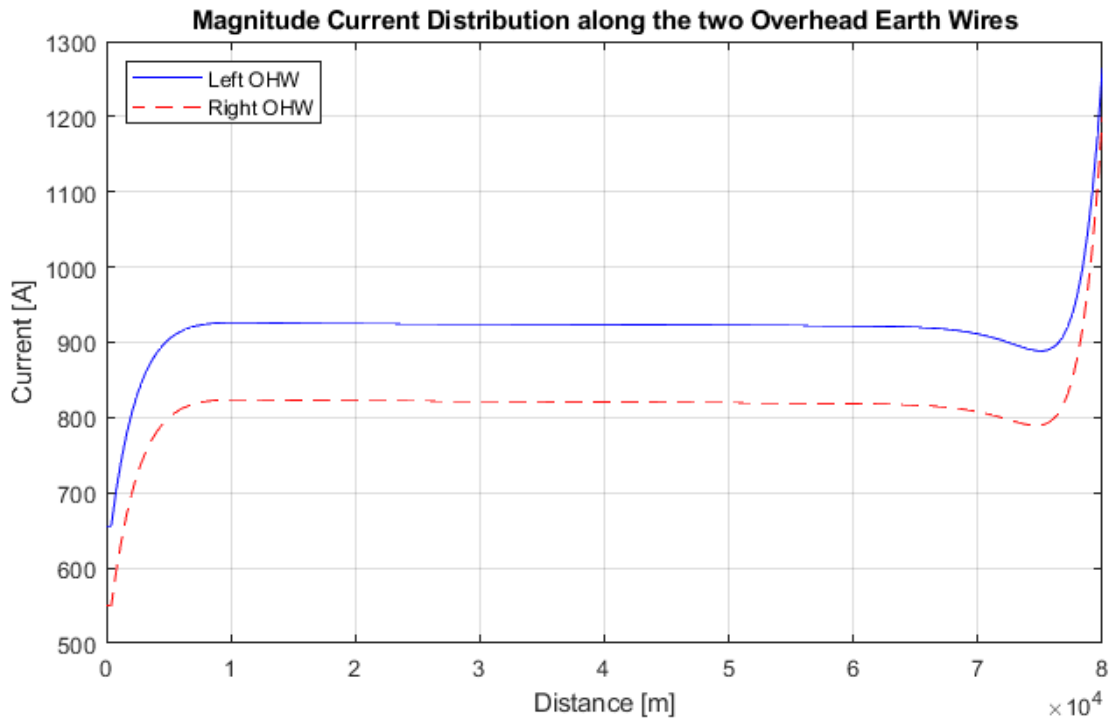


Figure 5-26: Magnitude Current Distribution along Left and Right Overhead Earth Wire – OpenDSS

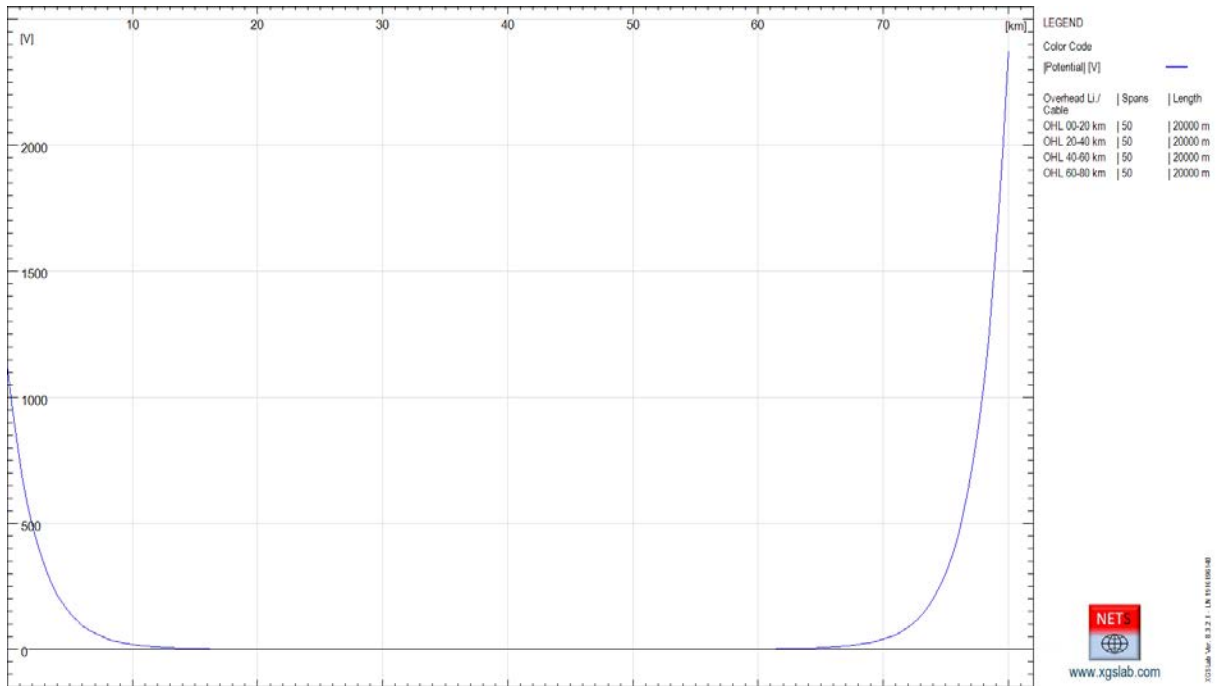


Figure 5-27: Magnitude Potential Distribution along Left Overhead Earth Wire – NETS

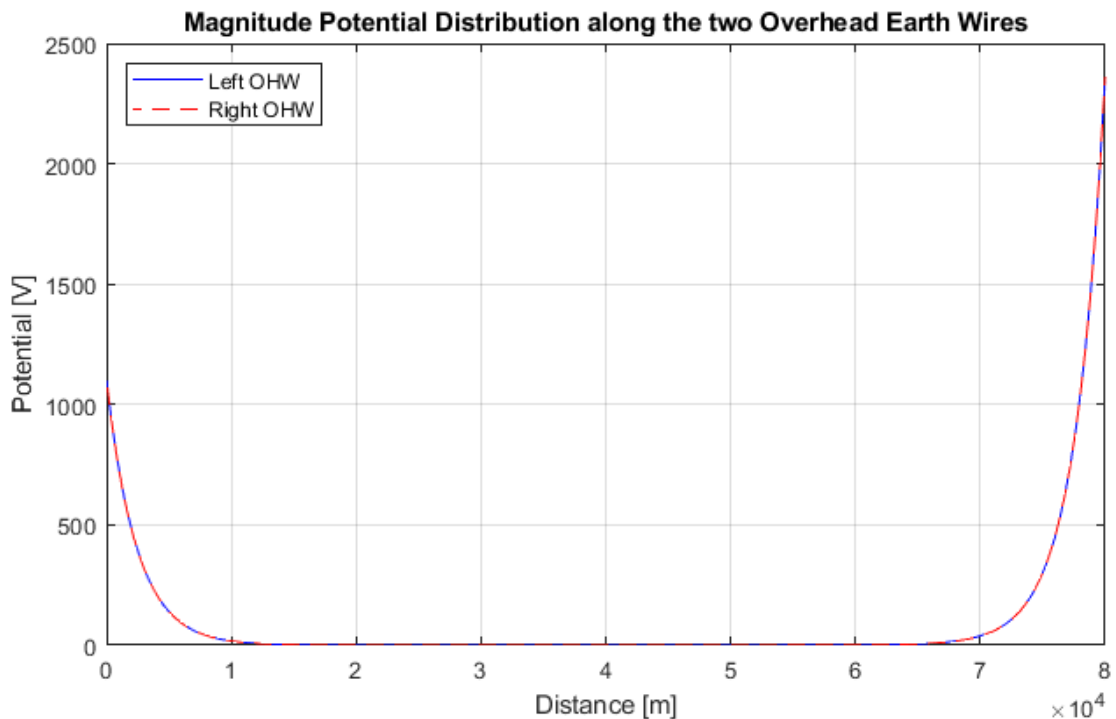


Figure 5-28: Magnitude Potential Distribution along Left and Right Overhead Earth Wire – OpenDSS

The phase to earth fault conditions are the most interesting for practical applications and allow to evaluate the split factor related to overhead earth wires.

In the specific case:

- Fault current magnitude (line out phase A): $I_f = 5331$ [A] $\angle 103.6$ [deg]
- Current to earth at line side out = $I_e = 2398$ [A] $\angle -87.37$ [deg]
- Split factor = $S_f = I_e / I_f = 2398 / 5331 = 0.4498$

In the specific case the split factor is rather low because the calculation has been performed with aluminum overhead earth wires (this because OpenDSS does not consider ferromagnetic conductors).

In phase to earth fault conditions, it's also interesting to observe, the same results could be obtained if the line is divided in only 3 sections with length $20 + 40 + 20$ [km] and with tower footing resistance infinite in the central section. This because as evident from previous results, along the central part, the overhead earth wires do not contribute to spread to earth the fault current.

Results in these conditions are represented in the following table and figures.

Table 5-6: The result does not change, modifying the length of each line in NETS

Cell and Phase	NETS 4x20 km				NETS 20+40+20 km			
	I [A]	∠ [deg]	U [V]	∠ [deg]	I [A]	∠ [deg]	U [V]	∠ [deg]
OHEW_in D	639.4	148.0	1124	-33.84	639.4	148.0	1124	-33.84
OHEW_in D	530.2	143.9	=	=	530.2	143.9	=	=
OHEW_out D	1331	-67.60	2373	-87.56	1331	-67.60	2373	-87.56
OHEW_out D	1265	-71.93	=	=	1265	-71.93	=	=

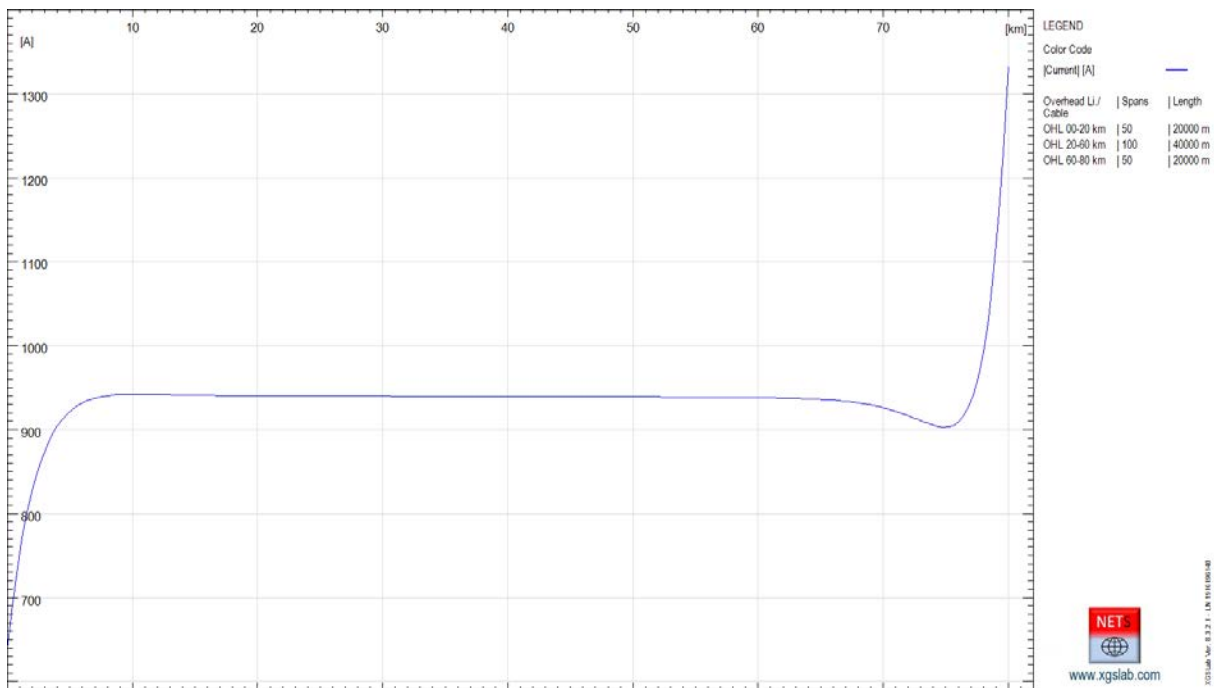


Figure 5-29: Magnitude Current Distribution along Left Overhead Earth Wire – NETS

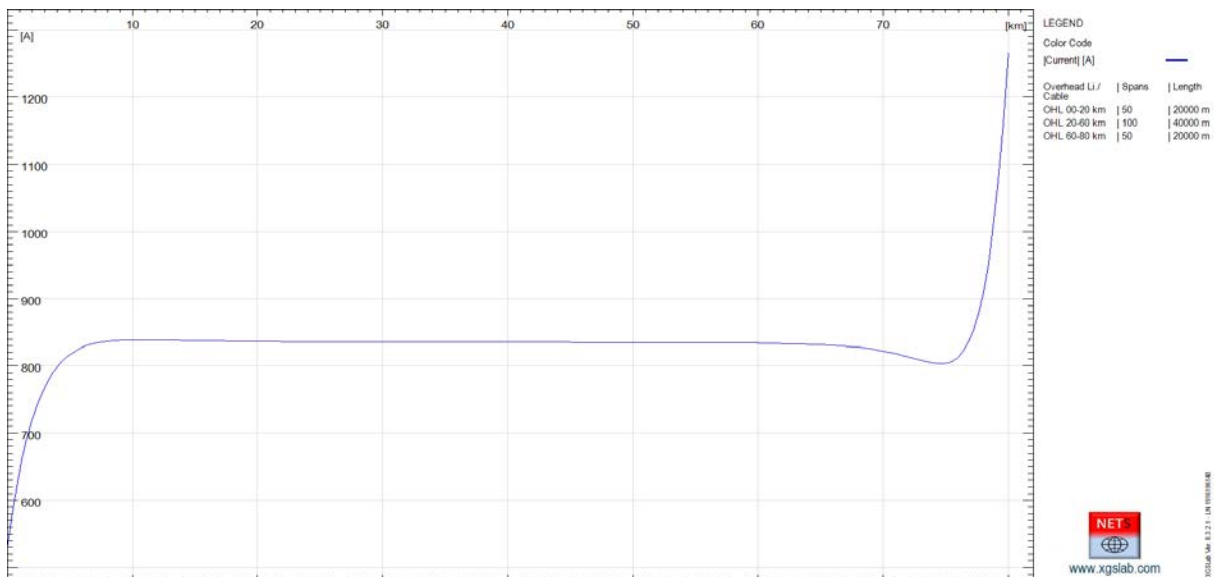


Figure 5-30: Magnitude Current Distribution along Right Overhead Earth Wire – NETS

Results in both cases are the same. This result is very important because in general cases, a very long line can be anyway represented using only 3 sections, the start and end sections with a length limited taking into account the (5.4) formula and the central part, with arbitrary length and with tower footing resistance infinite.

5.1.3 Overhead line, electromagnetic interaction – NETS vs OpenDSS

In the following, a calculation taking into account two parallel overhead line is shown in order to verify the agreement of the results obtained using NETS and OpenDSS (EPRI) in case of electromagnetic interactions.

The case study includes a real three-phase feeder and two parallel overhead lines with rated voltage 132 [kV], and with distance between the axes of 20 [m].

In the following the main input data.

Feeder

Main input data:

- Phases number: 3 (symmetrical and balanced)
- Rated line voltage: 132 [kV]
- Short circuit power: 5000 [MVA]
- $X/R = 20$
- $Z_e = 0.1 [\Omega]$

The equivalent internal impedance of the feeder can be calculated with the formulas (5.2) and (5.3).

It follows:

- $Z = 3.485 (0.04994 + j 0.9988) = 0.1740 + j 3.480 [\Omega]$ (for all phases)

Overhead Lines

The Figure 5-31 represents the cross section layout and the two parallel overhead lines.

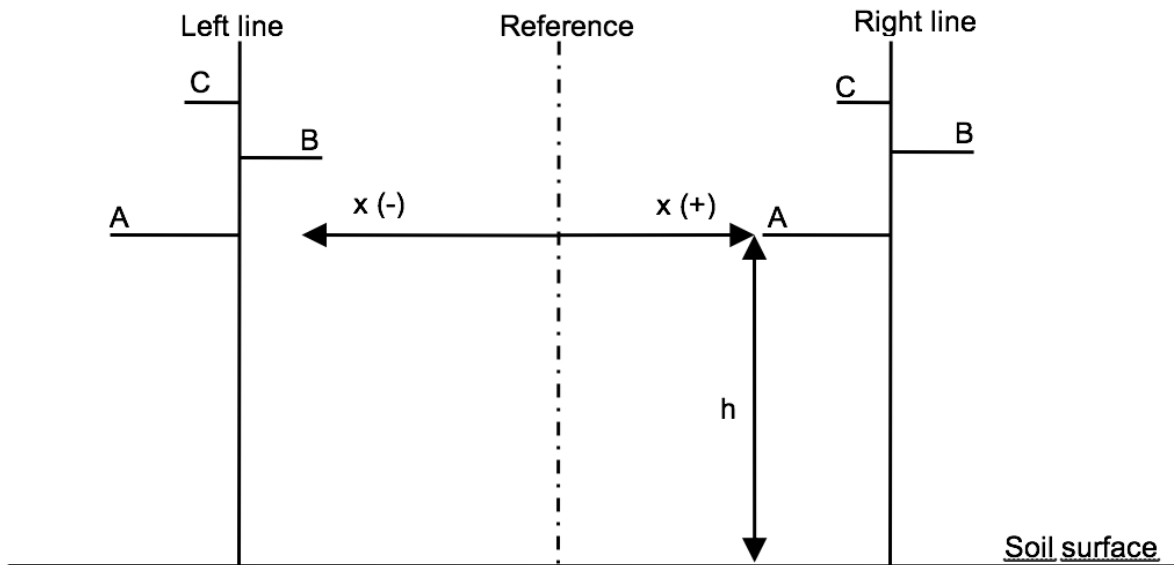


Figure 5-31: Tower lattices cross section layout

The two lines can be represented using a single equivalent overhead line with six phase conductors and two overhead earth wires.

Main input data:

- Phases numbers: 3 per line
- Rated line voltage = 132 [kV]
- Frequency = 50 [Hz]
- Low frequency soil resistivity = 100 [Ωm]
- High frequency soil relative permittivity = 6
- Line length = 10 [km]
- Span length = 250 [m] (40 spans)
- Phases conductors layout: A (left - down), B (right), C (left - up), for each tower
- Maximum and minimum distance to the soil surface phase A: 15.1 and 8 [m]
- Maximum and minimum distance to the soil surface phase B: 17.1 and 10 [m]
- Maximum and minimum distance to the soil surface phase C: 19.1 and 12 [m]
- Maximum and minimum distance to the soil surface overhead earth wires: 24.35 and 19.4 [m]
- Position with respect to reference:
 - Left line: A: -13.50 [m], B: -7.00 [m], C: -12.90 [m]
 - Right line: A: - 6.50 [m], B: 13.00 [m], C: 7.10 [m]
- Phase conductors: ACSR (Aluminium Conductor Steel Reinforced the steel is inside and the aluminium is outside) with external diameter = 31.5 [mm], cross section of steel and aluminium 65.81 and 519.5 [mm^2] respectively, resistance = 0.05564 [Ω/km] at 20 [$^{\circ}\text{C}$]

- Overhead wire: steel and aluminium conductors with external diameter = 11.5 [mm], cross section 80.66 [mm²] resistance = 1.062 [Ω /km] at 20 [°C]
- Resistance to earth of each single tower: 20 [Ω]

The resistance of phase conductors has to be referred to the operative temperature 75 °C using the formula (5.1).

Using the temperature coefficient of aluminum (0.0043 [1/°C]), the phase conductor resistance is 0.6879 [Ω /km] at 75 [°C].

The reference temperature for overhead earth wire can be 20 [°C].

The limit length for lines with overhead earth wires can be take into account using again formula (5.4); using $S = 250$ [m], $R_t = 20$ [Ω] and $R_s = 0.25 \cdot 1.062 = 0.2655$ [Ω] it follows $L =$ about 21.7 [km].

The line length is 10 [km] and then previous constraint is fulfilled.

The average height above ground of phase conductors and overhead earth wires can be calculated using the formula (5.5).

If follows:

- Phases A $h = 8 + (15.1 - 8) / 3 = 10.37$ [m]
- Phases B $h = 12.37$ [m]
- Phases C $h = 14.37$ [m]
- Overhead earth wires $h = 21.05$ [m]

Load

Main input data:

- Phases numbers: 3
- Rated line voltage: 132 [kV]
- Apparent power: 50 [MVA]
- $\cos \varphi = 0.8$

The load can be represented using a transverse impedance with:

- $Z = 348.5 (0.8 + j 0.6) = 278.8 + j 209.1$ [Ω] (for all phases)
- $Z_e = 1$ [M Ω]

The phase voltage and currents calculated with NETS and OpenDSS are displayed, in the following table.

Table 5-7: Current and voltage variations along the overhead line with electromagnetic interaction, NETS vs OpenDSS

Cell and Phase	NETS				OpenDSS			
	I [A]	∠ [deg]	U [V]	∠ [deg]	I [A]	∠ [deg]	U [V]	∠ [deg]
Line in A,left	105.4	-38.08	75740	-0.436	105.7	-37.9	75739	-0.400
Line_in B,left	110.5	-156.6	75739	-120.4	110.0	-156.6	75738	-120.4
Line_in C,left	105.2	84.99	75740	119.6	105.3	84.80	75741	119.6
OHEW_in D,left	1.614	-49.15	2.329	169.4	1.669	-50.80	2.347	168.9
Line in A,right	108.7	-34.92	75740	-0.436	108.3	-35.10	75740	-0.400
Line_in B,right	103.2	-156.6	75739	-120.4	103.7	-156.7	75740	-120.4
Line_in C,right	108.4	81.98	75740	119.6	108.3	82.20	75739	119.6
OHEW_in D,right	1.448	33.28	2.329	169.4	1.505	34.00	2.347	168.9
Line_out A,left	106.7	140.9	75459	-0.665	107.0	141.1	75454	-0.700
Line_out B,left	111.9	22.48	75439	-120.7	111.4	22.50	75436	-120.7
Line_out C,left	106.7	-95.99	75421	119.4	106.8	-96.20	75415	119.4
OHEW_out D,left	1.614	129.6	2.330	-11.75	1.670	128.0	2.348	-12.20
Line_out A,right	109.9	144.0	75459	-0.665	109.6	143.9	75454	-0.700
Line_out B,right	104.5	22.47	75439	-120.7	105.0	22.40	75434	-120.7
Line_out C,right	109.9	-98.98	75421	119.4	109.7	-98.80	75418	119.4
OHEW_out D,right	1.452	-147.8	2.330	-11.75	1.508	-147.1	2.348	-12.20

The agreement between NETS and OpenDSS results is excellent.

It is interesting to note that, because of the electromagnetic interactions, the current in the inner conductors (phase B of the line left and phases A and C of the right line) are higher than the current in the outer conductors.

This is due to the non-symmetrical disposition of the phases respect to the line axis.

5.2 Underground Cables

5.2.1 Underground cables, frequency domain – NETS vs OpenDSS

In the following, a calculation taking into account a short underground cable is shown in order to verify the agreement of the results obtained using NETS and OpenDSS (EPRI) in the frequency domain.

The comparison between NETS and OpenDSS in this case is interesting and useful but partial because as known, cable parameters like resistance, reactance and capacitance matrices have to be calculated externally and directly provided to OpenDSS. Of course, the formulas used in order to calculate these matrices are the same used by NETS. Anyway, OpenDSS does not

consider the conductance matrix and this has consequences in terms of application limits that will be highlighted in the following.

The case study is very simple and includes an ideal generator (symmetrical and balanced), a short underground cable with 3 single core 132 [kV] cables, without phases transposition and with a resistive load.

The comparison is performed both with solid and single bonding conditions.

The general layout is represented in the following figure.

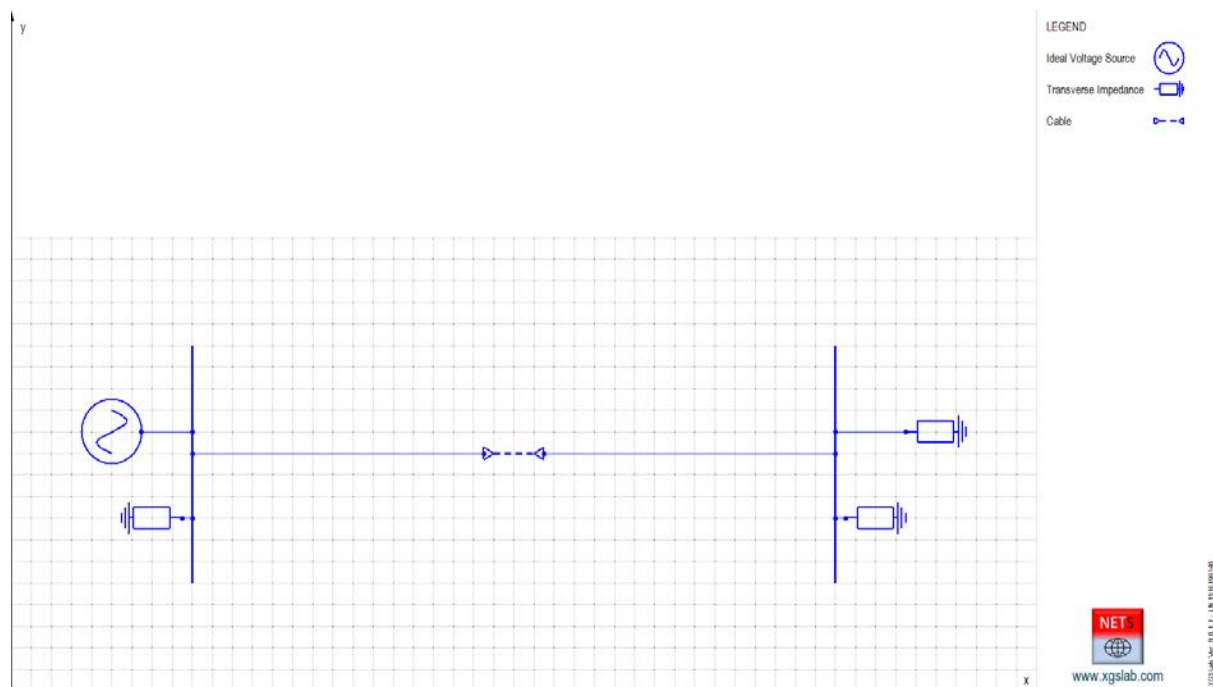


Figure 5-32: Single Line Diagram of an Ideal Voltage Source + Underground Cable + Solid Bonding + Load

In the following the main input data.

Ideal Voltage generator

Main input data:

- Phases number: 3 (symmetrical and balanced)
- Rated phase voltage: 100 [V]
- Frequency = DC, 1. 2. 5. 10. 20. 50. 100. 200. 500 [Hz], 1. 2. 5. 10. 20. 50. 100 [kHz]

In both cases, calculations cannot be provided exactly at DC condition.

If DC conditions are set, NETS automatically assumes a frequency 1 [mHz].

OpenDSS accepts a minimum frequency 1 [mHz].

Underground Cable

Main input data:

- Phases numbers: 3
- Low frequency soil resistivity = 100 [Ωm]
- High frequency soil relative permittivity = 6
- Line length = 500 [m] (automatically divided in spans)
- Phases conductors layout: A (left), B (center), C (right)
- Phases conductors depth = 1 [m]
- Phase conductor horizontal distance = 0.5 [m]
- Core: copper with external diameter = 34.2 [mm], cross section 800 [mm²] AC resistance 0.0326 [Ω/km] at 90 [$^{\circ}\text{C}$], inductance 0.36 [mH/km], capacitance 0.212 [$\mu\text{F}/\text{km}$]
- Insulating: XLPE (resistivity 10^{15} [Ωm], relative permittivity 2.3) with thickness 19.4 [mm] including semi-conductive screens
- Screen: copper wires with external diameter 74 [mm], cross section 50 [mm²]
- Sheath: Polyethylene (resistivity 10^7 [Ωm], relative permittivity 2.3) with thickness 4 [mm]
- Outer diameter: 82 [mm]
- Resistance to earth: 1 [Ω] at each cable ends

The resistance of cores and screens has to be referred to the operative temperature 90 $^{\circ}\text{C}$ using the formula (5.1).

Load

Main input data:

- Phases numbers: 3
- $Z = 1 + j0$ [Ω] (for all phases)
- $Z_e = 1$ [$\text{M}\Omega$]

5.2.1.1 Solid bonding condition

In this case, the screens are connected to earth at each termination.

The currents on phase A and screen of the phase A calculated with NETS and OpenDSS are displayed, in the following table.

Table 5-8: Differences between underground cable phase A core current and phase A screen current at difference frequencies, in solid bonding condition, NETS vs OpenDSS

f (Hz)	NETS Phase A		OpenDSS Phase A		Difference %	NETS Screen A		OpenDSS Screen A		Difference %
	I [A]	∠ [deg]	I [A]	∠ [deg]		I [A]	∠ [deg]	I [A]	∠ [deg]	
0.001	98.58	0.000	98.58	0	0.00	0.001	-97.58	2.64E-08	-90	-100.00
1	98.55	-0.143	98.55	-0.1	0.00	0.765	-98.18	0.765	-98.2	0.00
2	98.53	-0.286	98.53	-0.3	0.00	1.527	-98.78	1.527	-98.8	0.00
5	98.41	-0.712	98.41	-0.7	0.00	3.802	-100.6	3.802	-100.6	0.00
10	98.16	-1.405	98.16	-1.4	0.00	7.537	-103.5	7.536	-103.5	-0.01
20	97.43	-2.712	97.43	-2.7	0.00	14.7	-109.3	14.7	-109.3	0.00
50	94.15	-5.777	94.15	-5.8	0.00	32.62	-124.4	32.62	-124.4	0.00
100	88.67	-8.4	88.67	-8.4	0.00	50.49	-141.9	50.49	-141.9	0.00
200	82.55	-10.18	82.55	-10.2	0.00	64.22	-160	64.21	-160.1	-0.02
500	76.67	-14.55	76.67	-14.5	0.00	71.2	179.6	71.2	179.6	0.00
1000	71.18	-23.22	71.18	-23.2	0.00	69.11	164.2	69.11	164.2	0.00
2000	59.71	-38.2	59.71	-38.2	0.00	58.99	145.6	58.99	145.6	0.00
5000	35.11	-61.44	35.11	-61.4	0.00	34.98	120.1	34.98	120.1	0.00
10000	19.34	-73.95	19.34	-74	0.00	19.32	106.8	19.32	106.8	0.00
20000	9.762	-81.02	9.762	-81	0.00	9.765	99.39	9.765	99.4	0.00
50000	3.18	-84.46	3.18	-84.5	0.00	3.183	95.65	3.183	95.6	0.00
100000	0.19	40.03	0.1895	40	-0.26	0.191	-139.8	0.1909	-139.8	-0.05

Taking into account that the system is symmetrical and the load is balanced, only the values in the phase “A” are displayed in previous table. The values in the phases “B” and “C” are similar, the only differences are related to the asymmetrical conditions of phase conductors position.

The differences in the table are related to the currents magnitude.

The differences in phase currents up to 50 [kHz] are negligible.

The frequency 100 [kHz] is out of the application range.

The difference in screen current are negligible in the range 1 [Hz] – 50 [kHz].

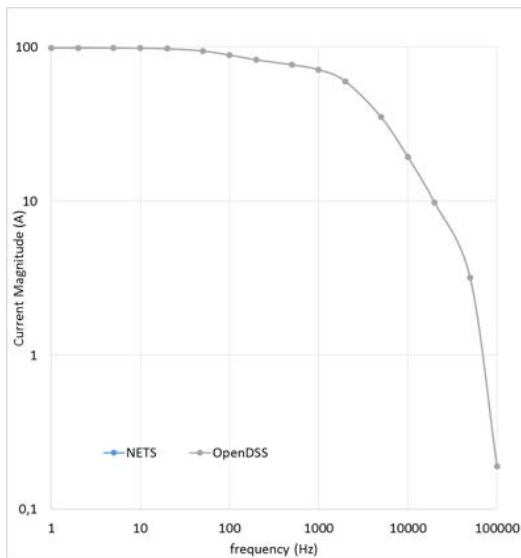
The large difference at 1 [mHz] is due to the different model used.

As known, OpenDSS does not consider insulating conductance.

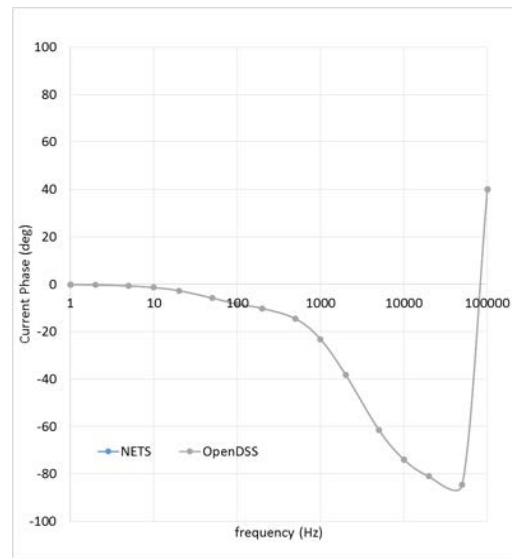
The conductance effects are in general negligible but at very low frequency these effects are predominant on the cable capacitance and cannot be neglected for a rigorous simulation.

Conservatively, 10 [kHz] can be assumed as application limits for NETS (for cables models).

The following figures represent the comparisons between results in graphical way.

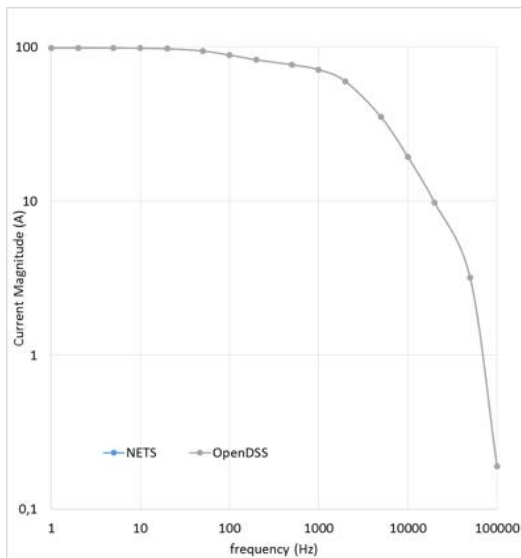


Magnitude (X log, Y log)

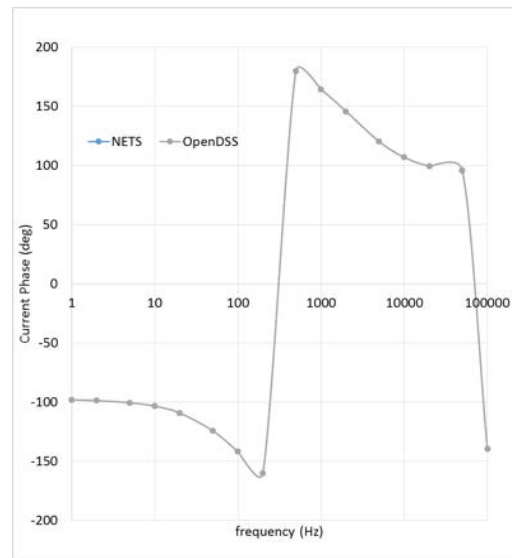


Phase (X log, Y linear)

Figure 5-33: Graphical differences between phase A core currents at difference frequencies in case of solid bonding, NETS vs OpenDSS (NETS = azure, OpenDSS = grey)



Magnitude (X log, Y log)



Phase (X log, Y linear)

Figure 5-34: Graphical differences between phase A screen currents at difference frequencies in case of solid bonding, NETS vs OpenDSS (NETS = azure, OpenDSS = grey)

As expected, the solid bonding is involved with strong currents along the screens. The current along screens depends on frequency and the ratio between screen and phase currents at high frequency tends to 1.

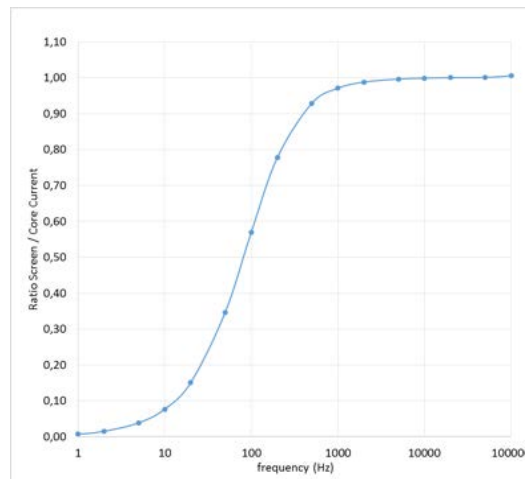


Figure 5-35: Ratio between current along screen and phase of the phase A (calculated by NETS)

The currents along screens are not desirable because of the consequent energy dissipation and the corresponding ampacity reduction. For this reason, solid bonding is seldom used. In case of short cable, the single bonding is usually the preferred bonding system.

5.2.1.2 Single bonding condition

In this case, the screens are connected to earth only at the termination at the same side of the generator.

The currents on phase A and screen of the phase A (at the side of the generator) calculated with NETS and OpenDSS are displayed, in the following table.

Table 5-9: Differences between underground cable phase A core current and phase A screen current at difference frequencies, in single bonding condition, NETS vs OpenDSS

f (Hz)	NETS Phase A		OpenDSS Phase A		Difference %	NETS Screen A		OpenDSS Screen A		Difference %
	I [A]	∠ [deg]	I [A]	∠ [deg]		I [A]	∠ [deg]	I [A]	∠ [deg]	
0.001	98.58	-0.001	98.58	0	0.00	0.00005	-99.74	5.26E-08	-90	-99.89
1	98.56	-0.144	98.56	-0.1	0.00	0.0005	-99.74	5.27E-05	-89.6	-89.46
2	98.53	-0.287	98.53	-0.3	0.00	0.001	-99.8	1.06E-04	-89.3	-89.41
5	98.45	-0.718	98.45	-0.7	0.00	0.002	-99.99	2.65E-04	-88.2	-86.74
10	98.3	-1.434	98.3	-1.4	0.00	0.0035	-100.3	5.36E-04	-86.4	-84.70
20	97.95	-2.859	97.95	-2.9	0.00	0.007	-100.98	0.001097	-82.9	-84.33
50	96.52	-7.053	96.52	-7.1	0.00	0.017	-102.87	0.003028	-74.4	-82.19
100	93.07	-13.66	93.07	-13.7	0.00	0.032	-105.7	0.007366	-66	-76.98
200	83.98	-24.97	83.99	-25	0.01	0.06	-109.8	0.02032	-62.1	-66.13
500	58.52	-45.97	58.54	-46	0.03	0.123	-112.5	0.07605	-70.1	-38.17
1000	36.04	-60.72	36.05	-60.8	0.03	0.212	-108.4	0.1778	-79.7	-16.13
2000	19.55	-70.67	19.55	-70.8	0.00	0.396	-103.1	0.3786	-86.9	-4.39
5000	7.627	-76.78	7.619	-77.3	-0.10	0.95	-100.3	0.953	-94.3	0.32
10000	2.847	-73.91	2.824	-75.5	-0.81	2.242	-89.46	2.273	-85.2	1.38
20000	2.164	63.77	2.133	69.8	-1.43	7.16	-99.53	7.226	-95.9	0.92
50000	2.829	48.24	2.764	53.1	-2.30	2.868	112.8	2.884	112	0.56
100000	16.07	-92.5	16.81	-108	4.60	8.287	109.1	7.969	95.4	-3.84

Again, only the values in the phase “A” are displayed in previous table.

The differences in the table are related to the currents magnitude.

The differences in phase currents up to 5 [kHz] are negligible and are acceptable up to 20 [kHz].

The frequency 100 [kHz] is clearly out of the application range.

The large difference in screen currents are due to the different model used.

As known, OpenDSS does not consider insulating conductance.

The conductance effects in this specific case, where the screen currents are only related to conductance and capacitance cannot be neglected. Results provided by NETS and OpenDSS are similar when frequency grow but frequency 100 [kHz] is clearly out of the application range.

It is evident that OpenDSS cannot be used to simulate the screen in the specific case.

Anyway, conservatively, 10 [kHz] can be assumed also as application limits for NETS (for cables models).

The following figures represents the comparisons between results in graphical way.

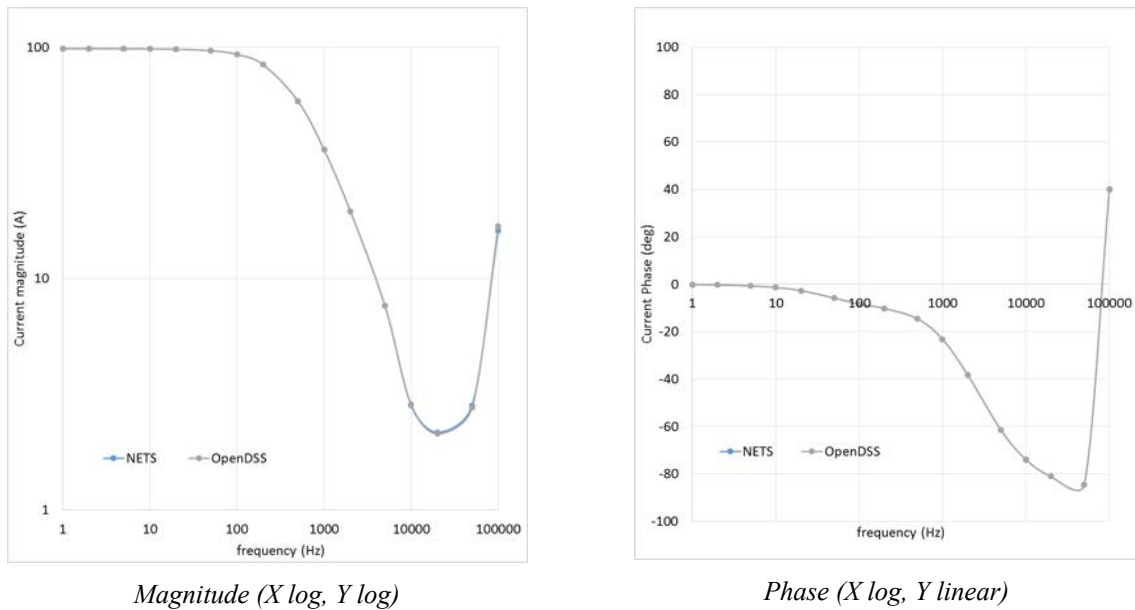


Figure 5-36: Graphical differences between phase A core currents at difference frequencies in case of single bonding, NETS vs OpenDSS (NETS = azure, OpenDSS = grey)

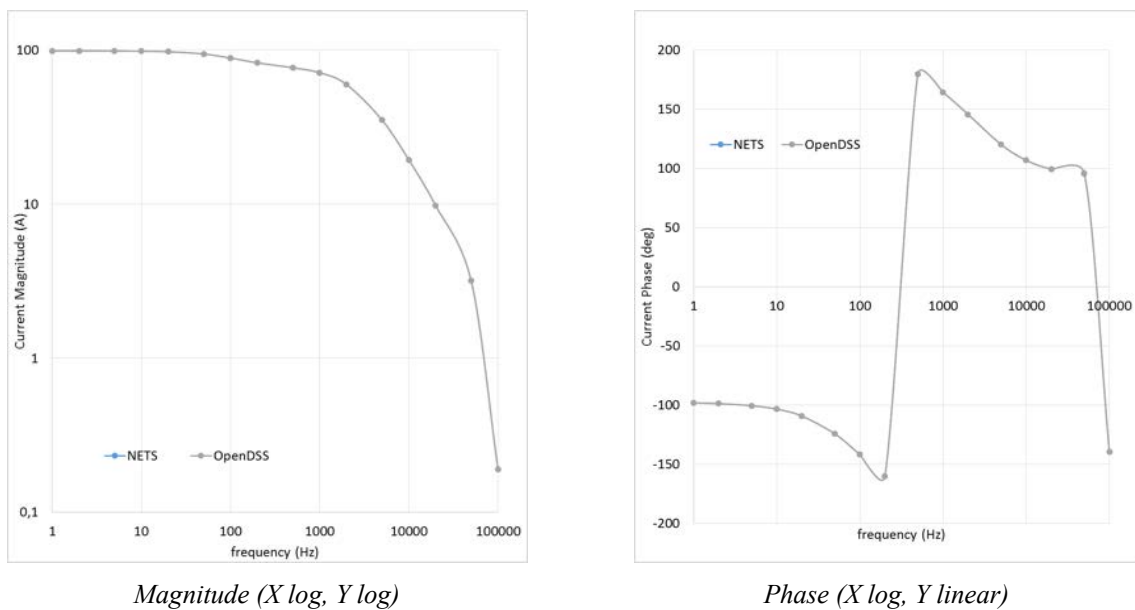


Figure 5-37: Graphical differences between phase A screen currents at difference frequencies in case of single bonding, NETS vs OpenDSS (NETS = azure, OpenDSS = grey)

As expected, with the single bonding, currents along the screens are very low and negligible at low frequency.

This bonding system is often used in case of short cables.

In case of long cables, this bonding system is not used because the voltages induced along screens could be dangerous.

Anyway, single bonding does not allow the drainage of fault currents in case of single-phase to earth fault.

5.2.2 Underground cables, various condition – NETS vs OpenDSS

In the following, a calculation taking into account a medium length underground cable is shown in order to verify the agreement of the results obtained using NETS and OpenDSS (EPRI) in various conditions.

The case study is quite simple and includes a real three-phase feeder and an underground cable 30 [km] long, with one or two complete intermediate transpositions. The bonding system is solid bonding at the cable ends while intermediate transposition points are connected to earth through a voltage limiter, and so in normal conditions, they are insulated to earth.

The general layout is represented in in the following figure.

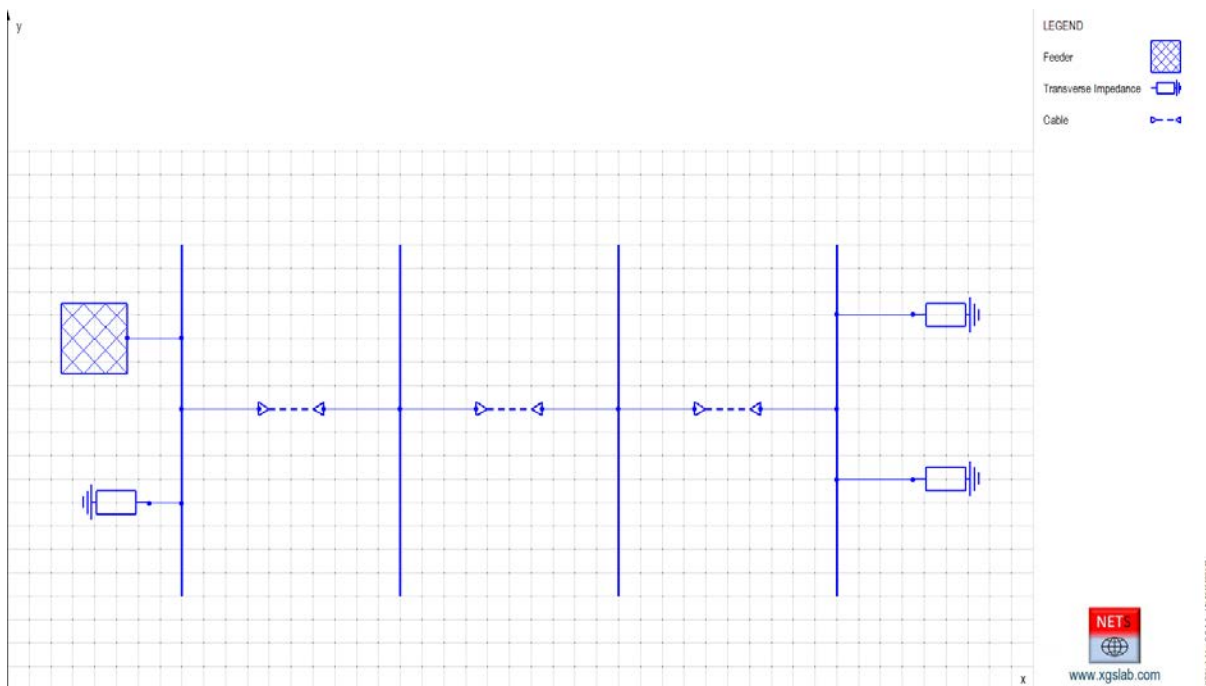


Figure 5-38: Single Line Diagram of Feeder + Underground Cable + Intermediate Transpositions + Solid Bonding + Load

In the following the main input data.

Feeder

Main input data:

- Phases number: 3 (symmetrical and balanced)
- Rated line voltage: 132 [kV]
- Short circuit power: 5000 [MVA]
- $X/R = 20$
- $Z_e = 0.1 [\Omega]$

The equivalent internal impedance of the feeder can be calculated with the formulas (5.2) and (5.3).

It follows:

- $Z = 3.485 (0.04994 + j 0.9988) = 0.1740 + j 3.480 [\Omega]$ (for all phases)

Underground Cable

- Main input data:
- Phases numbers: 3
- Rated line voltage = 132 [kV]
- Frequency = 50 [Hz]
- Low frequency soil resistivity = 100 [Ωm]
- High frequency soil relative permittivity = 6
- Line length = 30 [km]
- Phases conductors layout: A (left), B (center), C (right)
- Phases conductors depth = 1 [m]
- Phase conductor horizontal distance = 0.5 [m]
- Core: copper with external diameter = 34.2 [mm], cross section 800 [mm²], AC resistance 0.0326 [Ω/km] at 90 [°C], inductance 0.360 [mH/km], capacitance 0.212 [$\mu\text{F}/\text{km}$]
- Insulating: XLPE (resistivity 10^{15} [Ωm], relative permittivity 2.3) with thickness 19.4 [mm] including semi-conductive screens
- Screen: copper wires with external diameter 74 [mm], cross section 50 [mm²]
- Sheath: Polyethylene (resistivity 10^7 [Ωm], relative permittivity 2.3) with thickness 4 [mm]
- Outer diameter: 82 [mm]
- Trasposition locations: first step 10+10+10 [km], second step 2·(5+5+5) [km]
- Voltage Limiter Triggering: 1500 [V]
- Resistance to earth of each grounding system: 1 [Ω]

The resistance of cores and screens has to be referred to the operative temperature 90 [°C] using the formula (5.1).

5.2.2.1 Steady state condition

The steady state condition is represented by the following three-phase balanced load:

- $S = 50$ [MVA] referred to the rated voltage
- $\cos \varphi = 0.8$

The steady state condition can be represented using a transverse impedance with:

- $Z = 348.5 (0.8 + j 0.6) = 278.8 + j 209.1$ [Ω] (for all phases)
- $Z_e = 1$ [$M\Omega$]

The screen cables are connected together at the cable ends and then to earth using a transverse impedance with:

- $Z = 0.01$ [Ω]
- $Z_e = 1$ [Ω] (resistance to earth of terminal substations)

In the following, a resistance 0.01 [Ω] represents a short circuit condition.

The phase voltage and currents calculated with NETS and OpenDSS are displayed, in the following table.

Table 5-10: Current and voltage variations along the underground cable in steady state condition, NETS vs OpenDSS

Cell and Phase	NETS				OpenDSS			
	I [A]	L [deg]	U [V]	L [deg]	I [A]	L [deg]	U [V]	L [deg]
Core_in A	172.1	-4.348	76137	-0.448	172.2	-4.400	76137	-0.400
Core_in B	172.9	-124.3	76137	-120.5	172.9	-124.3	76137	-120.4
Core_in C	172.7	115.5	76135	119.6	172.8	115.5	76135	119.6
Screen_in A	38.10	-67.67	3.914	-116.1	29.02	-42.10	4.772	-119.8
Screen_in B	37.22	176.2	4.075	-107.2	26.20	-164.2	4.669	-114.1
Screen_in C	43.95	56.52	4.609	-113.2	31.45	79.3	5.145	-115.5
Core_out A	215.9	141.8	75264	-1.348	216.1	141.7	75308	-1.400
Core_out B	216.6	21.88	75465	-121.3	216.7	21.90	75497	-121.3
Core_out C	216.7	-98.34	75529	118.5	216.9	-98.40	75590	118.5
Screen_out A	17.80	-62.47	4.986	59.86	28.62	-106.2	5.170	66.5
Screen_out B	17.30	172.0	4.966	56.27	26.26	133.3	4.791	63.10
Screen_out C	11.17	55.58	4.781	58.15	24.31	9.300	4.757	68.50

It is interesting to note currents grow significantly along cable and load currents are higher than corresponding feeder currents. This is due to the cable capacitance.

The agreement between results provided by NETS and OpenDSS is excellent for cores but not adequate for screens.

The reason about this difference is unexpected and is related to the conductance between screen and earth.

As known, OpenDSS does not consider insulating conductance. The conductance effects are in general negligible but in case of long cables these effects cannot be neglected for a rigorous simulation.

Using a resistivity 10^{15} [Ωm] for the polyethylene sheath the conductance between screen and earth is very low and negligible for practical applications.

In these cases, the phase voltage and currents calculated with NETS and OpenDSS are displayed, in the following table.

Table 5-11: Current and voltage variations along the underground cable, neglecting the conductance effect between screen and earth, NETS vs OpenDSS

Cell and Phase	NETS				OpenDSS			
	I [A]	L [deg]	U [V]	L [deg]	I [A]	L [deg]	U [V]	L [deg]
Core_in A	172.2	-4.376	76137	-0.448	172.2	-4.400	76137	-0.400
Core_in B	172.9	-124.3	76137	-120.5	172.9	-124.3	76137	-120.4
Core_in C	172.8	115.5	76135	119.6	172.8	115.5	76135	119.6
Screen_in A	29.01	-42.05	4.855	-119.7	29.02	-42.10	4.772	-119.8
Screen_in B	36.18	-164.3	4.753	-114.1	26.20	-164.2	4.669	-114.1
Screen_in C	31.48	79.28	5.229	-115.5	31.45	79.3	5.145	-115.5
Core_out A	216.1	141.7	75308	-1.382	216.1	141.7	75308	-1.400
Core_out B	216.7	21.86	75496	-121.3	216.7	21.90	75497	-121.3
Core_out C	216.8	-98.36	75590	118.5	216.9	-98.40	75590	118.5
Screen_out A	28.65	-106.2	5.253	66.51	28.62	-106.2	5.170	66.5
Screen_out B	26.24	133.4	4.874	63.24	26.26	133.3	4.791	63.10
Screen_out C	24.29	9.214	4.841	68.50	24.31	9.300	4.757	68.50

The agreement between results provided by NETS and OpenDSS are excellent for both cores and screens.

A consideration about screen currents is treated in 7.1.

5.2.2.2 Phase to earth fault condition

In the following the calculations have been performed using a resistivity 10^{15} [Ωm] for the polyethylene sheath in order to have a conductance negligible for practical applications and a better agreement with OpenDSS results.

A single transposition (10+10+10 [km]) has been used in the following.

The phase to earth fault condition can be represented modifying the transverse impedance related to the screen connection at the side out of the underground cable and using a new transverse impedance with:

- $Z = 0.01$ [Ω] (for all screens)
- $Z = 0.01$ [Ω] (for the fault phase, for instance A)
- $Z_e = 1$ [Ω] (resistance to earth)

The Single Line Diagram is the same of the previous case.

The phase voltage and currents calculated with NETS and OpenDSS are displayed, in the following table.

Table 5-12: Current and voltage variations along the underground cable in phase to earth fault condition, NETS vs OpenDSS

Cell and Phase	NETS				OpenDSS			
	I [A]	\angle [deg]	U [V]	\angle [deg]	I [A]	\angle [deg]	U [V]	\angle [deg]
Core_in A	6223	-61.11	57142	-9.026	6236	-60.9	57139	-9.100
Core_in B	187.2	-110.5	75964	-120.9	187.1	-110.6	75964	-120.9
Core_in C	132.0	103.6	76681	119.7	132.2	103.7	76683	119.7
Screen_in A	1788	135.7	5533	-44.58	1794	135.6	5553	-44.70
Screen_in B	1855	136.2	5534	-44.58	1861	136.0	5553	-44.70
Screen_in C	1873	134.4	5534	-44.59	1880	134.2	5554	-44.80
Core_out A	6259	118.7	2044	-122.3	6271	118.8	2015	-122.2
Core_out B	174.3	32.88	68472	-144.3	174.2	32.90	68354	-144.4
Core_out C	220.4	-117.5	104094	116.9	220.6	-117.5	104290	116.8
Screen_out A	1809	-42.65	2013	-124.4	1816	-42.80	1983	-124.3
Screen_out B	1844	-42.52	2013	-124.4	1851	-42.70	1983	-124.3
Screen_out C	1867	-41.83	2013	-124.4	1873	-42.00	1983	-124.3

The agreement between results provided by NETS and OpenDSS are excellent for both cores and screens.

In previous condition, the potentials of screens at the transposition points (10 and 20 [km]) are displayed, in the following table.

Table 5-13: Potential rise in cable screen transposition points, NETS vs OpenDSS

Cell and Phase	NETS		OpenDSS	
	U [V]	∠ [deg]	U [V]	∠ [deg]
Screen_A Bus 2 in (D)	8842	-123.7	8872	-122.1
Screen_B Bus 2 in (E)	4897	-19.90	5066	-21.40
Screen_C Bus 2 in (F)	7163	-10.22	7278	-11.5
Screen_A Bus 3 in (E)	6408	-131.4	6355	-130.0
Screen_B Bus 3 in (F)	7828	8.960	7880	8.400
Screen_C Bus 3 in (D)	4813	-113.6	4906	-112.8

The little differences between results provide by NETS and OpenDSS can be also related to the little resistance 1 [mΩ] used in OpenDSS at any transposition.

Anyway, as expected, all the voltage limiter in these conditions will trigger.

This new scenario with voltage limiter triggered is represented in the following figure.

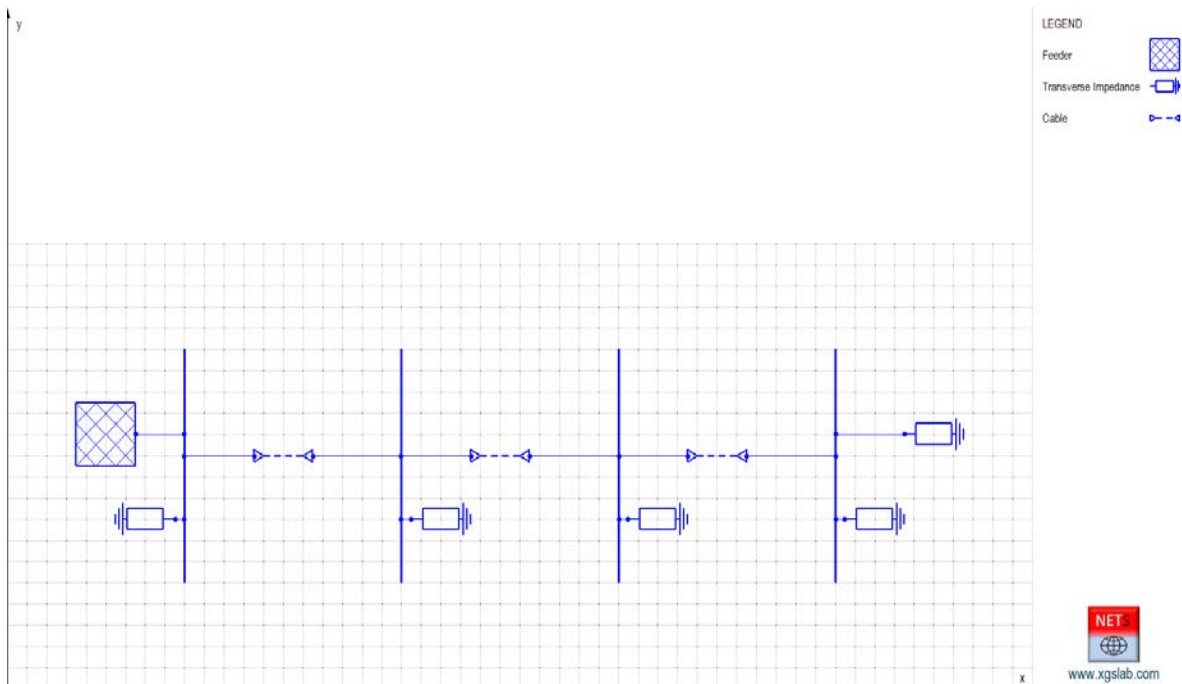


Figure 5-39: Single Line Diagram of Feeder + Underground Cable + Intermediate Transpositions with Voltage Limiter Triggered + Solid Bonding + Load

The phase voltage and currents calculated with NETS and OpenDSS are displayed, in the following table.

Table 5-14: Current and voltage variations along the underground cable with voltage limiter triggered, NETS vs OpenDSS

Cell and Phase	NETS				OpenDSS			
	I [A]	∠ [deg]	U [V]	∠ [deg]	I [A]	∠ [deg]	U [V]	∠ [deg]
Core_in A	6104	-54.49	58987	-10.72	6115	-54.30	59007	-10.80
Core_in B	186.1	-109.7	76040	-120.9	186.1	-109.8	76041	-120.9
Core_in C	119.3	104.9	76690	119.7	119.5	104.9	76691	119.7
Screen_in A	3024	169.7	5212	-31.95	3028	169.6	5237	-32.40
Screen_in B	1520	129.4	5198	-32.12	1533	128.9	5224	-32.50
Screen_in C	1132	113.6	5193	-32.14	1149	113.2	5219	-32.50
Core_out A	6134	125.2	1576	-113.4	6146	125.4	1575	-112.9
Core_out B	176.2	32.88	72483	-141.5	176.1	32.90	72379	-141.6
Core_out C	209.1	-116.1	97384	120.3	209.3	-116.1	97561	120.2
Screen_out A	3028	-16.15	1550	-116.4	3032	-16.00	1549	-116.0
Screen_out B	1638	-60.21	1536	-115.8	1640	-60.10	1535	-115.4
Screen_out C	1325	-71.57	1535	-115.6	1328	-71.40	1534	-115.2

The agreement between results provided by NETS and OpenDSS are excellent for both cores and screens.

The fault to earth fault conditions are the most interesting for practical applications and allow to evaluate the split factor related to screens.

In the specific case:

- Fault current magnitude (core out phase A): $I_f = 6134 \text{ [A]} \angle 125.2 \text{ [deg]}$
- Current to earth at line side out = $I_e = 1545 \text{ [A]} \angle 64.73 \text{ [deg]}$
- Split factor = $S_f = I_e / I_f = 1545 / 6134 = 0.2519$

In general, in high voltage cables, split factor could be very low.

The current to earth is in general a little fraction of the fault current.

Then, the evaluation of the split factor is crucial in order to avoid oversizing of grounding systems.

5.3 Transformers

In this paragraphs, two transformers families are took into consideration: in 5.3.1, will be shown a comparison with the typical European distribution transformer while, in 5.3.2, will be shown a rapid comparison about ZigZag transformers.

5.3.1 Two windings transformer

In the following, a calculation taking into account a distribution transformer is shown in order to verify the agreement of the results obtained using NETS and OpenDSS (EPRI) in various conditions.

The case study is quite simple and includes a real three-phase feeder, a 1800 [kVA] three-phase transformer (so, a transformer for distribution systems) and balanced or unbalanced load or fault conditions.

The general layout is represented in the following figure.

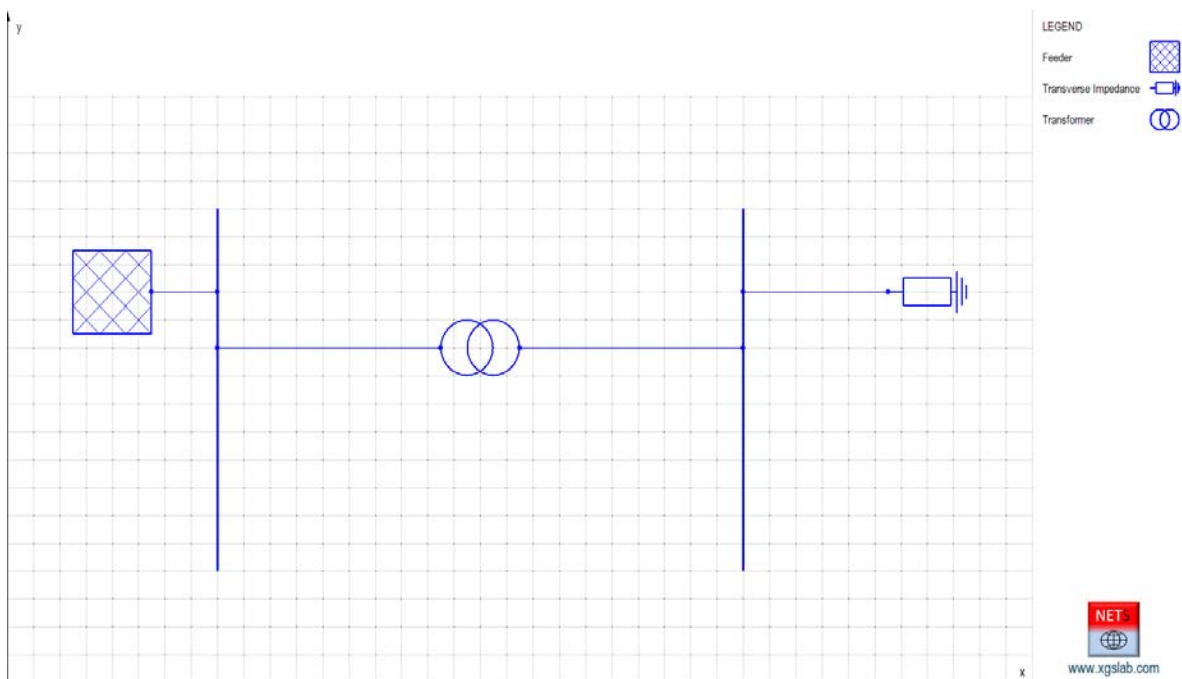


Figure 5-40: Single Line Diagram of Feeder – Transformer and Load

Feeder

Main input data:

- Phases number: 3 (symmetrical and balanced)
- Rated line voltage: 33 [kV]
- Short circuit power: 1800 [MVA]
- $X/R = 5$
- $Z_c = 100 [\Omega]$ (impedance set in order to limit the single-phase to earth current to about 200 [A])

The equivalent internal impedance of the feeder can be calculated with the formula (5.1).

It follows:

- $Z = 0.6050 (0.1961 + j 0.9806) = 0.1186 + j 0.5933 [\Omega]$ (for all phases)

Transformer

- Main input data:
- Phases numbers: 3
- Type: two windings transformer
- Apparent rated power: 1800 [kVA]
- Frequency = 50 [Hz]
- Rated line voltage in = 33 [kV]
- Rated line voltage out = 0.405 [kV]
- Short circuit voltage: 6%
- Short circuit losses: 0.902%
- No load current: 0.3%
- No load losses: 0.136%
- Connections and vector group: DYN11
- Neutral: distributed at side out (low voltage level)

5.3.1.1 Steady state condition - Balanced Load Without Neutral

The steady state condition is represented by the following three-phase balanced load (without neutral):

- $S = 1200$ [kVA]
- $\cos \varphi = 0.8$

The steady state condition can be represented using a transverse impedance referred to the rated voltage 405 V with:

- $Z = 0.1367 (0.8 + j 0.6) = 0.1094 + j 0.08202$ [Ω] (for all phases)
- $Z_e = 1$ [$M\Omega$]

The phase voltage and currents calculated with NETS and OpenDSS are displayed in the following table.

Table 5-15: Current and voltage at the primary side and at the secondary side, balanced load without neutral, in steady state condition, NETS vs OpenDSS

Cell and Phase	NETS				OpenDSS			
	I [A]	∠ [deg]	U [V]	∠ [deg]	I [A]	∠ [deg]	U [V]	∠ [deg]
Phase 1 in	20.47	-38.56	19044	-0.024	20.47	-38.60	19044	0.000
Phase 2 in	20.47	-158.6	19044	-120.0	20.47	-158.6	19044	-120.0
Phase 3 in	20.47	81.45	19044	120.0	20.47	81.40	19044	120.0
Phase 1 out	1661	171.6	227.2	28.42	1661	171.6	227.1	28.40
Phase 2 out	1661	51.56	227.2	-91.59	1661	51.60	227.1	-91.60
Phase 3 out	1661	-68.45	227.2	148.4	1661	-68.40	227.1	148.4
Neutral out	0	0	0	0	0	0	0	0

Results provided by NETS and OpenDSS are the practically same.

5.3.1.2 Steady state condition - Unbalanced Load Without Neutral

The steady state condition is represented by a three-phase unbalanced load (without neutral).

The conditions can be represented using a transverse impedance with:

- $Z_1 = 0.100 + j 0.080 \text{ } [\Omega]$
- $Z_2 = 0.080 + j 0.050 \text{ } [\Omega]$
- $Z_3 = 0.120 + j 0.100 \text{ } [\Omega]$
- $Z_e = 1 \text{ } [\text{M}\Omega]$

The phase voltage and currents calculated with NETS and OpenDSS are displayed in the following table.

Table 5-16: Current and voltage at the primary side and at the secondary side, unbalanced load without neutral, in steady state condition, NETS vs OpenDSS

Cell and Phase	NETS				OpenDSS			
	I [A]	∠ [deg]	U [V]	∠ [deg]	I [A]	∠ [deg]	U [V]	∠ [deg]
Phase 1 in	19.63	-36.72	19044	-0.024	19.63	-36.70	19044	0.000
Phase 2 in	24.74	-153.7	19042	-120.0	24.73	-153.7	19042	-120.0
Phase 3 in	23.60	74.17	19041	120.0	23.59	74.20	19041	120.0
Phase 1 out	1777	178.9	227.6	37.62	1777	179.0	227.6	37.60
Phase 2 out	2071	49.73	195.4	-98.27	2071	49.70	195.4	-98.30
Phase 3 out	1671	-74.81	261.0	145.0	1671	-74.80	261.0	145.0
Neutral out	0	0	0	0	0	0	0	0

Again, results provided by NETS and OpenDSS are practically the same.

5.3.1.3 Steady state condition - Unbalanced Load With Neutral

The steady state condition is represented by a three-phase unbalanced load (with neutral).

The conditions can be represented using a transverse impedance with:

- $Z_1 = 0.100 + j 0.080 \text{ } [\Omega]$
- $Z_2 = 0.080 + j 0.050 \text{ } [\Omega]$
- $Z_3 = 0.120 + j 0.100 \text{ } [\Omega]$
- $Z_4 = 0.001 \text{ } [\text{m}\Omega]$
- $Z_e = 1 \text{ } [\text{M}\Omega]$

The phase voltage and currents calculated with NETS and OpenDSS are displayed in the following table.

Table 5-17: Current and voltage at the primary side and at the secondary side, unbalanced load with neutral, in steady state condition, NETS vs OpenDSS

Cell and Phase	NETS				OpenDSS			
	I [A]	∠ [deg]	U [V]	∠ [deg]	I [A]	∠ [deg]	U [V]	∠ [deg]
Phase 1 in	19.83	-37.59	19044	0	19.83	-37.60	19044	0
Phase 2 in	24.90	-152.0	19043	-120.0	24.89	-152.0	19043	-120.0
Phase 3 in	24.60	75.23	19041	120.0	24.59	75.20	19041	120.0
Phase 1 out	1769	169.7	226.5	28.36	1769	169.7	226.5	28.40
Phase 2 out	2385	55.54	224.9	-92.46	2384	55.50	224.9	-92.50
Phase 3 out	1458	-71.12	227.7	148.7	1457	-71.10	227.6	148.7
Neutral out	906.7	-95.10	0	84.90	906.7	-95.10	0	84.80

Again, results provided by NETS and OpenDSS are practically the same.

5.3.1.4 Phase to earth fault condition

The initial condition is represented by the previous case (unbalanced load with neutral).

The phase to earth fault condition can be represented using an additional transverse impedance with:

- $Z = 0.01 \text{ } [\Omega]$ (for the fault phase, for instance A)
- $Z_e = 10.00 \text{ } [\Omega]$ (resistance to earth at the fault point)

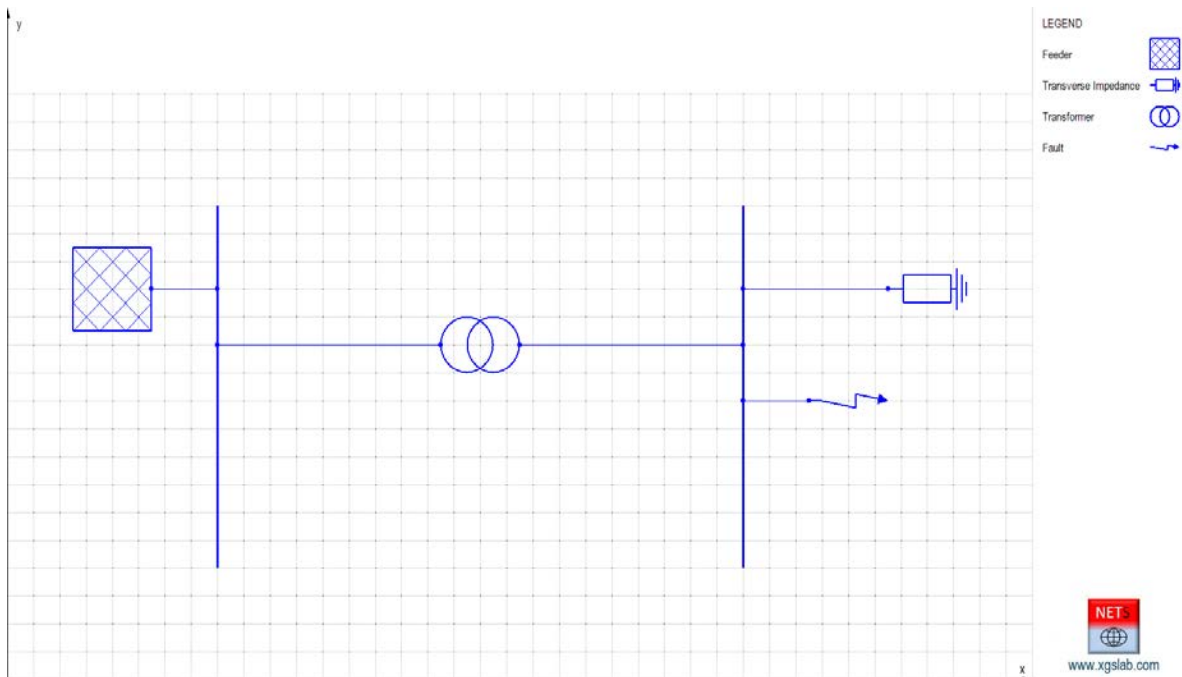


Figure 5-41: Single Line Diagram of Feeder – Transformer, Load and Fault

The phase voltage and currents calculated with NETS and OpenDSS are displayed in the following table.

Table 5-18: Current and voltage at the primary side and at the secondary side, balanced load without neutral in phase to earth fault condition, NETS vs OpenDSS

Cell and Phase	NETS				OpenDSS			
	I [A]	L [deg]	U [V]	L [deg]	I [A]	L [deg]	U [V]	L [deg]
Phase 1 in	309.4	-51.98	18886	-0.255	309.4	-52.00	18886	-0.300
Phase 2 in	295.2	-131.8	18898	-119.7	295.2	-131.8	18898	-119.7
Phase 3 in	24.59	75.31	19041	120.0	24.58	75.30	19041	120.0
Phase 1 out	42292	128.7	0.042	-51.30	42290	128.7	0	-51.30
Phase 2 out	2379	55.81	224.4	-92.19	2379	55.80	224.4	-92.20
Phase 3 out	1453	-71.38	227.0	148.40	1453	-71.40	227.0	148.40
Neutral out	41665	-53.76	0.042	128.7	41664	-53.80	0	128.7

Again, results provided by NETS and OpenDSS are practically the same.

5.3.2 Three windings transformers

In the following, a calculation taking into account two distribution transformers is shown in order to verify the agreement of the results obtained using NETS and OpenDSS (EPRI) with balanced and unbalanced conditions.

The transformers “YZ” and “Dz” have been treated separately because they are based on a specific model based on three windings transformers.

The general layout is represented in the following figure.

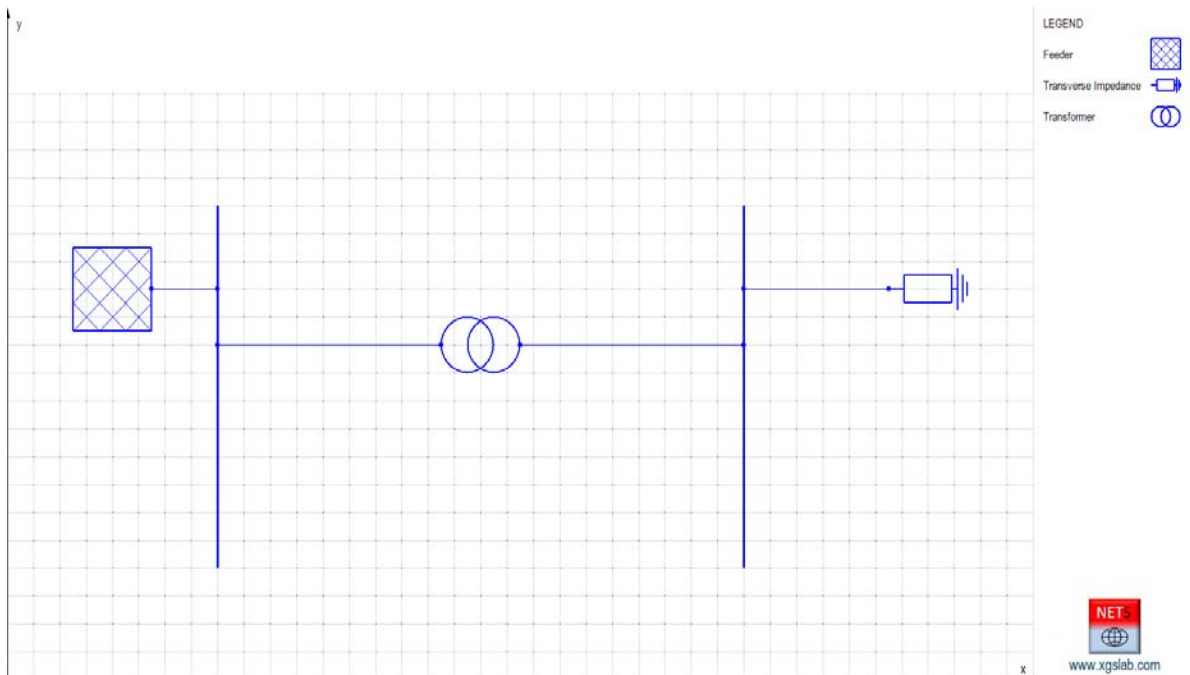


Figure 5-42: Single Line Diagram of Feeder – Transformer and Load

In the following the main input data.

Feeder

Main input data:

- Ideal Voltage Source
- Phases number: 3 (symmetrical and balanced)
- Rated line voltage: 33 [kV]

Transformer

Main input data:

- Phases numbers: 3
- Type: two windings transformer
- Apparent rated power: 1800 [kVA]

- Frequency = 50 [Hz]
- Rated line voltage in = 33 [kV]
- Rated line voltage out = 0.405 [kV]
- Short circuit voltage: 6%
- Short circuit losses: 0.902%
- No load current: 0.3%
- No load losses: 0.136%
- Connections and vector group: case A Yzn1, case B Dyn0
- Neutral: distributed at side out (low voltage level)

5.3.2.1 ZigZag transformer Yzn1

The balanced conditions are simulated using a resistive three-phase balanced load with neutral distributed and insulated to earth.

The load resistances for each phase vary from:

- $R = 0.001$ [m Ω] (short circuit condition)
- $R = 1$ [k Ω] (no load condition)

The unbalanced conditions are simulated using a resistive three-phase unbalanced load with neutral distributed and insulated to earth.

The load resistances for the phase 1 vary from:

- $R = 0.001$ [m Ω] (short circuit condition)
- $R = 1$ [k Ω] (no load condition)

The load resistances for the phases 2 and 3 remain fixed and equal to:

- $R = 1$ [M Ω] (no load condition)

The following figure represents the comparison between currents at the primary side in graphical way:

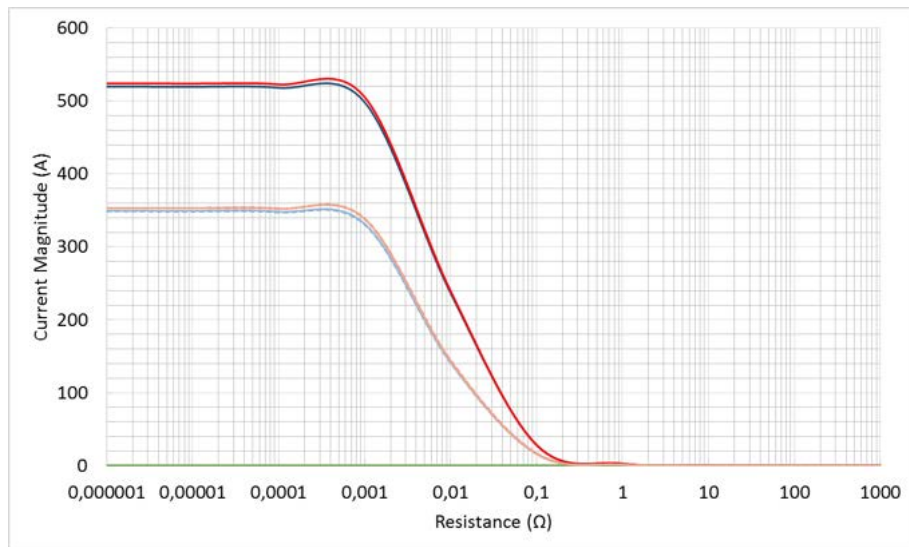


Figure 5-43: Graphical comparison between primary side currents in case of Yzn1 transformer, NETS vs OpenDSS (X log, Y linear)

Balanced condition:

- NETS: continuous blue line (all phases)
- OpenDSS: continuous red line (all phases)

Unbalanced condition:

- NETS: phase 1 and e 3 continuous light blue lines (overlapped), phase 2 continuous green line
- OpenDSS: phase 1 and e 3 continuous light red lines (overlapped), phase 2 continuous green line

As expected with unbalanced conditions (in this case a single-phase load at the secondary side), the currents at the primary side enters from the fase 1 and exits phase 3. The phase 2 is not interested to the load current.

Results provided by NETS and OpenDSS are practically same.

The maximum difference in results is related to unbalanced conditions and is lower than 2%.

5.3.2.2 ZigZag transformer Dzn0

The balanced and unbalanced conditions are represented as in the previous case A.

The following figure represents the comparison between currents at the primary side in graphical way:

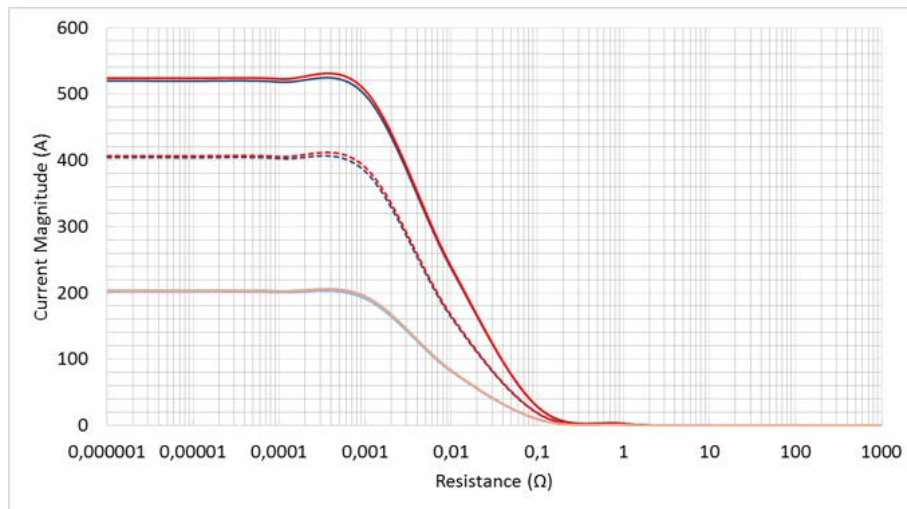


Figure 5-44: Graphical comparison between primary side currents in case of Dzn0 transformer, NETS vs OpenDSS (X log, Y linear)

Balanced condition:

- NETS: continuous blue line (all phases)
- OpenDSS: continuous red line (all phases)

Unbalanced condition:

- NETS: phase 1 dashed blue line, phases 2 and 3 continuous light blue lines (overlapped)
- OpenDSS: phase 1 dashed red line, phases 2 and 3 continuous light red lines (overlapped)

As expected with unbalanced conditions (in this case a single-phase load at the secondary side), the currents at the primary side enters from the phase 1 and exits in equal parts from phases 2 and 3.

Results provided by NETS and OpenDSS are practically same.

The maximum difference in results is related to unbalanced conditions and is lower than 2%.

5.4 Meshed Network

The scope of the following example is the calculation of the fault current distribution and of the split factor in case of single-phase fault current in a substation fed by a simple meshed network.

The results have been compared with results provided by OpenDSS (EPRI).

The general layout is represented in the following figure.

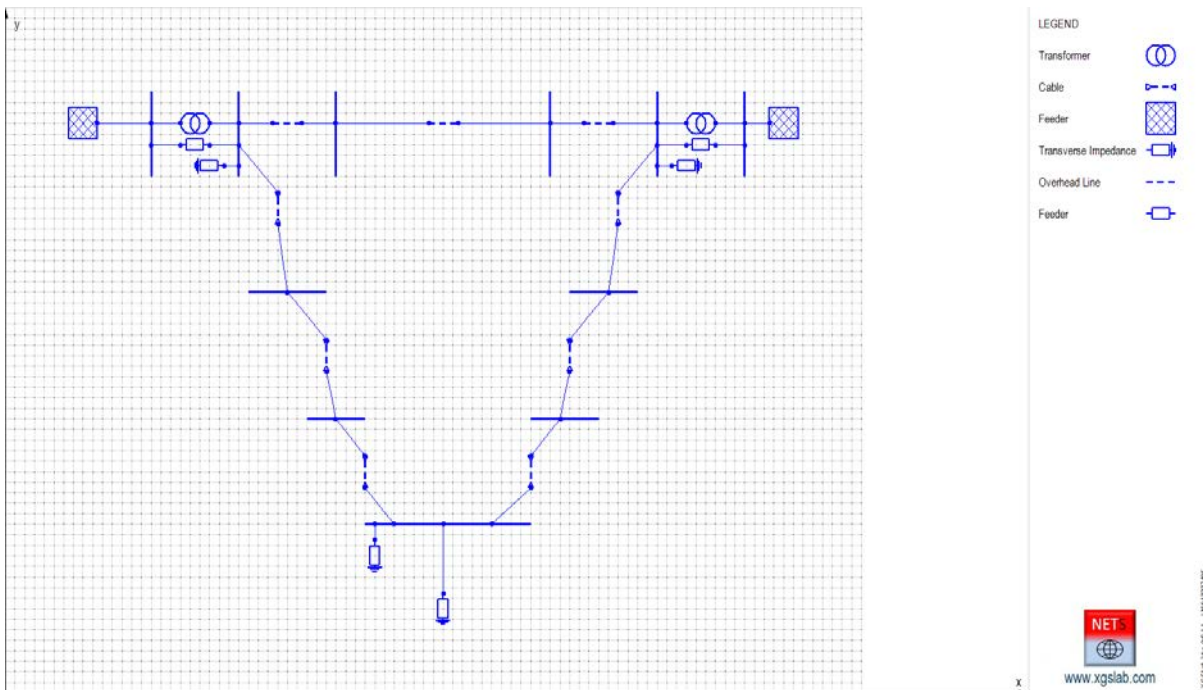


Figure 5-45: Single Line Diagram of a Meshed Network

The meshed network with a rated line voltage 132 [kV] is fed by two three-phase feeders and with two substations 400/132 [kV] and 230/1132 [kV] respectively and includes an overhead line 40 [km] long, two underground cables 30 [km] long and a substation with a load 10 [MVA].

In the following the main input data.

Feeder 400 [kV] (left side)

Main input data:

- Phases number: 3 (symmetrical and balanced)
- Rated line voltage: 400 [kV]
- Short circuit power: 40000 [MVA]
- $X/R = 25$
- $Z_c = 0.1 [\Omega]$

The equivalent internal impedance of the feeder can be calculated as in (5.1).

It follows:

- $Z = 4.000 (0.03997 + j 0.9992) = 0.1599 + j 3.997 = \text{about } j4.000 [\Omega]$ (for all phases)

Feeder 230 kV (right side)

Main input data:

- Phases number: 3 (symmetrical and balanced)
- Rated line voltage: 230 [kV]
- Short circuit power: 20000 [MVA]
- $X/R = 20$
- $Z_e = 0.1 [\Omega]$

As the same as before, the equivalent internal impedance is:

- $Z = 2.645 (0.04994 + j 0.9988) = 0.1321 + j 2.642 [\Omega] = \text{about } j2.645 [\Omega]$ (for all phases)

Substation 400/132 kV

- Main input data for transformer:
- Phases numbers: 3
- Type: two windings transformer
- Apparent rated power: 50 [MVA]
- Frequency = 50 [Hz]
- Rated line voltage in = 400 [kV]
- Rated line voltage out = 132 [kV]
- Short circuit voltage: 12%
- Short circuit losses: 0.4%
- No load current: 0.6%
- No load losses: 0.06%
- Connections and vector group: Yy0
- Neutral: grounded at both sides with a common grounding resistance: 1 [Ω]

Substation 230/132 kV

- Main input data for transformer:
- Phases numbers: 3
- Type: two windings transformer
- Apparent rated power: 20 [MVA]
- Frequency = 50 [Hz]
- Rated line voltage in = 230 [kV]
- Rated line voltage out = 132 [kV]
- Short circuit voltage: 12%
- Short circuit losses: 0.4%
- No load current: 0.8%
- No load losses: 0.08%

- Connections and vector group: Yy0
- Neutral: grounded at both sides with a common grounding resistance: 1 [Ω]

Overhead Line

The Figure 5-46 represents the tower lattice layout and the distances between phase conductors and overhead earth wire.

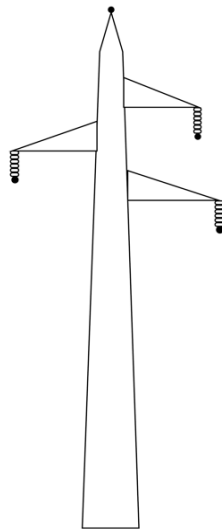


Figure 5-46: Tower lattice layout

Main input data:

- Phases numbers: 3
- Rated line voltage = 132 [kV]
- Frequency = 50 [Hz]
- Low frequency soil resistivity = 100 [Ωm]
- High frequency soil relative permittivity = 6
- Line length = 40 [km]
- Span length = 250 [m] (160 spans)
- Phases conductors layout: A (left - down), B (right), C (left - up)
- Maximum and minimum distance to the soil surface phase A: 15.1 and 8 [m]
- Maximum and minimum distance to the soil surface phase B: 17.1 and 10 [m]
- Maximum and minimum distance to the soil surface phase C: 19.1 and 12 [m]
- Maximum and minimum distance to the soil surface overhead earth wires: 24.35 and 19.4 [m]
- Position with respect to the tower axis: A -3.50 [m], B +3.00 [m], C - 2.90 [m]
- Phase conductors: ACSR (Aluminium Conductor Steel Reinforced the steel is inside and the aluminium is outside) with external diameter = 31.5 [mm], cross section of

- steel and aluminium 65.81 and 519.5 and [mm²] respectively, resistance = 0.05564 [Ω/km] at 20 [°C]
- Overhead wires: steel and aluminium conductors with external diameter = 11.5 [mm], total cross section 80.66 [mm²]: resistance = 1.062 [Ω/km] at 20 [°C]
 - Resistance to earth of each single tower: 20 [Ω]

The limit length for lines can be evaluated as in (5.4) and, using $S = 250$ [m], $R_t = 20$ [Ω] and $R_s = 0.25 \cdot 1.062 = 0.2655$ [Ω] it follows $L =$ about 21.7 [km].

The whole line should be divided in sections with length lower than 21.7 [km].

In this example the line has been divided in 3 sections 5 + 30 + 5 [km] and results are anyway good.

This means previous limit is quite conservative but anyway, when possible it has to be respected.

The average height above ground of phase conductors and overhead earth wire can be calculated using again the formula (5.5).

If follows:

- Phase A $h = 8 + (15.1 - 8) / 3 = 10.37$ [m]
- Phase B $h = 12.37$ [m]
- Phase C $h = 14.37$ [m]
- Overhead earth wire $h = 21.05$ [m]

Underground Cables (for both cables)

- Main input data:
- Phases numbers: 3
- Rated line voltage = 132 [kV]
- Frequency = 50 [Hz]
- Low frequency soil resistivity = 100 [Ωm]
- High frequency soil relative permittivity = 6
- Line length = 30 [km]
- Phases conductors layout: A (left), B (center), C (right)
- Phases conductors depth = 1 [m]
- Phase conductor horizontal distance = 0.5 [m]
- Core: copper with external diameter = 34.2 [mm], cross section 800 [mm²]: AC resistance 0.0326 [Ω/km] at 90 [°C], inductance 0.36 [mH/km], capacitance 0.212 [μF/km]

- Insulating: XLPE (resistivity 10^{15} [Ωm], relative permittivity 2.3) with thickness 19.4 [mm] including semi-conductive screens
- Screen: copper wires with external diameter 74 [mm], cross section 50 [mm^2]
- Sheath: Polyethylene (resistivity 10^7 [Ωm], relative permittivity 2.3) with thickness 4 [mm]
- Outer diameter: 82 [mm]
- Trasposition of screen: at 10 and 20 [km]
- Resistance to earth of grounding system at transposition points: 10 [Ω]
- Voltage Limiter Triggering: 1500 [V]

Load

- Main input data:
- Phases numbers: 3
- Rated line voltage: 132 [kV]
- Apparent power: 10 [MVA]
- $\cos \varphi = 0.8$
- Grounding resistance: 1 [$\text{M}\Omega$]

The load can be represented using a transverse impedance referred to the rated line voltage 132 [kV] with:

- $Z = 1742 (0.8 + j 0.6) = 1394 + j 1045$ [Ω] (for all phases)
- $Z_e = 1$ [$\text{M}\Omega$]

In the following the main results in various conditions.

5.4.1 Steady state condition

The phase voltage and currents calculated with NETS and OpenDSS are displayed in the following table.

Table 5-19: Current and voltage trends along phase A of longitudinal elements of the network in steady state condition, NETS vs OpenDSS

Cell and Phase	NETS				OpenDSS			
	I [A]	∠ [deg]	U [V]	∠ [deg]	I [A]	∠ [deg]	U [V]	∠ [deg]
Overhead Line - Phase A in	31.27	78.23	83537	-1.067	30.86	78.40	83464	-1.100
Overhead Line – OHEW in	0.070	95.60	1.342	-36.62	0.09679	125.6	1.353	-35.70
Overhead Line - Phase A out	21.06	-105.2	83904	-1.156	20.66	-104.9	83833	-1.200
Overhead Line - OHEW out	0.715	-49.10	0.642	-26.79	0.6789	-51.70	0.6669	-25.70
Cable Left - Phase A in	145.7	80.27	83537	-1.067	145.8	80.20	83464	-1.100
Cable Left – Screen Phase A in	30.28	-46.18	1.342	-36.62	30.26	-46.20	1.353	-35.70
Cable Left - Phase A out	24.06	-154.9	84066	-1.324	24.31	-154.7	83995	-1.300
Cable Left – Screen Phase A out	31.72	-102.5	3.151	145.4	31.69	-102.5	3.095	145.4
Cable Right - Phase A in	95.58	78.46	83904	-1.156	95.27	78.60	83833	-1.200
Cable Right – Screen Phase A in	30.67	-46.64	0.642	-26.79	30.65	-46.60	0.667	-25.70
Cable Right - Phase A out	43.16	111.9	84066	-1.324	43.22	111.6	83995	-1.300
Cable Right – Screen Phase A out	31.43	-102.4	3.151	145.4	31.40	-102.4	3.095	145.4
Load - Phase A	48.26	-38.18	84066	-1.324	48.22	-38.20	83995	-1.300
Load - Phase B	48.22	-158.1	84006	-121.3	48.18	-158.1	83935	-121.2
Load - Phase C	48.29	81.90	84141	118.8	48.25	81.90	84070	118.8

Taking into account that the system is symmetrical and the load is balanced, only the values in the phase “A” are displayed in previous table. The values in the phases “B” and “C” are similar.

The agreement between NETS and OpenDSS results is excellent.

From previous table, is interesting to note that the phase potential at the load ports is higher than the rated voltage (132000 [V] line to line and then 76210 [V] phase to earth).

This is due to the so called Ferranti’s effect and then to the effects of cables capacitance and to the relatively small load.

In the following the results in same conditions but with loads 1 [MVA] and 100 [MVA] respectively.

5.4.1.1 Steady state condition, 1 [MVA] load

If the apparent power is 1 [MVA] the load can be represented using a transverse impedance referred to the rated voltage 132 [kV] with:

- $Z = 17424 (0.8 + j 0.6) = 13940 + j 10454 \text{ } [\Omega]$ (for all phases)
- $Z_e = 1 \text{ } [M\Omega]$

The phase voltage and currents calculated with NETS and OpenDSS are displayed in the following table.

Table 5-20: Load current with a 1 [MVA] load

Cell and Phase	NETS				OpenDSS			
	I [A]	∠ [deg]	U [V]	∠ [deg]	I [A]	∠ [deg]	U [V]	∠ [deg]
Load - Phase A	4.887	-37.34	85149	-0.478	4.883	-37.30	85074	-0.500
Load - Phase B	4.881	-157.3	85058	-120.4	4.877	-157.3	84983	-120.4
Load - Phase C	4.889	82.76	85196	119.6	4.885	82.80	85121	119.6

This condition is similar to a no-load condition and the Ferranti's effect is even more evident than in the previous case.

The phase to earth potential values is about 10% higher than the rated values.

5.4.1.2 Steady state condition, 100 [MVA] load

If the apparent power is 100 [MVA] the load can be represented using a transverse impedance referred to the rated voltage 132 [kV] with:

- $Z = 174 (0.8 + j 0.6) = 139.2 + j 104.5 [\Omega]$ (for all phases)
- $Z_e = 1 [M\Omega]$

The phase voltage and currents calculated with NETS and OpenDSS are displayed in the following table.

Table 5-21: Load current with a 100 [MVA] load

Cell and Phase	NETS				OpenDSS			
	I [A]	∠ [deg]	U [V]	∠ [deg]	I [A]	∠ [deg]	U [V]	∠ [deg]
Load - Phase A	424.1	-45.56	73896	-8.680	423.9	-45.60	73856	-8.700
Load - Phase B	425.4	-165.4	74075	-128.6	425.1	-165.4	74036	-128.6
Load - Phase C	425.5	74.36	74150	111.2	425.3	74.4	74110	111.2

In this condition, the voltage drop effect prevails in the Ferranti's effect and the phase potential at the load ports is just below the rated voltage.

5.4.2 Phase to earth fault condition

The phase to earth fault condition can be represented modifying the transverse impedance related to the screen cables grounding system at the load side and using a new transverse impedance with:

- $Z = 0.01 \text{ } [\Omega]$ (for all screens)
- $Z = 0.01 \text{ } [\Omega]$ (for the fault phase, for instance A)
- $Z_e = 1 \text{ } [\Omega]$ (resistance to earth of the terminal substation)

The phase voltage and currents calculated with NETS and OpenDSS are displayed in the following table.

Table 5-22: Current and voltage trends along phase A of longitudinal elements of the network in phase to earth fault condition, NETS vs OpenDSS

Cell and Phase	NETS				OpenDSS			
	I [A]	∠ [deg]	U [V]	∠ [deg]	I [A]	∠ [deg]	U [V]	∠ [deg]
Overhead Line - Phase A in	199.7	-89.47	12341	-29.13	197.6	-89.40	12240	-28.80
Overhead Line – OHEW in	111.1	-17.84	367.4	-14.32	103.2	-19.80	372.1	-14.70
Overhead Line - Phase A out	202.0	90.17	7295	-34.42	199.9	90.20	7185	-34.00
Overhead Line - OHEW out	176.8	-80.73	356.3	-68.02	169.8	-82.50	361.7	-68.20
Cable Left - Phase A in	1362	-81.93	12341	-29.13	1363	-82.00	12240	-28.80
Cable Left – Screen Phase A in	449.2	113.7	367.4	-14.32	450.3	113.4	372.1	-14.70
Cable Left - Phase A out	1370	97.83	351.1	-142.2	1371	97.80	345.2	-142.1
Cable Left – Screen Phase A out	432.7	-64.40	333.1	-148.7	433.7	-64.70	327.3	-148.8
Cable Right - Phase A in	868.9	-85.98	7295	-34.42	865.2	-85.90	7185	-34.00
Cable Right – Screen Phase A in	267.7	98.86	356.3	-68.02	266.8	98.50	361.7	-68.20
Cable Right - Phase A out	873.5	93.80	351.1	-142.2	869.7	93.80	345.2	-142.1
Cable Right – Screen Phase A out	247.7	-78.15	333.1	-148.7	246.8	-78.50	327.3	-148.8
Load - Phase A	16.32	-45.21	351.1	-142.2	16.36	-45.40	345.2	-142.1
Load - Phase B	41.64	-139.8	80344	-123.8	41.59	-139.8	80227	-123.9
Load - Phase C	43.48	62.21	88463	117.1	43.48	62.20	88570	117.2

The agreement between NETS and OpenDSS results is excellent.

In previous condition, the potentials to earth of screens at the transposition points (10 and 20 km) for both cables are displayed, in the following table.

Table 5-23: : Potential rise in cables screen transposition points, NETS vs OpenDSS

Cell and Phase	NETS		OpenDSS	
	U [V]	∠ [deg]	U [V]	∠ [deg]
Screen_A Bus n262 in (D)	1645	-163.8	1644	-162.3
Screen_B Bus n262 in (E)	772.3	-13.34	796.9	-16.10
Screen_C Bus n262 in (F)	1238	1.603	1252	-0.300
Screen_A Bus n362 in (E)	1259	-161.1	1257	-160.2
Screen_B Bus n362 in (F)	1664	0.421	1674	-0.300
Screen_C Bus n362 in (D)	775.5	-158.1	774.1	-156.7
Screen_A Bus n562 in (D)	1328	-154.8	1334	-153.6
Screen_B Bus n562 in (E)	484.7	-40.08	503.2	-42.30
Screen_C Bus n562 in (F)	786.6	-16.94	793.8	-18.80
Screen_A Bus n662 in (E)	1033	-157.7	1032	-156.9
Screen_B Bus n662 in (F)	1044	-7.453	1044	-8.100
Screen_C Bus n662 in (D)	716.9	-144.5	720.8	-143.5

Again, the agreement between NETS and OpenDSS results is excellent.

The small differences between results provided by NETS and OpenDSS could be also related to the little resistance 1 mΩ used in OpenDSS at any transposition.

Because of fault conditions, the voltage limiter in the left cable will trigger (some voltage limiter will trigger because of the triggering of the other voltage limiter).

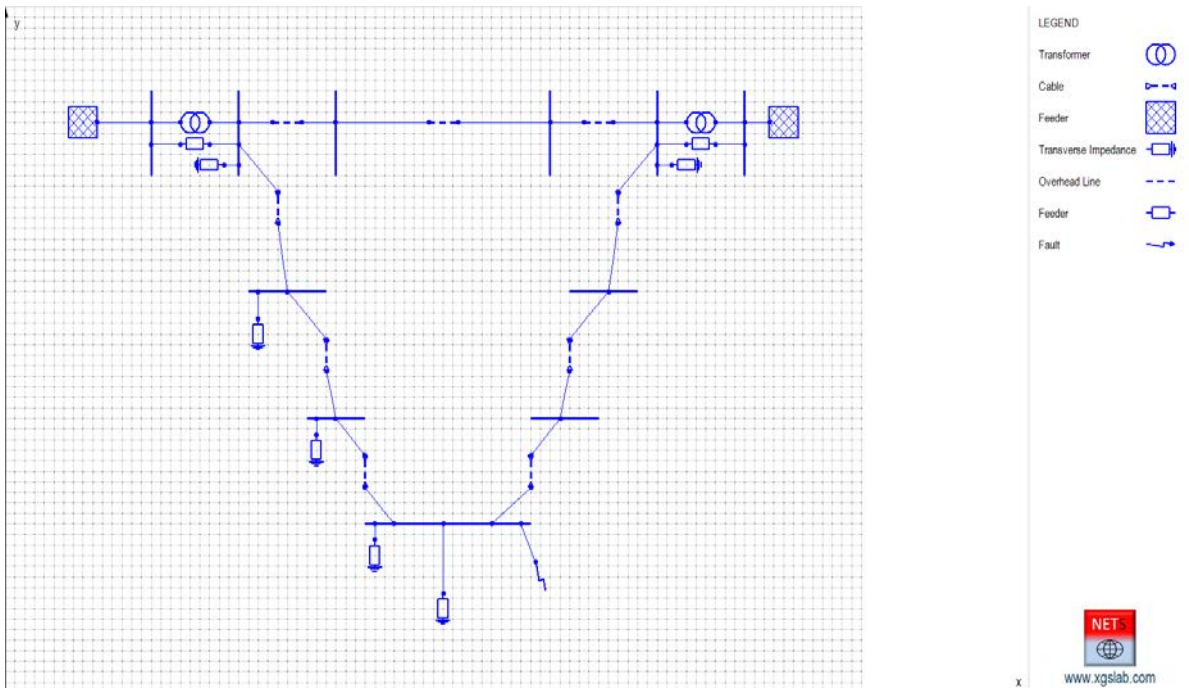


Figure 5-47: Single Line Diagram of an the Meshed Network (Voltage Limiter triggered in the Left Cable)

The phase voltage and currents calculated with NETS and OpenDSS are displayed in the following table.

Table 5-24: Current and voltage trends along phase A of longitudinal elements of the network in phase to earth fault condition with left underground cable voltage limiter triggered , NETS vs OpenDSS

Cell and Phase	NETS				OpenDSS			
	I [A]	∠ [deg]	U [V]	∠ [deg]	I [A]	∠ [deg]	U [V]	∠ [deg]
Overhead Line - Phase A in	208.1	-106.6	12931	-34.64	205.4	-106.7	12822	-34.40
Overhead Line – OHEW in	111.8	-15.20	367.5	-11.52	103.8	-17.40	372.1	-12.20
Overhead Line - Phase A out	210.7	73.21	7572	-37.34	208.0	73.10	7459	-37.00
Overhead Line - OHEW out	176.5	-79.50	357.7	-67.04	169.4	-81.30	363.1	-67.30
Cable Left - Phase A in	1381	-78.11	12931	-34.64	1383	-78.20	12822	-34.40
Cable Left – Screen Phase A in	708.4	139.3	367.5	-11.52	709.3	139.1	372.1	-12.20
Cable Left - Phase A out	1388	101.6	345.5	-142.0	1389	101.5	340.6	-141.8
Cable Left – Screen Phase A out	710.1	-39.98	328.0	-148.8	710.2	-40.1	323.0	-148.6
Cable Right - Phase A in	866.3	-89.74	7572	-37.34	861.9	-89.7	7459	-37.00
Cable Right – Screen Phase A in	268.1	100.0	357.7	-67.04	267.3	99.60	363.1	-67.30
Cable Right - Phase A out	871.1	90.03	345.5	-142.0	866.7	90.1	340.6	-141.8
Cable Right – Screen Phase A out	248.2	-77.00	328.0	-148.8	247.2	-77.30	323.0	-148.6
Load - Phase A	16.37	-44.32	345.5	-142.0	16.41	-44.50	340.6	-141.8
Load - Phase B	41.61	-139.8	80729	-123.7	41.56	-139.8	80617	-123.8
Load - Phase C	43.22	62.37	87788	117.6	43.22	62.40	87893	177.6

Again, the agreement between NETS and OpenDSS results is excellent.

The single-phase to earth fault condition is interesting for practical applications and allow to evaluate the split factor related to cables screens.

In the specific the split factor can be evaluated as in the following:

- Fault current from cable right (line out phase A): $I_f = 1388$ [A] $\angle 101.6$ [deg]
- Fault current from cable left (line out phase A): $I_f = 871.1$ [A] $\angle 90.03$ [deg]
- Fault current magnitude: $I_f = 1428$ [A]
- Current to earth magnitude: $I_e = 328$ [A]
- Split factor = $S_f = I_e / I_f = 328 / 1428 = 0.2297$

The split factor calculated with OpenDSS is:

- Split factor = $S_f = I_e / I_f = 323 / 1449 = 0.2229$

The agreement between NETS and OpenDSS results is excellent (the difference is about 3%).

CONCLUSIONS

The aim of this thesis was the study of the phase component method for the solution of unsymmetrical and unbalanced networks and the testing and validation of the new module NETS of the software XGSLab.

This work has been focused on the study of multi-conductor approach, which has been applied to study steady state currents and potentials of the network, mainly along overhead lines, underground cables and transformers.

Results are very close between the two software with all the test cases, and this means that the formulations used in the two codes are comparable. This is mainly highlighted in the frequency domain tests, because it can be noted that the formulas used in the software work well in a large range of frequencies.

It is clear that the results cannot be expected to be identical, because of the different formulas implemented and the different simplifications adopted.

Considering that OpenDSS does not allow, by default, to take into account the screened cables, it has been necessary to feed the OpenDSS script with R, X, C matrices calculated externally. These matrices were calculated with the same formulas implemented on NETS, making the underground cable case the one with the closest results between the two software.

In the two windings transformers comparison, results are the same in all conditions.

The analysis in different loading conditions, from balanced loads to short circuit cases, has allowed to test the robustness of the models implemented in the software.

Mutual couplings among the active parts and their interaction with the passive parts of the system (as overhead earth wires or cable screens) was analyzed. Knowing the feeder and load characteristics of each transversal components and their geometrical and physical parameters, it is possible to test a network in conditions as close to the real-life as possible.

As reported in 5.1.3, it is worth noting that even in case of balanced load, if the line (or a double circuit, as in the example) is displaced in a wrong way, there will be an unbalanced distribution of current in that line.

In addition, it was highlighted that, in case of screen transposition of underground cables, the screen current maintains a value very different to zero, as better described in 7.1

The under test NETS version is the first release, hence it is expected that in the future many improvements will be considered and implemented. The actual component models will be reconsidered and models with a larger frequency range to permit time domain transient analysis will be developed.

ANNEXES

7.1 Cross Bonding Transposition

As shown in 5.2.2.1 it's interesting to note that the trasposition is not so effective.

The cable is divided in three equal parts 10 [km] long and the load is balanced, so a good effets of trasposition was expected but despite that, the currents along screen are significant if compared to the phase currents. The reason of the limited effectiveness of trasposition is related to the current distribution along cores that is not uniform because the capacitance effets.

In the following, the magnitude of currents distribution along phase A and screen on phase A (the distribution is similar for phases and screens B and C, hence it is not represented) calculated with NETS.

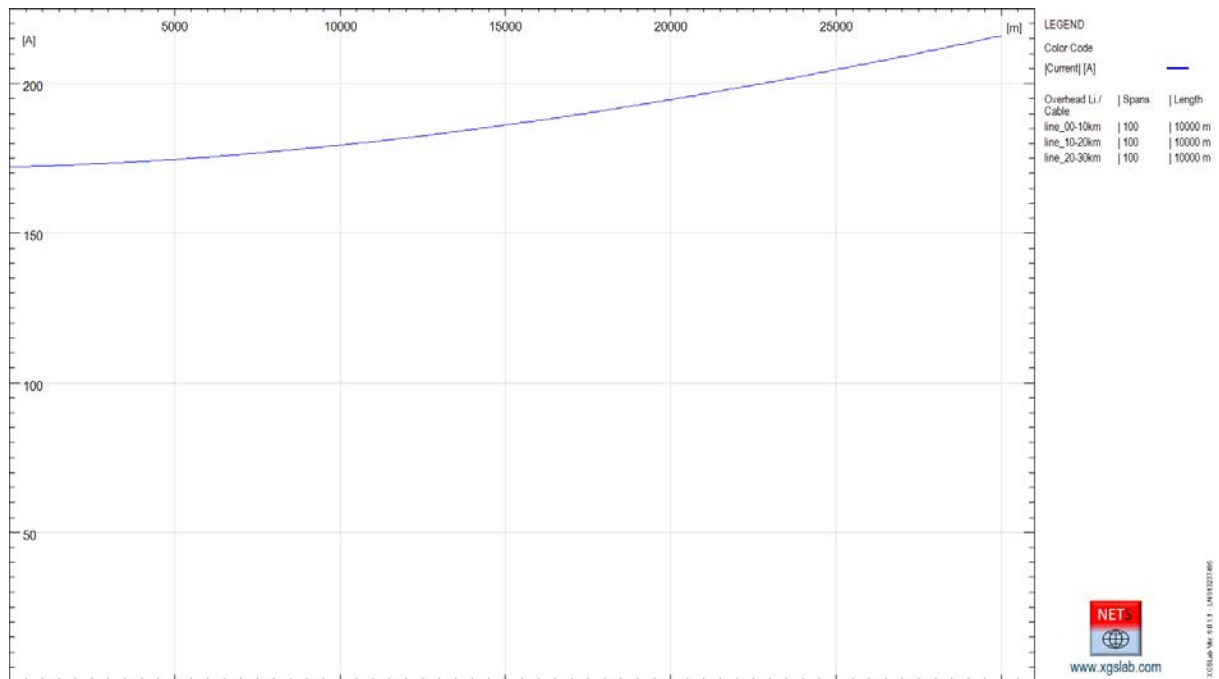


Figure 7-1: Magnitude Current Distribution along phase A – Transposition 10+10+10 [km] – NETS

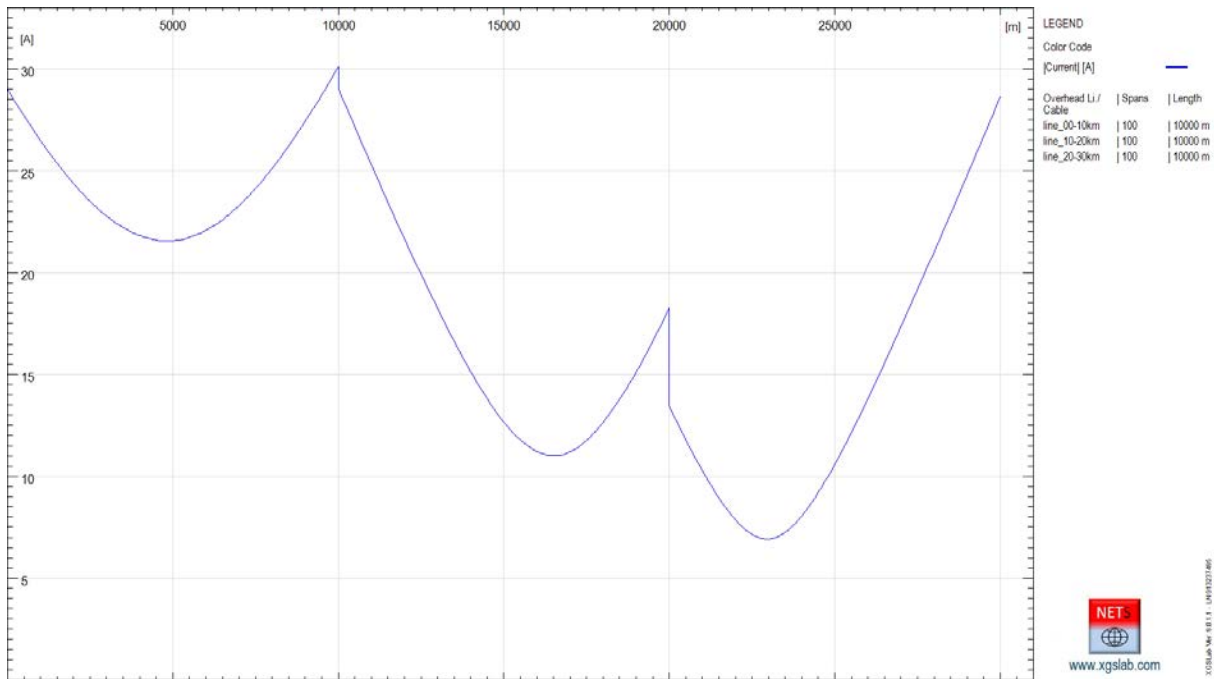


Figure 7-2: Magnitude Current Distribution along screens on phase A – Transposition 10+10+10 [km] – NETS

Of course, the discontinuity on current distribution along screen on phase A is due to the traspositons.

As expected, the trasposition is more effective if the cable is divided in six equal parts 5 [km] long. In the following, the magnitude of currents distribution along phase A and screen on phases A, B and C calculated with NETS.

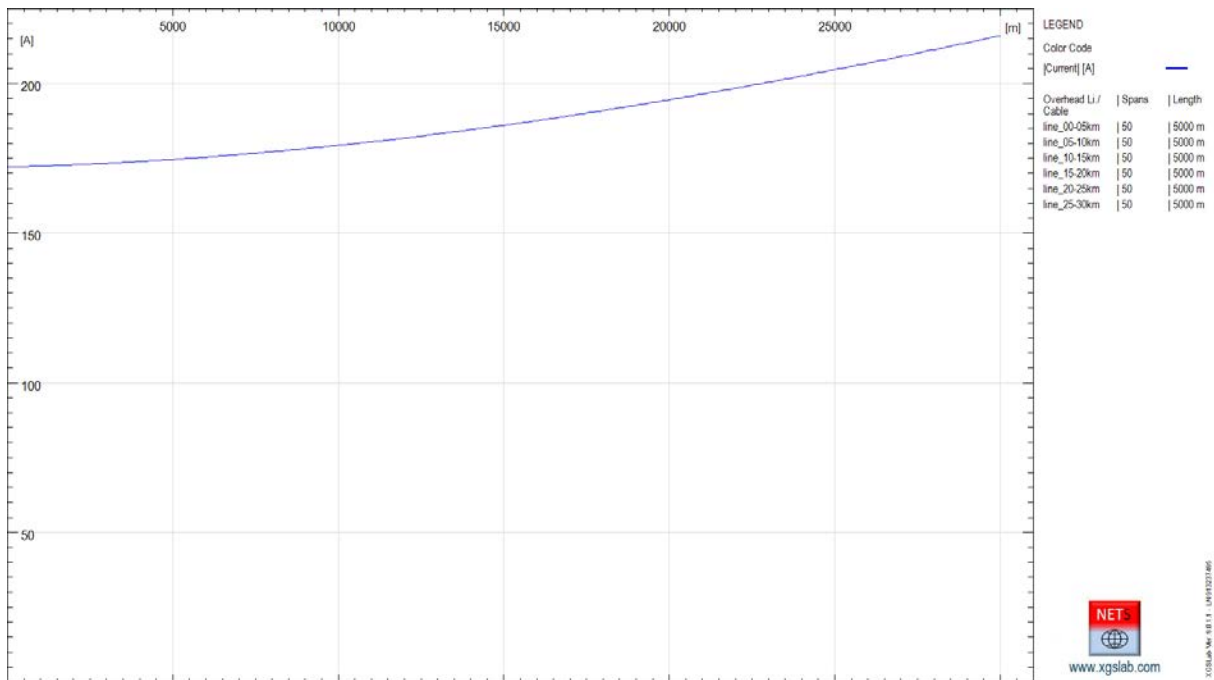


Figure 7-3: Magnitude Current Distribution along phase A – Transposition 2·(5+5+5) [km] – NETS

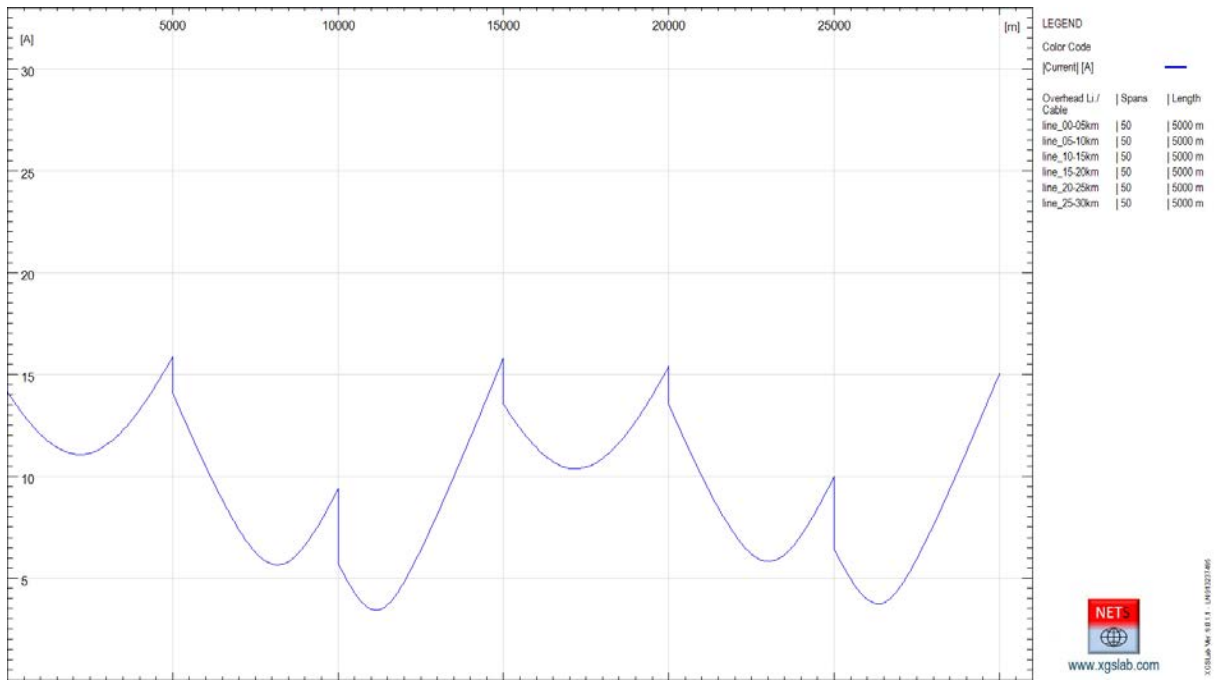


Figure 7-4: Magnitude Current Distribution along screens on phase A – Transposition 2·(5+5+5) [km] – NETS

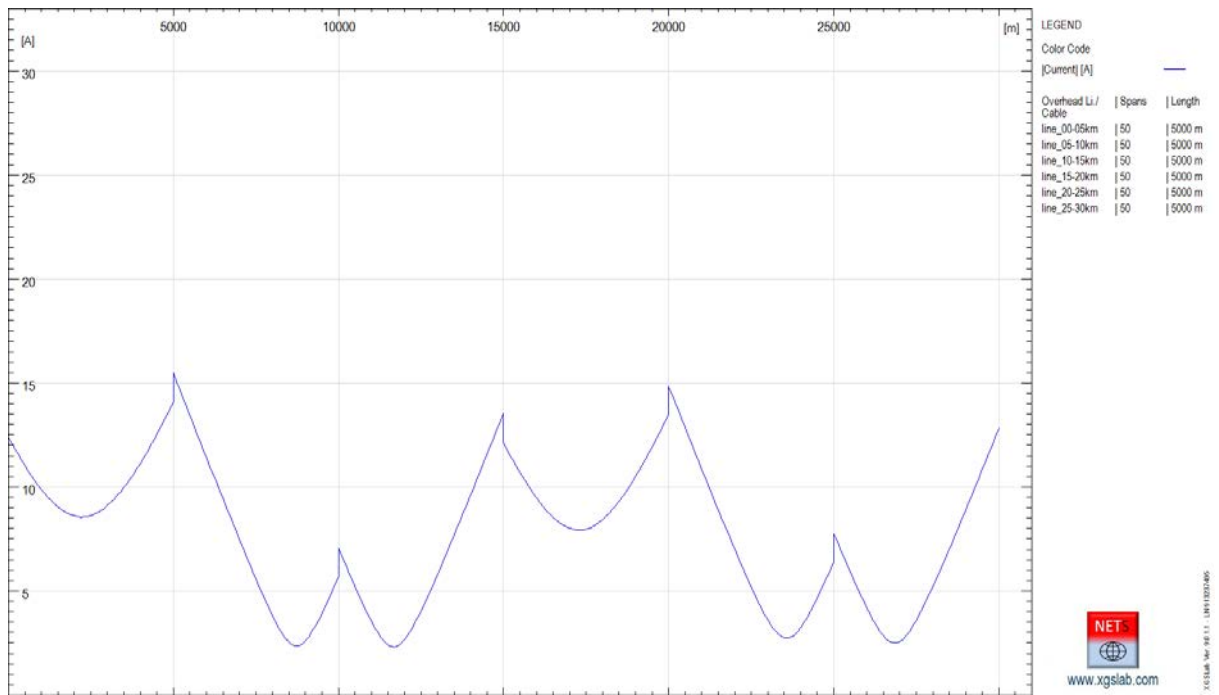


Figure 7-5: Magnitude Current Distribution along screens on phase B – Transposition 2·(5+5+5) [km] – NETS

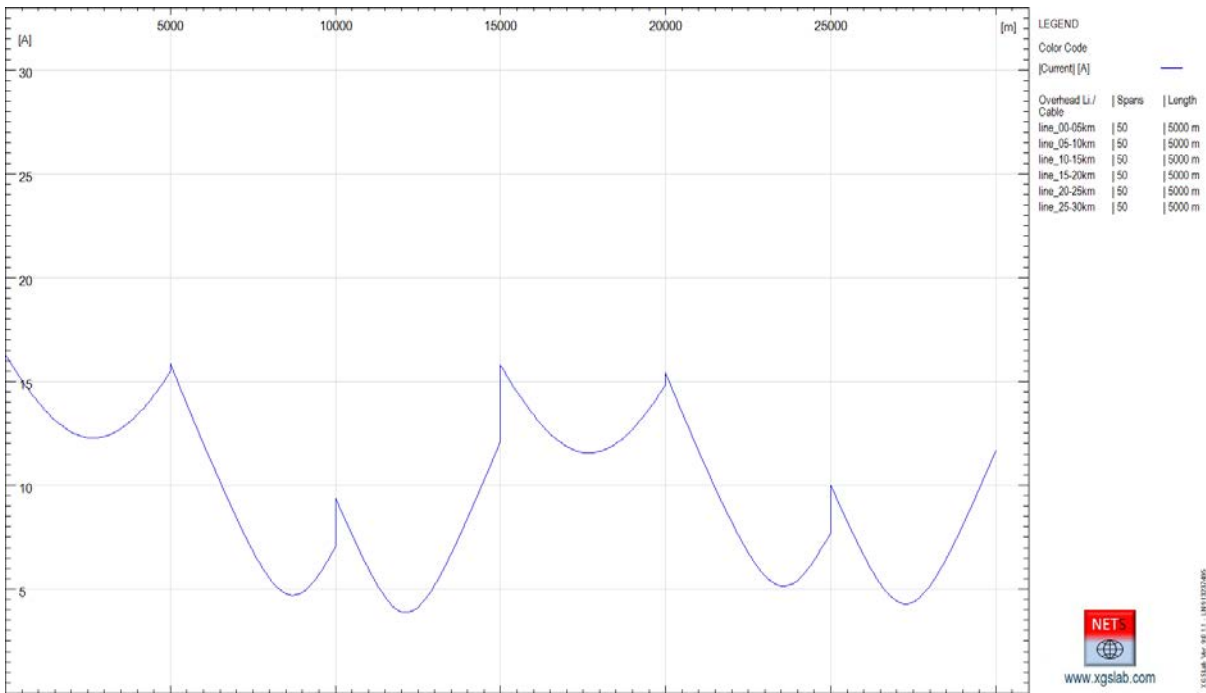


Figure 7-6: Magnitude Current Distribution along screens on phase C – Transposition 2·(5+5+5) [km] – NETS

Again, the discontinuity on currents distribution are due to the traspositons. About that, the following superposition of previous figures is interesting.

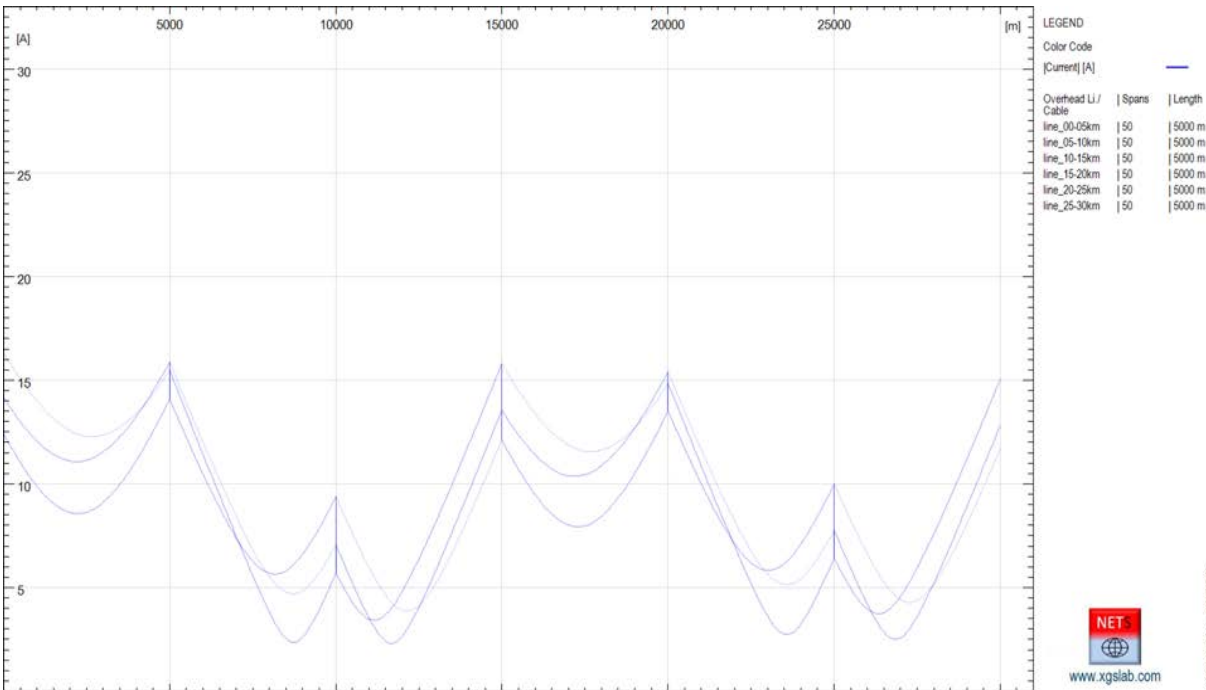


Figure 7-7: Magnitude Current Distribution along screens on phases A+B+C – Transposition 2·(5+5+5) [km] – NETS

With a double trasposition, the current along screens is about a half than with a single trasposition.

As consequence the losses on screens are reduced about to a quarter, with a great advantage for the cable ampacity.

BIBLIOGRAPHY

- [1] C. L. FORTESCUE, "Method of symmetrical co-ordinates applied to the solution of polyphase networks," *Trans. Am. Inst. Electr. Eng.*, vol. 37, pp. 1027–1140, 1918.
- [2] R. Benato and L. Fellin, *Impianti elettrici*. Wolters Kluwer Italia, 2014.
- [3] M. Coppo, R. Turri, H. Griffiths, N. Harid, and A. Haddad, "A procedure for detailed assessment of ground fault-current distribution in transmission networks," *Proc. - 2016 51st Int. Univ. Power Eng. Conf. UPEC 2016*, vol. 2017–Janua, pp. 1–6, 2017.
- [4] "Electro Magnetic Transient Program (EMTP), Theory book."
- [5] R. C. Dugan, "Reference Guide The Open Distribution System Simulator (OpenDSS) - Program Revision 7.6," no. June, 2013.
- [6] "<https://www.sestech.com/Product/Package/CDEGS>."
- [7] "<http://emtp-software.com/page/overview>."
- [8] "CCITT_vol_III.pdf."
- [9] A. Paolucci, *Lezioni di impianti elettrici*. CLEUP, 1989.
- [10] Intel, "Intel Math Kernel Library 10.2," no. March, 2009.
- [11] Y. Baghzouz, "EE 740 – Transmission Lines," 2013.
- [12] J. R. Carson, "Wave Propagation in Overhead Wires with Ground Return," *Bell Syst. Tech. J.*, vol. 5, no. 4, pp. 539–554, 1926.
- [13] E. Demirok, S. B. Kjær, and R. Teodorescu, "Three-Phase Unbalanced Load Flow Tool for Distribution Networks," *2nd Sol. Integr. Work.*, p. 9, 2012.
- [14] M. Albano, R. Turri, S. Dessanti, A. Haddad, H. Griffiths, and B. Howat, "Computation of the electromagnetic coupling of parallel untransposed power lines," *41st Int. Univ. Power Eng. Conf. UPEC 2006, Conf. Proceedings*, vol. 1, no. 2, pp. 303–307, 2006.
- [15] D. E. R. R., A. Padilha-Feltrin, and L. F. Ochoa, "Distribution transformers modeling with angular displacement: actual values and per unit analysis," *Sba Control. Automação Soc. Bras. Autom.*, vol. 18, no. 4, pp. 490–500, 2008.
- [16] C. G. Someda, *Elementi di elettrotecnica generale*, 9th ed. 1979.
- [17] J. Cedeño, "A Three-Phase Unbalanced Load Flow Solver for Large- Scale Distribution Power Systems," 2017.
- [18] M. Coppo, F. Bignucolo, and R. Turri, "Generalised transformer modelling for power flow calculation in multi-phase unbalanced networks," *IET Gener. Transm. Distrib.*, vol. 11, no. 15, pp. 3843–3852, 2017.
- [19] S. Serafin, "Modello generalizzato di trasformatore variatore per lo studio di reti elettriche dissimmetriche col metodo correction current injection," Master Thesis in Electrical Energy Engineering, University of Padova, 2014.